TO DEVELOP AN EFFICIENT VARIABLE SPEED COMPRESSOR MOTOR SYSTEM

(PEMBINAAN SEBUAH SISTEM MOTOR KOMPRESSOR KELAJUAN BOLEHUBAH YANG CEKAP)

ABDUL HALIM MOHD YATIM

RESEARCH VOTE NO:

74535

Jabatan Pertukaran Tenaga

Fakulti Kejuruteraan Elektrik

Universiti Teknologi Malaysia

2007

UNIVERSITI TEKNOLOGI MALAYSIA

BORANG PENGESAHAN
LAPORAN AKHIR PENYELIDIKAN

TAJUK PROJEK :   TO DEVELOP AN EFFICIENT VARIABLE SPEED COMPRESSOR

MOTOR SYSTEM

Saya _____ ABDUL HALIM MOHD YATIM _____

Mengaku membenarkan **Laporan Akhir Penyelidikan** ini disimpan di Perpustakaan   Universiti Teknologi Malaysia dengan syarat-syarat kegunaan seperti berikut :

1. Laporan Akhir Penyelidikan ini adalah hakmilik Universiti Teknologi Malaysia.

2. Perpustakaan Universiti Teknologi Malaysia dibenarkan membuat salinan untuk tujuan rujukan sahaja.

3. Perpustakaan dibenarkan membuat penjualan salinan Laporan Akhir Penyelidikan ini bagi kategori TIDAK TERHAD.

4. * Sila tandakan (/)

    ☐   SULIT   (Mengandungi maklumat yang berdarjah keselamatan atau
                        Kepentingan Malaysia seperti yang termaktub di dalam
                        AKTA RAHSIA RASMI 1972).

    ☐   TERHAD   (Mengandungi maklumat TERHAD yang telah ditentukan oleh
                        Organisasi/badan di mana penyelidikan dijalankan).

    ☐   TIDAK
         TERHAD

_____
TANDATANGAN KETUA PENYELIDIK

_____
Nama & Cop Ketua Penyelidik

Tarikh : _____

CATATAN :   *Jika Laporan Akhir Penyelidikan ini SULIT atau TERHAD, sila lampirkan surat daripada pihak berkuasa/organisasi berkenaan dengan menyatakan sekali sebab dan tempoh laporan ini perlu dikelaskan sebagai SULIT dan TERHAD.

DEDICATION

ABSTRACT

TO DEVELOP AN EFFICIENT VARIABLE SPEED COMPRESSOR MOTOR SYSTEM

(Keywords: Variable speed drive, induction motor, compressor, efficiency optimization, neural network controller)

This research presents a proposed new method of improving the energy efficiency of a Variable Speed Drive (VSD) for induction motors. The principles of VSD are reviewed with emphasis on the efficiency and power losses associated with the operation of the variable speed compressor motor drive, particularly at low speed operation.

The efficiency of induction motor when operated at rated speed and load torque is high. However at low load operation, application of the induction motor at rated flux will cause the iron losses to increase excessively, hence its efficiency will reduce dramatically. To improve this efficiency, it is essential to obtain the flux level that minimizes the total motor losses. This technique is known as an efficiency or energy optimization control method. In practice, typical of the compressor load does not require high dynamic response, therefore improvement of the efficiency optimization control that is proposed in this research is based on scalar control model.

In this research, development of a new neural network controller for efficiency optimization control is proposed. The controller is designed to generate both voltage and frequency reference signals simultaneously. To achieve a robust controller from variation of motor parameters, a real-time or on-line learning algorithm based on a second order optimization Levenberg-Marquardt is employed. The simulation of the proposed controller for variable speed compressor is presented. The results obtained clearly show that the efficiency at low speed is significant increased. Besides that the speed of the motor can be maintained. Furthermore, the controller is also robust to the motor parameters variation. The simulation results are also verified by experiment.

Key researchers :

Prof. Dr. Abdul Halim Mohd Yatim (Head)
Mr. Wahyu Mulyo Utomo

E-mail :   halim@ieee.org
Tel. No. :   07-5535202
Vote No. :   74535

ABSTRAK

PENGEMBANGAN KECEKAPAN PADA SISTEM MOTOR KOMPRESSOR KELAJUAN BOLEHUBAH

(Keywords: Sistem pemacu kelajuan bolehubah, motor aruhan, kompesor, optimisasi kecekapan, kendali neural network)

Kajian ini membentangkan implementasi serta mencadangkan kaedah memperbaiki kecekapan untuk Sistem Pemacu Kelajuan Bolehubah (VSD). Perinsip berhubung VSD diulang kaji dengan penekanan terhadap permasalahan kecekapan dan pembaziran kuasa yang timbul bagi implementasi pemacu kelajuan bolehubah untuk motor kompresor, terutamanya untuk tindakan laju rendah.

Kecekapan motor aruhan untuk tindakan kelajuan dan muatan daya kilas nominal adalah tinggi. Namun untuk tindakan dengan muatan daya kilas rendah, kecekapannya turun. Untuk memperbaiki kecekapan, ialah penting untuk menentukan tingkatan fluks motor yang dapat menghasilkan rugi-rugi motor paling sedikit. Cara ini dikenali sebagai pengawal kecekapan atau kuasa secara optimal. Pada amalannya, jenis muatan daya kilas kompressor tidak memerlukan tanggapan dinamik yang tinggi, karenanya kaedah memperbaiki kecekapan yang dicadangkan ialah didasarkan pada metode scalar control.

Kajian ini mencadangkan pengawalan kelajuan yang baru menggunakan kecerdasan buatan,untuk menghasilkan kecekapan yang optimal dalam tindakan perubahan kelajuan. Pengawal kelajuan ini menghasilkan dua tahap pengeluaran, iaitu acuan voltan dan frekuensi dikira secara bersama-sama. Untuk meningkatkan kekokohan pengawal ini terhadap perubahan parameter motor, sebuah pembelajaran neural network secara terus, menggunakan optimisasi tingkat ke dua Levenberg-Marquardt adalah di gunakan. Simulasi untuk pengawal kecekapan yang yang digunakan pada pemacu kelajuan bolehubah motor kompressor dibentangkan. Keputusan yang diperoleh jelas menunjukkan efficiency pada laju rendah adalah ditingkatkan. Selain itu kelajuan pada motor juga dapat di kawal dan stabil terhadap perubahan parameter motor. Keputusan simulasi ini disahkan dengan keputusan ujikaji.

Key researchers :

Prof. Dr. Abdul Halim Mohd Yatim (Head)
Mr. Wahyu Mulyo Utomo

E-mail : halim@ieee.org
Tel. No. : 07-5535202
Vote No. : 74535

TABEL OF CONTENTS

LIST OF TABELS

TABLE NO.	TITLE	PAGE

LIST OF FIGURES

LIST OF SIMBOLS LIST OF SIMBOLS AND ABBREVIATIONS

a	: per-unit frequency.
A	: the Hessian matrix
ADC	: Analogue to Digital Converter
a_i	: the neuron output.
ANN	: Artificial Neural Network
$ANN\text{-}C$	: Artificial Neural Network Controller
$ANN\text{-}I$	: Artificial Neural Network Identifier
b_j	: bias parameter
c_{fw}	: mechanical losses coefficient.
C_{zb} , C_s, C_e	: constantans.
DAC	: Digital to Analogue Converter
d_{be}	: average diameter on the roller elements.
D_c	: desire response signal
d_s	: diameter of seal.
DSP	: Digital Signal Processor
E	: the air-gap emf.
e	: controller error signal
EIA	: Energy Information Administration
f	: stator voltage frequency.
F	: the neural network performance index function
f^*	: the frequency reference signal
f_1	: fundamental frequency
f_{actv}	: the activation function
F_{mbe}	: radial force in the bearing.
F_{ms}	: force between rubber V-ring seal and end-shield.

f_n	: harmonics frequency.
H_{mw}	: fan pressure.
$HVAC$	: Heating Ventilating and Air Conditioning System
I_d	: torque current
$I_{d,opt}$	: optimum torque current
$IGBT$	: Insulated Gate Bipolar Transistors
I_m	: magnetic current.
I_n	: harmonic current.
I_r	: rotor current.
$I_r^{'}$	: rotor current referred to the stator.
I_s	: stator current.
J	: the Jacobian matrix
k_c	: core coefficient.
k_e	: eddy current coefficient.
k_h	: hysteresis coefficient.
k_L	: load torque coefficient
k_s	: stray load coefficient.
$k_{s,n}$	: stray load coefficient.
k_{te}	: constantan.
LMC	: Loss-Model-based Controller
L_σ	: leakage inductance.
m_f	: modulation frequency
m_i	: modulation index
MLP	: Multilayer Perceptron
MSE	: Mean-Square Error
n	: harmonic number.
N	: rotor speed (rpm).
n_j	: neuron transfer function
NNC	: Neural Network Controller
$NNEOC$	: Neural Network Efficiency Optimization Controller
NNV/f	: Neural Network Constant Volt per Hertz
p	: pole pairs number.
P_{ref}^{*}	: the input power motor reference.

P_{cr}	: rotor core power loss.
P_{cs}	: stator core power loss.
$P_{cu,r}$	: rotor copper losses.
$P_{cu,rn}$	: harmonic rotor winding power loss.
$P_{cu,s}$	: stator copper losses per phase.
$P_{cu,sn}$	: harmonic stator winding power loss.
P_e	: eddy power loss.
P_h	: hysteresis power loss.
$P_{im,losses}$	: the induction motor power losses
P_{in}	: the input power
$P_{inv,losses}$	: the inverter power losses
P_{load}	: compressor load power
P_{loss}	: power losses.
P_{mbe}	: friction loss in bearing.
$P_{mech,losses}$	: the mechanical power losses
P_{ms}	: friction power loss of V-ring seals.
P_{mw}	: windage power loss.
P_{mwin}	: friction air power loss.
P_{out}	: mechanical output power.
P_{stray}	: total stray load power losses.
$P_{stray,1}$	: stray load power losses at fundamental frequency.
$P_{stray,n}$	: stray load power losses at harmonic frequency.
$PWM\text{-}VSI$	: Pulse Width Modulation Voltage Source Inverter
Q	: coolant output volume.
R_r	: rotor resistance.
$R_r^{'}$	: rotor resistance referred to the stator.
R_{rT}	: rotor resistance at temperature T.
R_{rt}	: rotor resistance at temperature t.
R_s	: stator resistance.
R_{sT}	: stator resistance at temperature T.
R_{st}	: stator resistance at temperature t .
R_{str}	: stator stray losses resistance
R_{th}	: the Thevenin equivalent resistance.

s	: slip.
s_1, s_2 and s_3	: constants.
SC	: Search Controller
$SVPWM$	: Space Vector Pulse Width Modulation
t	: the time variable.
T_0	: 234.5 for cooper and 212.9 for aluminium.
T_e	: electromagnetic torque
T_L	: the load torque.
T_{load}	: compressor load torque
V_m	: air-gap voltage.
V_{mbe}	: perimeter speed on the bearing race surface.
V_n	: harmonic voltage.
V_s^*	: the stator voltage reference signal
$V_{s,opt}$	: the optimal stator voltage.
VSD	: Variable Speed Drive
VSI	: Voltage Source Inverter
$V_{stray,n}$	: stray leakage voltage at harmonic frequency.
w^*	: the speed reference signal
w_i	: the weight connection
X_{in}^{max}	: maximal input value
X_{in}^{min}	: manimal input value
x_i	: the neuron inputs
X_{in}	: input value
X_{lr}'	: rotor leakage reactance referred to the stator.
X_m	: mutual reactance.
X_{nor}	: normalized input value
X_{nor}^{max}	: maximal normalized input value
X_{nor}^{min}	: minimal normalized input value
X_{th}	: the Thevenin equivalent reactance.
Y_c	: actual response signal
Y_{den}	: normalized output value
Y_{den}^{max}	: maximal normalized output value
Y_{den}^{min}	: minimal normalized output value

Y_{out}	: output value
Y_{out}^{max}	: maximal output value
Y_{out}^{min}	: manimal output value
Z^1	: unit-delay element
α	: the learning rate or step size.
η_e	: fan energetic efficiency.
η_{nom}	: the nominal motor efficient.
μ_{ms}	: coefficient of friction.
Φ	: air gap flux/motor flux.
Φ_{opt}	: optimal air-gap flux.
ω	: motor speed (r/s).
ω_b	: base speed (r/s).
ω_e	: supply frequency(r/s).
ω_{sl}^{*}	: the slip frequency reference signal

LIST OF APPENDICES

CHAPTER 1

INTRODUCTION

1.1   Background

Electricity today is mostly generated from non-renewable or fossil fuel resources such as oil, natural gas and coal. During the energy crisis of the early 1970's, that cause increasing energy costs and the impact of greenhouse gases on world climate are among the key forces that encourage efforts and progress for electrical energy efficiency or saving (Bose, 2000).

World wide, approximately around 70% of total electrical energy is consumed by electric motor (Sen *et al.,* 1996). In 1994 the production of the electric motor used as a driver accounts over 4 billion motors (Valentine, 1998). This is an equivalent manufacturing rate of nearly 11 million motors per day. With an expected 8.5% combined average growth rate, the number will increase to 29 million motors per day before the end of this year 2006. In additions, around 96% of the total electric motors are consumed by the induction motor (Abrahamsen *et al.,* 1998).

Induction motors have many advantages compared to DC motors. Therefore, today induction motors are used in various appliances including households, industrial, commerce, public service, traction and agriculture. These motors have direct impact on the quality of life and providing essentials such as heating, cooling and work machines driver. Because of high energy consumption and the very large

number of installed units, even a small increase in efficiency improvement can have major impact on the total electrical energy consumptions (Callcut *et al.*, 1997).

The important segment to save the energy consumed by induction motors is heating ventilating and air conditioning system (HVAC) application (Domijan *et al.*, 1992; Stebbins, 1994 and Abrahamsen *et al.*, 2001). This segment constitutes a high percentage of electrical energy consumption and spends considerable time running at low loading.

In developed country such as the USA, based on Energy Information Administration (EIA) survey, it is estimate that the energy used to operate the HVAC can represent over half of the total electrical energy use in a typical commercial building (Johnson *et al.*, 1994). In Malaysia electrical consumption for cooling system, refer to previous works on energy audit and surveys of official building by ASEAN USAID was reported that the energy consumed to cooling the building is about 68% of the total electrical energy consumptions (Loewen *et al.*, 1992).

In cooling systems such as air conditioning or refrigerator-freezers system, electric motors are used for inlet fan drive, outlet blower and compressor. The main consumption of electric energy in air conditioning is consumed by the compressor motor drive which is about 80% (Domijan *et al,* 1992). In most existing air-conditioning systems the compressor is driven by an induction motor and set at constant speed or control by thermostat technique.

Usually, motor drives in the cooling system is designed for nominal capacity, although historically its fully loaded occurs only for a few times per day (Domijan *et al,* 1992 and Stebbins, 1994). Therefore without prejudice to occupant thermal comfort filling, implementation of variable speed drives in air conditioner to avoid the wasteful use of energy associated with its overuse can result in substantial saving of energy. Besides that, it has the potential to increase the energy saving because the typical load torque profile of the compressor is proportional to the square of the speed, hence the input power profile is proportional to cubic speed (Bose, 2000).

Furthermore, replacing the fixed speed motor compressor driver with variable speed drive also can be used to increase the lifespan of the air conditioner (Chen and Tsay, 2004). The reason is with the thermostat technique, the switching on-off of the compressor at high speed and high torque suddenly will produce the huge starting current and cause stress on the compressor bearings.

1.2   Energy Saving of a Variable Speed Induction Motor Drive

Variable speed electrical drives have facilitated the revolution of industrial automation leading to better quality and higher productivity in various industries and home appliances. Over the past decades, DC motors have been used extensively in variable speed drive systems. This is because; DC motors offer simple control structure. In addition, the speed and armature voltage are always linear.

Despite their simple control structure, there are some major limitations associated with the DC motor. For instance, they require regular maintenance and cannot be operated in explosive environment, their speed is limited by the mechanical commutator and they are heavy and also expensive. Although, the induction motor is more rugged and reliable, however its control is very complex and needs intricate signal processing to obtain the comparable performance of the DC motor drive (Bose, 1982).

Not until a decade later, when semiconductor and fast microprocessors or digital signal processor become available, the implementation of a variable speed induction motor drive system becomes popular and widely employed (Sen, 1990). In addition, due to the superiority of the induction motor drive, for the next decade it will encourage to replace the application of the DC motor drives in many industrial and home appliances.

In terms of the efficiency, operation of the induction motor at rated flux results in good utilization of the motor iron hence high efficiency and torque per stator ampere can be achieved. At rated flux the nominal electromagnetic torque can be developed at all frequencies. However, at light load the motor flux may be greater than necessary for development of required load torque. In this condition the iron and stator copper losses increase excessively hence the total losses become high and the efficiency drops dramatically (Domijan *et al.,* 1992; Abrahamen *et al.,* 1998 and Bose, 1997).

According to the load condition, the induction motor drive efficiency can be obtained by reducing the motor air gap flux. In scalar control method, the flux can be indirectly controlled by adjusting both stator voltage and frequency (Ohnishi *et al*, 1988; Couto and Martin, 1994; Cleland *et al.*, 1995 and Zidani *et al.*, 2002).

The main problem of the efficiency optimization control of the induction motor drive system at variable load operation is to obtain the optimum motor flux level that minimizes the total motor losses and the maximum efficiency is achieved (Abrahamen *et al.,* 2001; Kioskederis and Margaris, 1996 and Ohnishi *et al.,* 1988). At the same time it is also important to ascertain that the rotor speed of the motor is still stable. In addition, the nonlinearities of the induction motor characteristic and the varying of the motor variable parameters due to the temperature variations and magnetic saturation need to be considered when designing a robust efficient optimization control.

1.3   Research Objectives and Contributions

The objective of this research is to investigate, implement and improve efficiency of the variable speed compressor motor drive, particularly at low speed and load operation. The controller is based on the implementation of a scalar control model of the induction motor drive system.

This research proposes an improvement of efficiency optimization control of the variable speed induction motor for driving compressor by developing the neural network with on-line/real-time learning algorithm of a second order Levenberg-Marquardt optimization. The controller is designed to generate both voltage and frequency reference signals simultaneously. The design of the controller is verified by simulation and laboratory experiment. While performing the study, the significant contributions are listed as follows:

1. A new efficiency optimization control scheme for the variable speed compressor motor drive using neural network control is developed, in which the technique does not require knowledge of the motor parameters.

2. A new structure neural networks controller as a combination between recurrent and feed forward networks with multiple outputs is developed. This controller generates voltage and frequency reference signals simultaneously. By this approach both of the speed and efficiency of the motor can be control simultaneously too.

3. A new neural network controller scheme with real-time/on-line learning algorithm with the second order Levenberg-Marquardt optimization method is developed. By this technique the controller becomes adaptive hence completely insensitive to motor parameters variation and more robust.

4. The simulation and experimental set-up to verify the proposed neural network efficiency optimization control for the variable speed compressor motor drive was developed. The simulation is conducted using S-Function on MATLAB/SIMULINK. from the Borland C++, Inc. and the experimental set-up is centered on TMS320C31 Texas Instruments DSP.

1.4   Project Report Organizations

The broad outline of this report is as follows:

Chapter 2 describes the basic principles of the efficiency optimization control of the induction motors drive. Various aspects and problems associated with the efficiency optimization control are discussed. The losses of the induction motor drive system and various methods for minimizing the motor losses are explained. Besides that, reviews of previous and current research conducted in efficiency optimization control of the induction motor drive system are described.

Chapter 3 presents the development of the proposed method. The prospective of the neural network control on the efficiency optimization control is discussed. The design of the neural network efficiency optimization control is described in detail.

Chapter 4 provides an explanation on the hardware and experimental setup used in this research. The major components of the experimental set-up, which centered on the TMS320C31 Digital Signal Processor are presented and described.

Chapter 5 verifies the proposed controller. To show the feasibility of the proposed controller scheme, the simulation studies by using Simulink-Matlab are presented with the results verified by relevant experimental results.

Finally, main conclusions of the research and recommendation for future research directions are presented in Chapter 6.

CHAPTER 2

OVERVIEW AND PREVIOUS WORK OF EFFICIENCY OPTIMIZATION CONTROL OF VARIABLE SPEED INDUCTION MOTOR DRIVE SYSTEMS

2.1   Introduction

This chapter presents an overview of efficiency optimization control of variable speed induction motor drive, followed by its theoretical background. The equivalent circuit and related equations of the induction motor drive is first described. Then the concept of efficiency optimization control is described. Some control strategies which have been implemented in the induction motor drive system are discussed. Advantages and disadvantages of previous work are also discussed.

2.2   Variable Speed Induction Motor Drive System

Variable speed electrical motor drive technology has advanced dramatically in the last two decades with the advent of new power semiconductor devices and magnetic materials (Sen, 1990 and Shepherd *et al.*, 1995). This technique provides continuous wide ranges speed compared to the mechanical variable speed drive. Therefore, compared to the mechanical variable speed drive, the electrical variable speed drives have potential for energy savings (Rice, 1988).

Before the emergence of Power Electronic, the DC motor with its mechanical commutator and brushes was the undisputed choice for variable speed drive application. The DC motor provide inherent decouple of torque and flux and hence is simple to control (Sen *et al.*, 1996). In that time, the induction motors were commonly applied as fixed speed machines due to their connection to a fixed voltage and frequency supply.

Recent advantages in power electronic, microelectronic and microcomputer technologies have made it possible to implement variable speed induction motor in many applications (Sen, 1990 and Bose, 1997).

Induction motor was first developed by Galileo Ferraris in 1885 and Nicola Tesla in 1886 (Boldea and Nasar, 2002). They were rugged and easier to construct and have many advantages compared to the DC motor. However, its motor has a highly coupled, multivariable structure and nonlinear characteristic. By these reasons, control performance of the induction motor drive generally requires more complicated control algorithms implemented by fast real-time signal processing unit (Sen, 1990; Bose, 1997 and Cirstea *et al.*, 2002).

Basically, the variable speed induction motor drive is composed of some distinguish elements such as a controllable power converter, an electric motor which drives a mechanical load at an adjustable speed and also driver controller (Murphy and Turnbull, 1988 and Shepherd *et al.*, 1995). The main elements of the Variable Speed Drive (VSD) system are shown in Figure 2.1.
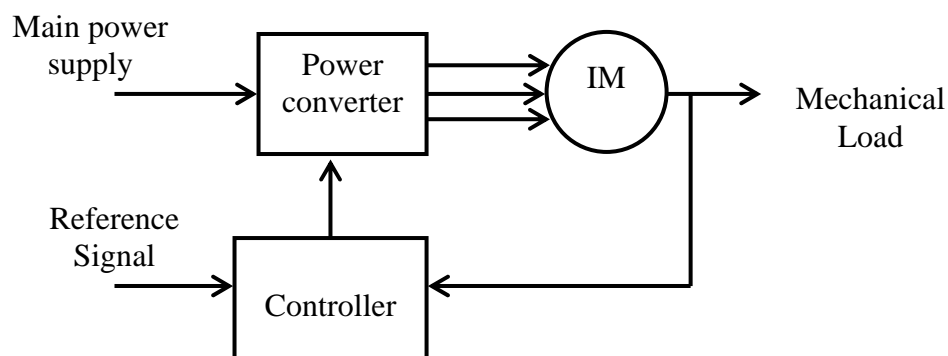
Figure 2.1: Block diagram of a variable speed induction motor drive

The power converter receives ac or dc supply voltages from the main power supply and feeds the motor with appropriately condition voltage, current and frequency. In close loop the controller receives command from reference signal and actual speed information from the load. The actual speed should follow the reference signal command value as accurately as possible in a short time without ripple and overshoot. The mechanical load has a torque-speed characteristic representing the counter torque which must be overcomed by the drive motor.

2.3   Power Losses of A Variable Speed Induction Motor Drive

The output power developed by the motor is proportional to the product of the shaft torque and the shaft rotational speed. The value of the development torque usually varies automatically to satisfy the demand of the load torque plus any torque associated with friction and windage. Any significant change in motor speed, however must be obtained in a controlled manner by making some adjustment to its electrical supply.

Associated to the power flow of the motor drive system, the input power of the system generates mechanical output and power losses. The power losses occur in components of the VSD which includes the power converter and the induction motor losses. Correlation between input, losses and output power of the VSD is given by following equation:

$$P_{in} = P_{inv,losses} + P_{im,losses} + P_{mech,losses} \qquad (2.1)$$

where: P_{in} : the input power

$P_{inv,losses}$: the inverter power losses

$P_{im,losses}$: the induction motor power losses

$P_{mech,losses}$: the mechanical power losses

2.3.1 Inverter Losses

Nowadays, the Pulse Width Modulation Voltage Source Inverter (PWM-VSI) converter topology is used as a standard power converter for variable speed induction motor drive system (Cirstea *et al.*, 2002). Configuration of the three phases Voltage Source Inverter (VSI) using Insulated Gate Bipolar Transistors (IGBT) and diode for the induction motor drive system is shown in Figure 2.2.
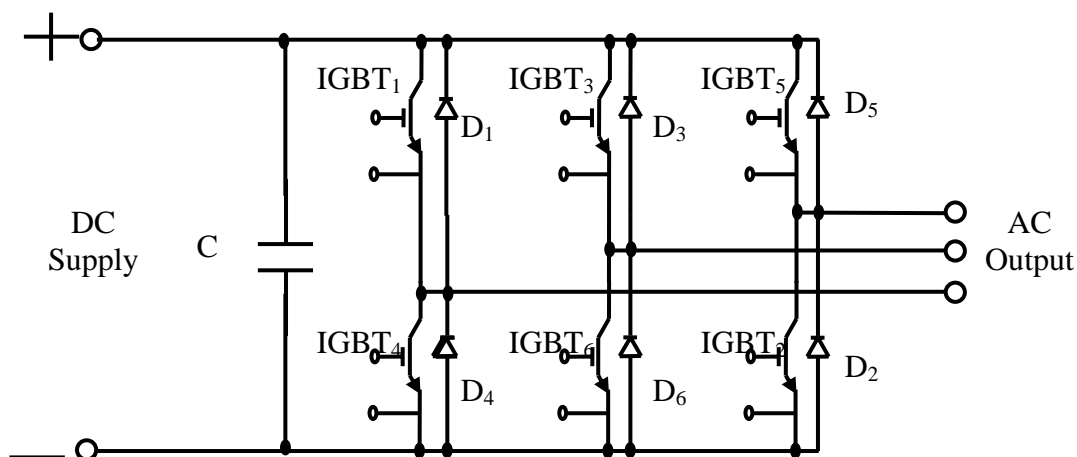
Figure 2.2: Circuit of a three phase IGBT inverter

The inverter is used to convert the DC supply (fixed) to variable frequency/voltage AC supply. The losses powers of the inverter occur in the power semiconductor devices such as IGBTs and diodes. These losses compose of conduction and switching losses (Rashid, 1993 and Mohan *et al*., 1995).

Conduction losses are due to the fact that the voltage across the switch in the on state is not zero, but typically in the range of 1 to 2 V for IGBTs (Skvarenina, 2002). In addition, a resistive element of the semiconductor device will generate power dissipation.

In the ideal case of a switching event, there would be no power loss in the switch since either the current in the switch is zero (switch open) or the voltage across the switch is zero (switch closed). In reality, the switching losses are the second major loss mechanism and are due to the fact that, during the turn-on and turn-off transition, current is flowing while voltage is present across the device. Also the losses will generate in the dc-link capacitor and the filter components. However the losses in the dc-link capacitor are disregarded (Grigsby, 2001).

In order to avoid audible noise being radiated from motor windings or transformers, most modern inverters operate at switching frequencies substantially above 10 kHz (Bose, 2001). The maximum switching frequency needs to be carefully considered due to Electromagnetic Interference (EMI) factor.

The inverter losses are also influence by the inverter modulation strategy (Trzynadlowski and Legowski, 1994 and Emadi, 2005). For drives with the size of some kilowatts, the inverter losses only constitute a small fraction of the total motor drive losses (Abrahamsen *et al*., 1998). By this reason, it is not commented further in this thesis.

2.3.2   Induction Motor Losses

Power losses in the induction motor are portions of the input power that eventually transform to heat rather than driving the load. Losses in induction motor occur in windings, magnetic cores, besides mechanical friction and windage losses (Boldea and Nasar, 2002). These losses can be classified as follows (Garcia *et al.*, 1994):

1. Stator Resistance - current losses in the windings.
2. Rotor Resistance - current losses in the rotor bars and end rings.
3. Iron Core Losses - magnetic losses in laminations, inductance and eddy current losses.
4. Stray Losses - magnetic transfer loss in the air gap between stator and rotor.
5. Windage and Friction - mechanical drag in bearings and cooling fan.

Losses in the induction motor also can be classified based on their electrical frequency such as: fundamental and harmonic losses. Frequency harmonics are to be considered only when the induction motor is static converter fed, and thus the voltage time harmonics content depends on the type of the converter and the pulse width modulation used with it (Boldea and Nasar, 2002).

2.3.2.1 Stator Resistance Losses

It is known that resistor components in the stator winding will generate heat proportional to the square of the current. The stator power losses are a function of the current flowing in the stator winding as defined by:

$$P_{cu,s} = I_s{}^2 R_s \qquad (2.2)$$

where: $P_{cu,s}$: stator copper losses per phase.

        I_s : stator current.

        R_s : stator resistance.

The stator resistance will vary in accordance to the temperature, correction for the resistance of the stator winding is given by (IEEE standard-112, 2004):

$$R_{sT} = R_{st} \frac{T_0 + T}{T_0 + t} \qquad (2.3)$$

where: R_{sT} and R_{st} : stator resistance at temperature T and t.

        T_0 : 234.5 for cooper and 212.9 for aluminium.

High frequency time harmonics in the supply voltage of IMs may occur either because the induction motor itself is fed from a PWM static power converter for variable speed or because, in the local power grid, some other power electronic devices produce voltage time harmonics at the induction motor terminals. For voltage-source static power converters, the time harmonics frequency content and distribution depends on the PWM strategy and the switching period (Boldea and Nasar, 2002).

The variation of resistance R and leakage inductance L_l for conductors in slots with frequency is at first rapid, being proportional to f^2. As the frequency increases further, the field penetration depth gets smaller than the conductor height and the rate of change of R and L_l decreases to become proportional to $f^{1/2}$ as shown in Figure 2.3 (Boldea and Nasar, 2002).
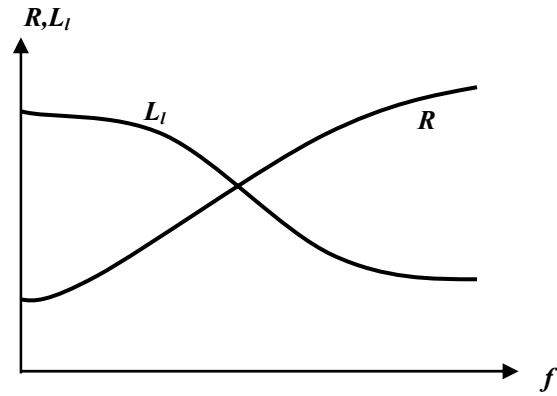
Figure 2.3: R and L_l variation with frequency

For high frequencies, the equivalent circuit of the induction motor can be simplified by eliminating the magnetization branch as given in Figure 2.4.
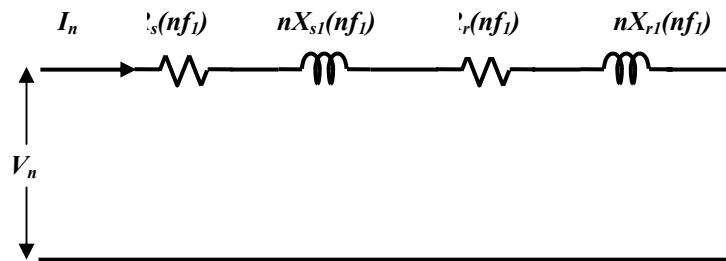
Figure 2.4: Equivalent circuit for voltage time harmonic

In general, the reactance prevails at high frequencies and a value of the current harmonic is defined:

$$I_n \approx \frac{V_n}{2\pi f_n L_\sigma(f_n)} \tag{2.4}$$

$$L_\sigma(f_n) = L_{sl}(f_n) + L_{rl}(f_n) \tag{2.5}$$

where: I_n : harmonic current.

L_σ : leakage inductance.

V_n : harmonic voltage.

f_1 : fundamental frequency.

f_n : harmonics frequency.

n : harmonic number.

The frequency harmonic loss in the stator winding time harmonic losses is given by:

$$P_{cu,sn} = 3I_n^2 R_s \left(f_n \right)$$ (2.6)

where: $P_{cu,sn}$: harmonic stator winding power loss.

2.3.2.2 Rotor Resistance Losses

The rotor copper loss is a function of the current flowing in the rotor winding or rotor bar as defined by:

$$P_{cu,r} = I_r^2 R_r$$ (2.7)

where: $P_{cu,r}$: rotor copper losses.

I_r : rotor current.

R_r : rotor resistance.

The rotor resistance will vary accordance to the temperature, correction for the resistance of the rotor winding is given by (IEEE standard-112, 2004):

$$R_{rT} = R_{rt} \frac{T_0 + T}{T_0 + t}$$

(2.8)

where: R_{rT} and R_{rt} : rotor resistance at temperature T and t.

The most common rotor bar is developed by aluminium, although copper may also be used.

The frequency harmonic loss in the rotor winding time harmonic losses is given by:

$$P_{cu,rn} = 3I_n^2 R_r \left(f_n \right)$$

(2.9)

where: $P_{cu,rn}$: harmonic rotor winding power loss.

2.3.2.3 Core Losses

The core losses in the induction motor comprise the hysteresis and eddy current power losses. The losses occur in both the stator and rotor core. There are several variant of the calculation core losses, the core loss due to fundamental frequency mutual flux in the stator can be approached by (Sousa *et al.*, 1992):

$$P_{hs} = k_h f \Phi^2$$

(2.10)

$$P_{es} = k_e f^2 \Phi^2$$

(2.11)

$$P_{cs} = P_{hs} + P_{es} \tag{2.12}$$

$$= k_h f \Phi^2 + k_e f^2 \Phi^2 \tag{2.13}$$

where: P_{cs} : stator core power loss.

       P_h : hysteresis power loss.

       P_e : eddy power loss.

       k_h : hysteresis coefficient.

       k_e : eddy current coefficient.

       Φ : air gap flux/motor flux.

       f : stator voltage frequency.

Corresponding rotor core losses is approached as:

$$P_{cr} = k_h s f \Phi^2 + k_e (sf)^2 \Phi^2 \tag{2.14}$$

where: P_{cr} : rotor core power loss.

       s : slip.

The total core losses can be rearranged as follows:

$$P_c = P_{cs} + P_{cr} \tag{2.15}$$

$$= \left(k_h \frac{(1+s)}{f} + k_e (1+s)^2 \right) f^2 \Phi^2 \tag{2.16}$$

As the air gap flux is related to air-gap voltage as given by:

$$\Phi = \sqrt{k_c} \frac{V_m}{f} \tag{2.17}$$

where: k_c : core coefficient.

       V_m : air-gap voltage.

The total power losses can be rewritten as:

$$P_c = k_c \left(k_h \frac{(1+s)}{f} + k_e (1+s)^2 \right) V_m^2$$

(2.18)

The equivalent core loss resistance can be derived as:

$$R_m = \frac{1}{k_c \left(k_h \dfrac{(1+s)}{f} + k_e (1+s)^2 \right)}$$

(2.19)

Assuming that the coefficients of hysteresis and eddy current losses remain the same at harmonic frequency and since the harmonic slip is unity, the equivalent core losses resistance at harmonic frequency can be obtained from the fundamental core resistance as:

$$R_{m,n} = \frac{0.5}{k_c \left(\dfrac{k_h}{f_n} + k_e \right)}$$

(2.20)

2.3.2.4 Stray Load Losses

The stray load losses are additional core and eddy current losses caused by the increase in air-gap leakage flux with load and losses caused by high frequency pulsation fluxes. These losses can be divided into six components as follows (Sen and Landa, 1990):

1) The eddy current loss in the stator copper due to slot leakage flux.
2) The losses in the motor end structure due to end leakage flux.
3) The high-frequency rotor and stator surface losses due to zig-zag leakage flux.

4) The high-frequency tooth pulsation and rotor I^2R losses also due to the zig-zag leakage flux.

5) The six-times-frequency (for three-phase machines) rotor I^2R losses due to circulating currents induced by the stator belt leakage flux.

6) The extra iron losses in motors with skewed slots due to skew leakage flux.

For the fundamental current, the stray losses essentially concentrate at the stator, this losses can be approached by (Sousa *et al.*, 1992):

$$P_{stray,1} = k_s \left[\ k_h f + k_e f^2 \ \right] I_S^2$$

(2.21)

where: $P_{stray,1}$: stray load power losses at fundamental frequency.

k_s : stray load coefficient.

The equivalent resistance R_{stray} can be represented in series with the stator leakage reactance as given by:

$$R_{stray,1} = k_s \left[k_h f + k_e f^2 \right]$$

(2.22)

The stator per phase stray loss at harmonic frequency f_n is given by (Sousa *et al.*, 1992):

$$P_{stray,n} = k_{s,n} \left[\frac{k_h}{f_n} + k_e \right] V_{s,n}^2$$

(2.23)

where: $P_{stray,n}$: stray load power losses at harmonic frequency.

$k_{s,n}$: stray load coefficient.

$V_{stray,n}$: stray leakage voltage at harmonic frequency.

The loss can be represented by an equivalent resistance $R_{stray,n}$ in parallel with the leakage inductance as:

$$R_{stray,n} = \frac{1}{k_{s,n}\left[\dfrac{k_h}{f_n} + k_e\right]}$$

(2.24)

Kioskeridis and Margaris (1996) approach the stray loss arise on the copper and iron of the induction motor as:

$$P_{stray} = c_{zb}I_s^2 + c_s\Phi^2 I_s^2 + c_e a I_s^2$$

(2.25)

where: P_{stray} : total stray load power losses.

   C_{zb} , C_s and C_e: constantans.

   a : per-unit frequency.

Sen and Landa (1990) described that the value of the C_{zb} , C_s and C_e are dependent on the skin effect, flux density, no-load current, stator current and other empirical factors.

2.3.2.5 Mechanical Loss

The mechanical loss which consists of friction and windage power losses is due to friction of the bearing and air friction caused by the motion of the moving part through the surrounding medium. These losses are relatively fixed and a small percentage of the total motor losses, which can be broken down by the following equations (Dabala, 2001):

1. Friction power loss in bearing is approximated by:

$$P_{mbe} = 1.5 F_{mbe} \frac{v_{mbe}}{d_{be}} 10^{-5}$$

where: P_{mbe} : friction loss in bearing.

         F_{mbe} : radial force in the bearing.

         d_{be} : average diameter on the roller elements.

         V_{mbe} : perimeter speed on the bearing race surface.

2. Windage power loss of outside fan is approximated by:

$$P_{mw} = \frac{H_{mw} Q}{\eta_e}$$

where: P_{mw} : windage power loss.

         H_{mw} : fan pressure.

         Q : coolant output volume.

         η_e : fan energetic efficiency.

3. Friction air power losses of rotor and windage losses of two internal fans are approximated by:

$$P_{mwin} = 2 p P_{mw}$$

where: P_{mwin} : friction air power loss.

         p : pole pairs number.

4. Friction power loss of V-ring seals is approximated by:

$$P_{ms} = 52.33 \mu_{ms} F_{ms} N d_s 10^{-3} \qquad (2.29)$$

where: P_{ms} : friction power loss of V-ring seals.

μ_{ms} : coefficient of friction.

F_{ms} : force between rubber V-ring seal and end-shield.

N : rotor speed (rpm).

d_s : diameter of seal.

In simple calculation, Sen and Landa (1990) described that the total friction and windage losses are approximately proportional to the square of the speed and to the contact surface area. The total mechanical induction motor losses can be approximated by:

$$P_{mech,losses} = c_{fw} N^2 \qquad (2.30)$$

where: $P_{mech,losses}$: mechanical power losses.

c_{fw} : mechanical losses coefficient.

Sen and Landa (1990) assumed that the mechanical induction motor losses to be unaffected by voltage harmonic distortion.

2.4 Efficiency Optimization of an Induction Motor Drive System

The efficiency of the induction motor is determined by the relationship between input power, power losses and output power as given by:

$$\eta = \frac{P_{out}}{P_{in}}$$

(2.31)

$$\eta = \frac{P_{out}}{P_{out} + P_{loss}}$$

(2.32)

where: P_{loss} : power losses.

P_{out} : mechanical output power.

Equation 3.32 shows that the only way to increase the efficiency of an induction motor operating at a given level of output power is to reduce the losses within the motor (Umans, 2004).

To optimize the efficiency of induction motor drive by means of power losses reduction reports that, Kusko and Galler in 1983 suggest three categories of efficiency optimization motor drive (Ta and Hori, 2001) i.e.:

1. Motor selection and design improvement.
2. Improvement of the waveforms supplied by power inverter.
3. Utilizing a suitable control method.

In the case of the motor drive duty cycle operating less than the rated torque and speed condition most of the time, it is not possible to improve the efficiency by machine design or by waveform shaping techniques. Utilizing of the suitable control flux method that optimized the motor efficiency is more flexible.

2.4.1. Relationship of Induction Motor Variables

The three phase induction motor with balance input voltage can be analysed by single phase equivalent circuit. In steady state mode, the per-phase equivalent circuit of the induction motor in fundamental frequency is given in Figure 2.5.
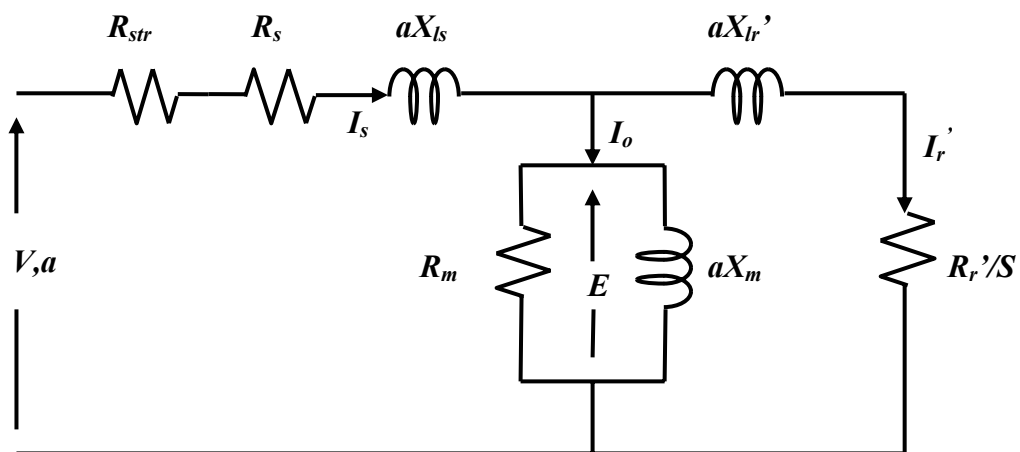
Figure 2.5: Per-phase induction motor equivalent circuit

In the equivalent circuit of Figure 2.5, the stray losses are represented by equivalent resistance R_{str} in the stator branch. The stray losses are mainly attributed to the rotor current, since the rotor current in the squirrel cage induction motor is not measurable, the stray losses are expressed as a function of the stator current (Kioskeridis and Margaris, 1996).

Referring to the Figure 2.5, in the per-unit system, the induction motor equation will be determined. The per-unit frequency is given by:

$$a = \frac{\omega_e}{\omega_b} \tag{2.33}$$

$$= \frac{\omega}{1-s} \tag{2.34}$$

Where: ω_e : supply frequency(r/s).

     ω_b : base speed(r/s).

     ω : motor speed (r/s).

The magnetizing current is determined by:

$$I_m = \frac{E/a}{X_m} \tag{2.35}$$

$$= \frac{\Phi}{X_m} \tag{2.36}$$

where: I_m : magnetizing current.

     E : the air-gap emf.

     X_m : mutual reactance.

The rotor current is determined by:

$$I_r^{'} = \frac{\Phi}{\sqrt{\left(R_r^{'}/s\ a\right)^2 + X_{lr}^{'2}}} \tag{2.37}$$

where: $I_r^{'}$: rotor current referred to the stator.

     $R_r^{'}$: rotor resistance referred to the stator.

     $X_{lr}^{'}$: rotor leakage reactance referred to the stator.

From Equation (2.37) the air-gap flux can be obtained by:

$$\Phi = I_r' \sqrt{\left(R_r'/s\ a\right)^2 + X_{lr}'^2} \tag{2.38}$$

The electromagnetic torque is given by:

$$T_e = I_r'^2 \frac{R_r'}{s\ a} \tag{2.39}$$

Substitution Equation (2.36) into (2.38) the electromagnetic torque can be obtained by:

$$T_e = \Phi^2 \frac{R_r'/s\ a}{\left(R_r'/s\ a\right)^2 + X_{lr}'^2} \tag{2.40}$$

Usually, the induction motor operates with a small slip and the condition $R_r'/sa >> aX_{lr}'$ holds. By this assumption, the air-gap flux and torque electromagnetic can be approached by:

$$\Phi \cong \frac{R_r' I_r'}{s\ a} \tag{2.41}$$

$$T_e \cong \frac{s\ a}{R_r'} \Phi^2 \tag{2.42}$$

$$T_e \cong \Phi\ I_r' \tag{2.43}$$

The stator current of the induction motor can be determined by (Kioskeridis and Margaris, 1996):

$$I_s^2 = I_m^2 + c_L I_r'^2 \qquad (2.44)$$

where:

$$c_L = 1 + 2\frac{X_{lr}'}{X_m} \qquad (2.45)$$

The magnetization current curve can be approximated by (Kioskeridis and Margaris, 1996):

$$I_m = s_1\Phi + s_2\Phi^3 + s_3\Phi^5 \qquad (2.46)$$

Hence the magnetizing reactance is given by:

$$X_m = \frac{\Phi}{I_m} \qquad (2.47)$$

$$= \frac{1}{s_1 + s_2\Phi^2 + s_3\Phi^4} \qquad (2.48)$$

where: s_1, s_2 and s_3 : constantans.

2.4.2. Efficiency Control of an Induction Motor

The efficiency of the induction motor is high when it is operated at the rated flux, load and speed. However, at light loads the flux at rated operation causes excessive core loss, thus impairing the efficiency of the induction motor drive (Sousa *et al.*, 1995 and Bose *et al.*, 1997). In this condition the motor flux is more than the necessary for the development of the required torque. Therefore to improve the induction motor efficiency, the motor air gap flux must be reduced.

The technique to minimise the motor drive by adjusting the motor flux level according to the motor load is called energy optimal control (Abrahamsen *et al.*, 1998). This technique is also known as efficiency optimization control (Garcia *el al.*, 1994 and Sousa *et al.*, 1995) or loss minimization control (Vukosavic and Levi, 2003)

The optimal operating point is achieved when the sum of the induction motor losses components is minimum (Abrahamsen *et al.*, 1998; Kioskeridis and Margaris, 1996; Moreno *et al.*, 1997; Sousa *et al.*, 1995 and Bose *et al.*, 1997).

The basic principle of the efficiency optimization control is hereafter described with the main focus on the motor losses minimization. The electromagnetic torque of the induction motor can be approximated by (Bose, 2001):

$$T_e = k_{te} I_m I_r \qquad\qquad (2.49)$$

where: T_e : electromagnetic torque.

        I_m : magnetizing current.

        I_r : rotor current.

        k_{te} : constantan.

From Equation (2.49), the electromagnetic torque of the induction motor can be generated by the numbers of combinations of magnetizing and torque producing rotor current. It is thus possible to obtain the same torque with different combination of flux and current value. For every load and speed condition, there exists a magnetizing current where the motor losses are minimal (Abrahamsen *et al.*, 1998)

Illustration of its combination associated to the phasor diagram of the voltage and current of the motor is as shown in Figure 2.6 (Murphy and Turnbull, 1988).
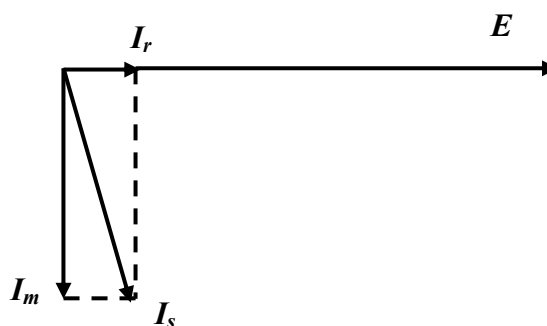
(a)
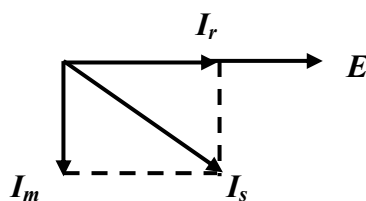
(b)

Figure 2.6: Phasor diagram of the induction motor voltage and current at light load operation: (a) at rated stator voltage and (b) at half rated stator voltage.

From Figure 2.6 the influence of the stator voltage to the motor losses can be described as follows. At light load operation and at rated stator voltage, the rotor current I_r is quite small, but the stator current I_s and magnetic current I_m are high as shown in Figure 2.6(a). If the voltage E is reduced by half, as shown in Figure 2.6(b), the rotor current I_r must double in order to develop the same electromagnetic

torque as before. The motor flux and magnetizing current I_m are also halved and the total stator current I_s is reduced.

By a proper adjustment of the magnetic flux, an appropriate balance between copper and iron losses can be achieved to minimize the total motor drive losses. Beside that, from Equation (2.25), the stray loss reduces while the motor flux decreases.

However, the motor speed decrease while the magnetizing current decrease and in order to maintain the speed, the speed component of supply such as stator current for vector control and the stator frequency for scalar control must be increased.

A number of methods have been published on efficiency optimization control of the induction motor drive system. The technique allowing the efficiency improvement can be divided into two categories (Kioskeridis and Margaris, 1996; Moreno *et al.,* 1997; Bernal *et al.*, 2000; Ta and Hori, 2001 and Chakraborty *et al.*, 2002):

1. A Loss-model-based controller (LMC).
2. A search controller (SC).

The following section shows that by controlling the motor flux level or its equivalent variable command, the required speed and electromagnetic torque can be established.

2.4.3. Loss-Model-Based Controller Method

The loss-model-based approach consisting of computing the losses by using the machine model and selecting the flux level that minimizes these losses. In the literatures, different LMC approach model can be found.

2.4.3.1. Principle of Loss-Model-Based Controller Method

Basically, the LMC method determines the optimum flux function by deriving the equation of the power losses of the motor drive. If rotor iron and inverter losses are neglected and expressing stray and mechanical losses using a simple assumption, the total power losses in the induction motor drive are given by (Kioskeridis and Margaris, 1996):

$$P_{loss} = R_s I_s^2 + R_r I_r^2 + \left(k_h \omega + k_e \omega^2 \right) \Phi^2 + c_{str} \omega^2 I_r^2 + c_{fw} \omega^2 \qquad (2.50)$$

where: $c_{str} \omega^2 I_r^2$: stray power loss.

$c_{fw} \omega^2$: mechanical power loss.

Eliminating the stator and rotor current in Equation (2.50) by substituting Equations (2.36) and (2.44) yield:

$$P_{loss} = \left(c_L R_s + R_r' + c_{str} \omega^2 \right) \frac{T_e^2}{\Phi^2} + \left(k_h \omega + k_e \omega^2 + \frac{R_s}{X_m^2} \right) \Phi^2 + c_{fw} \omega^2 \qquad (2.51)$$

The sensitivity function of input power motor drive with respect to the air gap flux at steady state is determined as follows:

$$S_{\Phi_m}^{P_{loss}} = \left. \frac{\partial P_{loss}}{\partial \Phi} \right|_{T_e \omega} \qquad (2.52)$$

$$S_{\Phi_m}^{P_{loss}} = 2\left[-\left(c_L R_s + R_r^{'} + c_{str}\omega^2\right)\frac{T_e^2}{\Phi^3} + \left(k_h\omega + k_e\omega^2 + \frac{R_s}{X_m^2}\right)\Phi \right] \qquad (2.53)$$

The second derivative of the function in Equation (2.51) is given by:

$$\frac{\partial^2 P_{loss}}{\partial \Phi^2} = 2\left[3\left(c_L R_s + R_r^{'} + c_{str}\omega^2\right)\frac{T_e^2}{\Phi^4} + \left(k_h\omega + k_e\omega^2 + \frac{R_s}{X_m^2}\right) \right] \qquad (2.54)$$

At any motor flux value, the Equation (2.54) is:

$$\frac{\partial^2 P_{loss}}{\partial \Phi^2} > 0 \qquad (2.55)$$

Based on Equation (2.55) it can be concluded that function of Equation (2.51) is concave and it means that there is a value of flux that will generate minimum power losses (Blanusa and Vukasovic, 2003).

The losses minimization condition with respect to air-gap flux of the induction motor can be determined by the sensitivity power losses Equation (2.53) equal to zero. Substitution of the Equation (2.43) for the loss minimization condition is given by:

$$\left(c_L R_s + R_r^{'} + c_{str}\omega^2\right)I_r^{'2} = \left(k_h\omega + k_e\omega^2 + \frac{R_s}{X_m^2}\right)\Phi^2 \qquad (2.56)$$

Condition of the Equation (2.56) can be used in the wound-rotor induction motor, but in the squirrel cage induction motor, the rotor current must be substituted by the stator current, since the former cannot be measured. Solving for optimum air-gap flux by substituting Equation (2.40) and (2.48) in Equation (2.56) yields:

$$\Phi_{opt} = I_s G_s \sqrt{\frac{1 + \omega^2 T_s^2}{1 + \omega^2 T_{cs}^2}} \tag{2.57}$$

where:

$$G_s = X_m \sqrt{\frac{C_L R_s + R_r^{'}}{2 C_L R_s + R_r^{'}}} \tag{2.58}$$

$$T_s = \sqrt{\frac{C_{str}}{C_L R_s + R_r^{'}}} \tag{2.59}$$

$$T_{cs} = \sqrt{\frac{C_L R_s}{2 C_L R_s + R_r^{'}} \left(T_c^2 + \frac{C_L R_s + R_r^{'}}{C_L R_s} T_s^2 \right)} \tag{2.60}$$

$$T_c = X_m \sqrt{\frac{k_e + k_h/\omega}{R_s}} \tag{2.61}$$

where: $\boldsymbol{\Phi_{opt}}$: optimal air-gap flux.

An example of a block diagram of the LMC of the induction motor drive that had been proposed by Kioskeridis and Margaris (1996) is given in Figure 2.7.
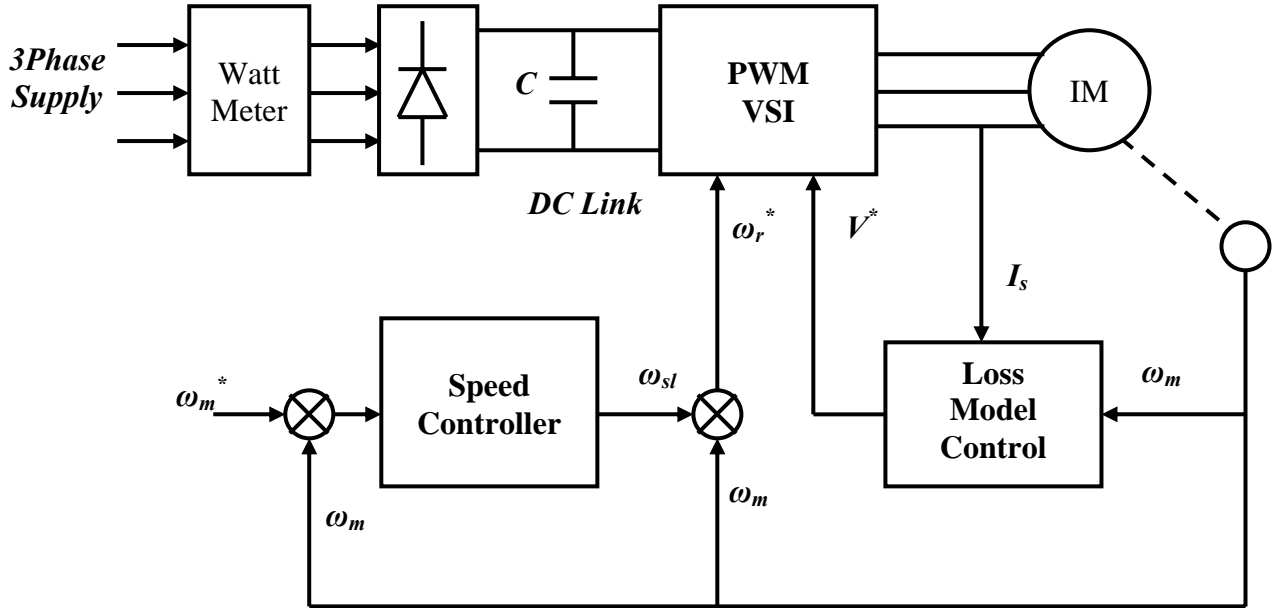
Figure 2.7: Block diagram of the LMC of the induction motor drive

2.4.3.2. Previous Work on the Loss-Model-Based Controller Method

Under specific speed and torque, Chen and Yeh (1992) derive the induction mathematic model for efficiency optimization. Without harmonic frequency effect consideration, the optimum voltage and slip frequency to achieve the minimum power losses are obtained by:

$$V_{s,opt} = \sqrt{\frac{T_L \omega_s \left(\left(R_{th} + R_r/s \right)^2 + X_{th}^2 \right)}{R_{th} + R_r/s}} \tag{2.62}$$

$$\omega_{sl} = \omega_{r} \frac{R_{r}}{s} \tag{2.63}$$

where: $V_{s,opt}$: the optimal stator voltage.

T_L : the load torque.

R_{th} : the Thevenin equivalent resistance.

X_{th} : the Thevenin equivalent reactance.

Wasynczuk *et al.* (1998) described efficiency optimization in vector control of induction motor drives. They suggested that in order to maintain maximum efficiency, the induction motor should operate at a constant slip. The function of the efficiency in terms of slip frequency is derived after considerable algebraic expression is given by:

$$\omega_{sl,opt} = \frac{1 - \sqrt{1 - 4(T_e)^2 d}}{2T_e c} \tag{2.64}$$

The slip frequency that result the maximum efficiency is determined by:

$$i_{s,opt} = \sqrt{T_e} \frac{\sqrt{X_{rr}}}{X_m} \sqrt{\frac{1}{\tau_r \omega_{sl,opt}} + \tau_r \omega_{sl,opt}} \tag{2.65}$$

Garcia *et al.* (1994) and Leindhold and Garcia (1998) described efficiency optimization in vector control induction motor drive. The focus of these papers is the minimization of the copper and core losses at steady state. The optimum torque current (I_d) for maximizing the efficiency is determined by differentiating the power losses function with respect to the torque current (I_d) and equalling it to zero. With M_d the mutual inductance between the stator and rotor of the induction motor equivalent circuit, the optimal torque current (I_d) for maximum efficiency is given by:

$$I_{d,opt} = I_q \sqrt{\frac{R_s(R_c + R_r) + R_c R_r}{R_s(R_c + R_r) + M_d^2 \omega^2}} \tag{2.66}$$

Bernal *et al.* (2000) proposed loss minimising control scheme for induction motors in vector control. With neglecting saturation and L_d is d-axis inductance, the optimal torque current (I_d) to achieve the minimum losses is given by:

$$I_{d,opt} = I_q \sqrt{\frac{(R_s + R_r)R_c + L_d^2\omega^2}{R_s R_c + L_d^2\omega^2}}$$

(2.67)

2.4.4   Search Controller Method

Search controller (SC) method also known as on-line efficiency optimization controller is a control technique based on the minimum input power tracking approach. The operation principle of the search controller is that the input power is first measured and then the motor flux function is gradually decreased to achieve the minimum input power associated to the minimum power losses or maximum efficiency.

2.4.4.1 Principle of a Search Controller Method

The philosophy of search controller is to minimize the motor drive input power by iterative adjustment of the motor flux or its equivalent variable command. The input power of the motor drive is a parabolic function of the flux, that has strictly positive second derivative with regime-dependent minimum that can be found by various search procedures (Sousa *et al.*, 1995; Kioskeridis and Margaris, 1996; Moreno *et al.*, 1997; Hasan *et al.*, 1997; Bose *et al.*, 1997; Vukosavic and Levi, 2003; Abdin *et al.*, 2003; Chakraborti and Hori, 2003 and Pryymak *et al.*, 2005).

Assume that the machine operates initially at rated flux in steady state with low load torque at a certain speed as indicated in Figure 2.8 (Cleland *et al.,* 1995).

P_{in} , T_q, ω_m
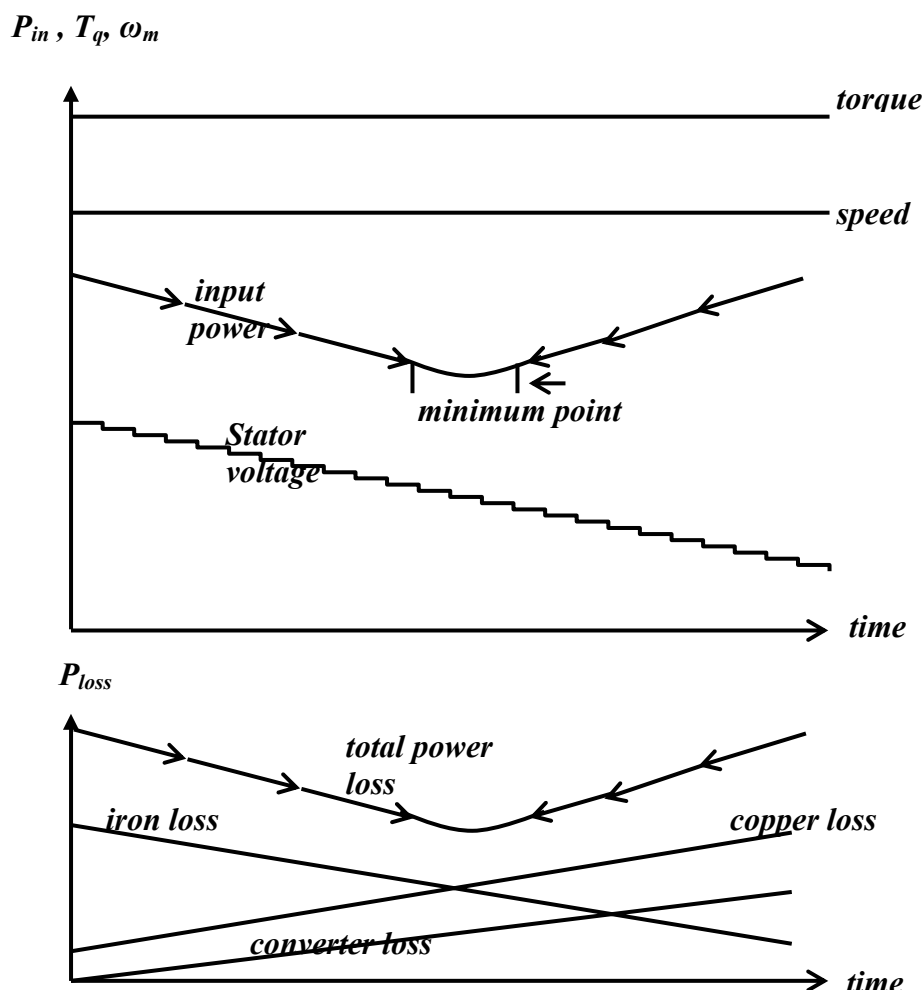
Figure 2.8: On-line search method of flux programming efficiency optimization control.

The motor flux is decreased gradually by reducing the stator voltage of the supply. As the core losses decrease with a decrease of flux, the copper losses increase but the total losses on the system decrease, hence the overall efficiency is improved. This is reflected in the decrease of the dc link power, as shown for the same output power.

Decreasing the stator voltage is continued until the system settled at the minimum input power, which means that the power losses become minimum and the efficiency become maximum. Any search attempt beyond minimum point adversely affects efficiency and forces the search direction such that operation always settles at minimum point.

This method has the advantage of the control not requiring knowledge of the motor parameters and it is universally applicable to any arbitrary machine.

An example of a block diagram of the search controller method of the induction motor drive that had been proposed by Kioskeridis and Margaris (1996) is given in Figure 2.9.
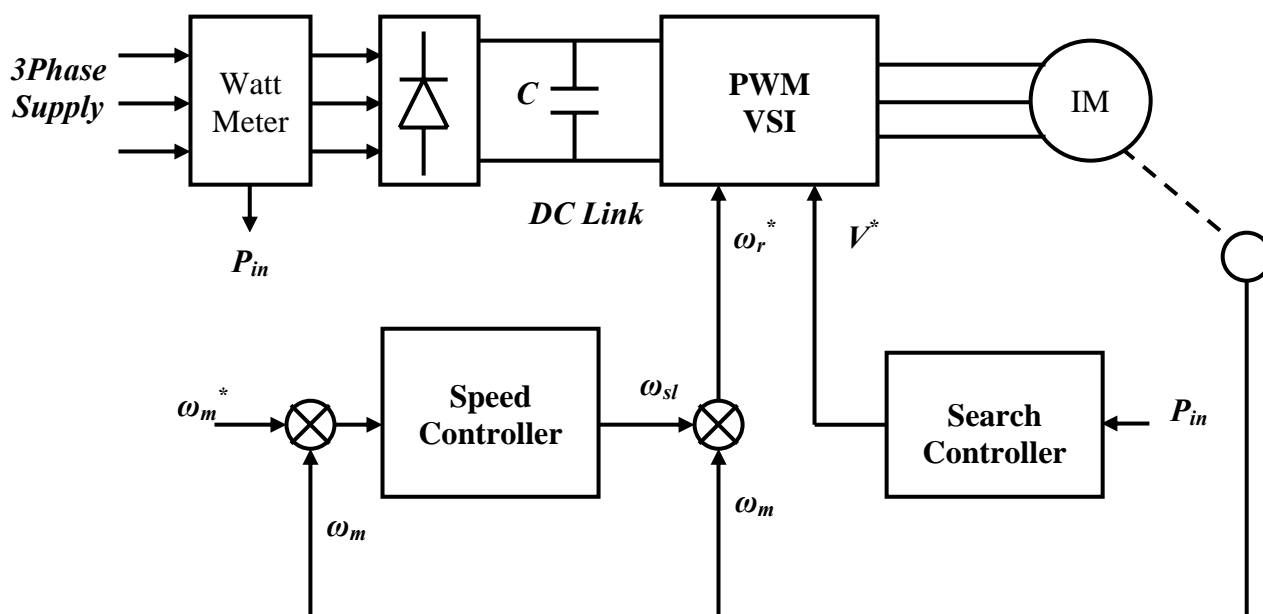
Figure 2.9: Block diagram of the search controller method of the induction motor drive

2.4.4.2 Previous Work on the Search Controller Method

Sul and Park (1988) proposed a technique that maximizes the efficiency by means of optimal slip in scalar control model. To find the optimal slip, a given torque-speed curve is automatically sectioned by the microprocessor according to the torque and speed. The optimal slip is first searched hence the minimum input power is achieved, and stored in the microprocessor memory as a lookup table. The controlled system is then forced to track the optimal slip given in the lookup table. The technique can be considered as an indirect way to minimize the input power.

Famouri and Cathey (1991) proposed an adaptive perturbing controller that minimizes the input power of a variable speed motor drive system on the scalar control model. A proportional-integral controller is developed to regulate the value of the stator voltage that adjusts the volt per hertz ratio. The subcontroller also added to control the inverter output frequency that obtains the motor speed.

Sousa *et al.* (1995) proposed the search controller on the vector control model by adaptively reducing the flux current reference compensator by the fuzzy logic controller. Input of the fuzzy logic controller is stator current and the output is the flux current reference compensator. The block diagram of the proposed fuzzy logic control is given in Figure 2.10.
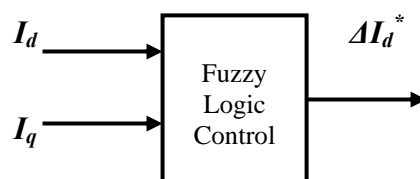
Figure 2.10: The block diagram of the fuzzy logic control scheme proposed by Sousa *et al.*

Huang and El-Sharkawi (1996) proposed the search controller in the scalar control model by adaptively obtaining the stator voltage per hertz ratio use fuzzy logic controller. Input of the fuzzy logic controller is the change of input power and volt per hertz ratio. The output is the new change of volt per hertz ratio. The block diagram of the fuzzy logic control of the proposed model is given in Figure 2.11.

$ΔP(k)$ → Fuzzy Logic Control → $ΔV/Hz(k)$

$ΔV/Hz(k-1)$ →
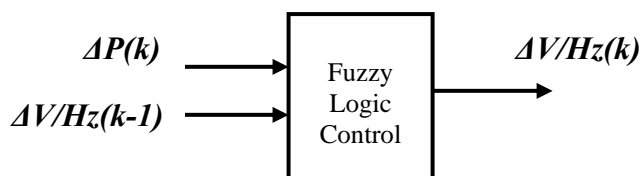
Figure 2.11: The block diagram of the fuzzy logic control scheme proposed by Huang and El-Sharkawi.

Cleland and Turner, (1996) proposed the search controller in the scalar control model by adaptively reducing the stator voltage reference with the use of a fuzzy logic controller. The torque pulsation problem is overcome with the help of feed-forward pulsating torque compensation. Input of the fuzzy logic controller is stator voltage and input power and the output is the voltage reference compensator. The block diagram of the fuzzy logic control of the proposed model is given in Figure 2.12.

$ΔV_s$ → Fuzzy Logic Control → $ΔV^*$

$ΔP_{in}{}^*$ →
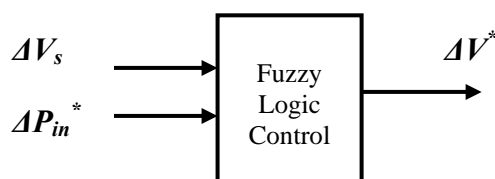
Figure 2.12: The block diagram of the fuzzy logic control scheme proposed by Cleland and Turner

Choy *et al*. in 1996 used a neural network to perform the search control. Based on the steady state induction motor model calculation, the neural network controller is trained in different operating points. The back propagation learning algorithm is employed. The neural controller consists of three layers, two neurons in the input layer and the output layer is slip speed reference. Input of the proposed controller consists of torque and speed of the motor. The network structure of the proposed efficiency optimization is given in Figure 2.13.
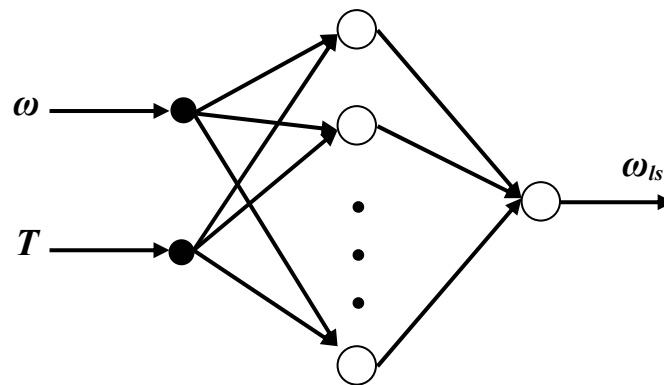
Figure 2.13: The structure of neural network-based efficency optimization control scheme proposed by Choy *et al*.

Hasan *et al.* in 1997 and Zang and Hasan (1999) used a neural network to perform the search controller function in the vector control induction motor drive system. Based on the steady state induction motor model, the motor power losses are calculated as a training data. The back propagation learning algorithm is employed to train the neural network controller in different operating point.

Their proposed neural control model has one input layer, two hidden layer and one output layer. The input layer consists of speed and load torque reference signals. The output layer has only one neuron for the magnetizing current. The first hidden layer has ten neurons and the second hidden layer has five neurons. The proposed network structure model is given in Figure 2.14.
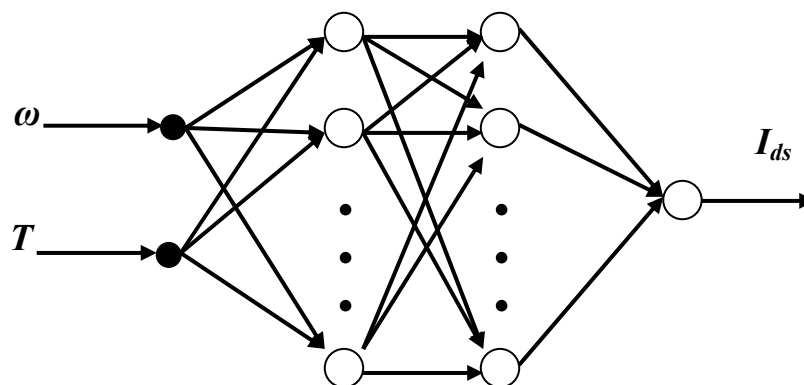
Figure 2.14: The structure of neural network-based efficency optimization control scheme proposed by Hasan *et al* .

Moreno *et al.* (1997) compare the different flux optimization algorithms to improve efficiency at steady state in a vector controlled induction motor drive. In this paper the conventional numeric search algorithm such a Rosenbrock, proportional, gradient, Fibonacci method and intelligent search fuzzy logic control is reviewed. The fuzzy logic control employed 14 rule based, with the error speed signal as an input. The block diagram of the proposed fuzzy logic control is given in Figure 2.15.
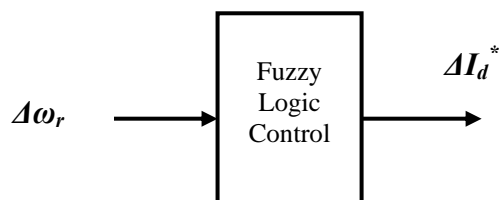
Figure 2.15: The block diagram of the fuzzy logic control scheme proposed by Moreno *et al*.

Bose *et al.* (1997) stated that the main advantage of using fuzzy control instead of classical search control scheme. The controller was implemented in a sensorless stator flux oriented vector control motor drive. However, it was the first time that search control was realized in sensorless drive. He proposed the input power and flux current error as an input of the controller. The block diagram of the fuzzy logic control is given in Figure 2.16.
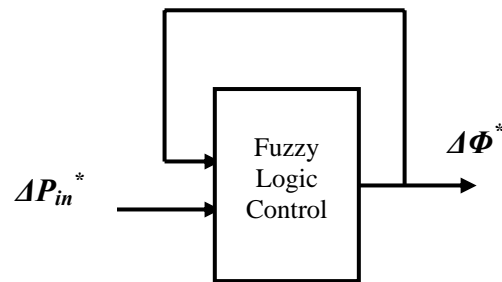
Figure 2.16: The block diagram of the fuzzy logic control scheme proposed by Bose *et al.*

Ta and Hori (2001) proposed a technique that maximizes the efficiency model in vector control for electrical vehicle load model. The optimal torque current reference is searched by golden section scheme. To limit torque pulsation by the stepwise decrease in the flux current, the low pass filter is added in the controller.

Chakraborty et al., (2002) and Chakraborty and Hori (2003) proposed a technique that maximizes the efficiency model in vector control by two steps. The optimal flux current reference is calculated based on the steady state loss model. The optimal flux current estimation employed is the same as that had been developed by Garcia *et al.* (1994) and Leindhold and Garcia (1998). In real-time application the optimal current flux reference is searched around the optimal current that has been determined by the LMC method. They claim that the convergence time can be reduced.

Pryymak *et al.* in 2005 used a neural network to perform the search controller in the vector control induction motor drive system. The difference to Hassan *et al.,* (1997) paper is that the changes of the resistance value due to temperature variation and the change of the inductances due to core saturation curves are considered in the power losses calculation.

Pryymak *et al.,* use the Levenberg-Marquardt learning algorithm, the neural network was trained with an off-line scheme. The neural controller consists of three layers, three neurons in the input layer and the output layer is the current flux reference. Input of the proposed controller consists of electromagnetic torque, rotor resistor and speed of the motor. However, they did not perform an experimental validation. The structure of the proposed controller is given in Figure 2.17.
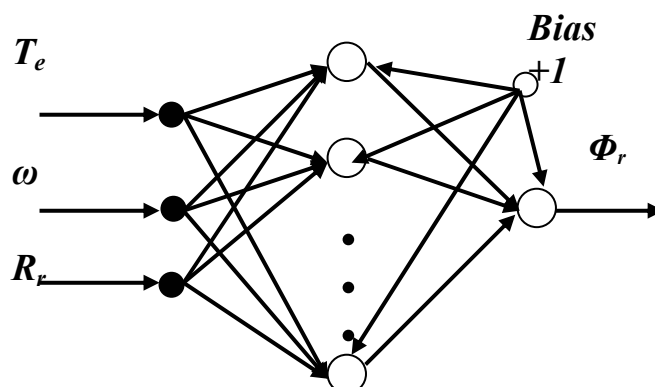
Figure 2.17: The structure of neural network-based efficiency optimization control scheme proposed by Pryymak *et al*.

2.5   Summary

The principle of the efficiency on the VSD mainly on the induction motor has been described. The review of the efficiency optimization control on VSD also has been reported. It is clear that the implementation of the efficiency optimization control is focused on minimizing the losses of the induction motor drive by controlling the motor flux function. The concept of efficiency optimization control has been described and shown that maintaining the flux of a motor is ideal to optimize the efficiency during speed and load variation.

The previous work on LMC method shows that the main advantage is simplificity of this method i.e. does not require extra hardware. However, it is mandatory that an accurate knowledge of motor parameters is known, which change considerably with temperature, saturation and skin effect. In real-time application, the difficulty in measuring the motor parameters of the loss model does not permit the implementation of the LMC (Sul and Park, 1988; Kioskeridis and Margaris, 1996; and Famouri and Cathey, 1991).

The previous works on the SC method show that to achieve optimal efficiency, the flux is decremented in steps until the measured input power for a certain load torque and speed condition settles down to the lowest value. This method does not require any knowledge of the motor parameters, is completely insensitive to motor parameter variation and the algorithm is applicable universally to any arbitrary drive (Bose *et al*., 1997).

CHAPTER 3

DEVELOPMENT OF A NEURAL NETWORK EFFICIENCY FOR EFFICIENCY OPTIMIZATION

3.1   Introduction

This chapter discusses the development of an efficiency optimization control technique of a variable speed compressor motor drive system. The prospective of adaptive neural-network on the search control method of the efficiency optimization control will be described first. Before proceeding to the detail of development of the adaptive neural network efficiency optimization controller scheme, it is essential to understand the concept of the on-line learning neural network controller strategy itself. Finally, the function of the proposed adaptive neural network controller for efficiency optimization of variable speed compressor motor drive is presented.

3.2   The Neural Network Perspective on the Efficiency Optimization Control Method

A linear control system with invariant plant parameters can be designed easily with classical design techniques, such as Nyquist and Bode plots. However in induction motor drive applications, where the parameters of the drive hardly remain constant, the performance of a conventional feedback controller is difficult to maintain. The effect of the parameters variations can be compensated to some extent

by a high-gain negative feedback loop, but excessive gain may cause an under-damping or instability problem (Bose, 2001).

The plant parameters variation require adaptation of the controller parameters in real-time known as adaptive control technique (Astrom and Wittenmark, 1995; Narendra and Annaswami, 1989; Mills *et al.*, 1996; Gupta and Sinha, 1996 and Lu, 1996). Generally, the adaptive control system can be thought of as having two loops. The first loop is a normal feedback based on the process and the other loop is the parameter or mechanism adjustment loop.

Referring to the previous works that have been described in the Chapter 2, Choy *et al.*, (1996); Hasan *et al.,* (1997); Zang and Hasan (1999) and Pryymak *et al.,* (2005) employees Neural Network Controller (NNC) to perform the search efficiency optimization control function. In these cases the neural network controller is trained off-line or through a batch learning algorithm. Initially, in training mode a model of the induction motor drive is developed to train the neural network in different operating points. In running mode, the controller is performed by the neural network alone.

The development of the neural network controller for the efficiency optimization control produce good results, however these developments are still limited to simulation work or off-line learning experimental work. Therefore its real-time application, with the induction motor parameters not constant, the performance of the off-line learning neural network controller is doubted (Abrahamsen, 2000).

Based on the reason mentioned, to successfully implement neural network controller of the efficiency optimization control of a variable speed compressor motor drive, a real-time or on-line learning algorithm of the neural network controller known as adaptive neural network control is proposed.

3.3   Concept of a Neural Network Control

Inspired by the successful function of the human brains, the Artificial Neural Network (ANN) was developed for solving many large scale and complex problems. The need to meet demanding control requirements in increasingly complex dynamical control systems under significant uncertainty makes the use of Neural Networks in control systems very attractive (Widrow and Lehr, 1990).

The main reasons behind this are their ability to learn to approximate functions and classify patterns and their potential for massively parallel hardware implementation. Beside that, development of on-line/real-time learning technique, makes the controller become adaptive and robust to the dynamic plant system or known as adaptive neural network controller (Narendra and Annaswami, 1989; Mills *et la.*, 1996 and Gupta and Sinha, 1996).

Neural networks consist of many simple computational elements called nodes or neurons each of which collects the signals from other nodes which are connected to it directionally. Among the neurons are connected by weighted links passing signals from one neuron to another. The architecture of these models is specified by:

1. Neuron/node characteristics,
2. Network topology and
3. Learning algorithm.

3.3.1   Structure of the Neuron

The basic processing element of the connectionist architecture is often called neuron by analogy with neurophysiology. Other names such as Perceptron by Rosenblatt in 1958 or Adaline by Widrow and Hoff in 1960 are also used. Neurons in artificial neural networks are very simple processors inspired by their biological counterparts.

The basic model of a neuron is illustrated in Figure 3.1 (Haykin, 1994). The neuron is composed of three components:

1. A set of synapses or connecting links, each of which is characterized by a weight or strength of its own.
2. A weight summer or an adder for summing the input signals, weighed by the respective synapses of the neuron. The operations could constitute a linear combiner.
3. A non dynamical, nonlinear function which is also called activation function, use for limiting the amplitude of the output of a neuron
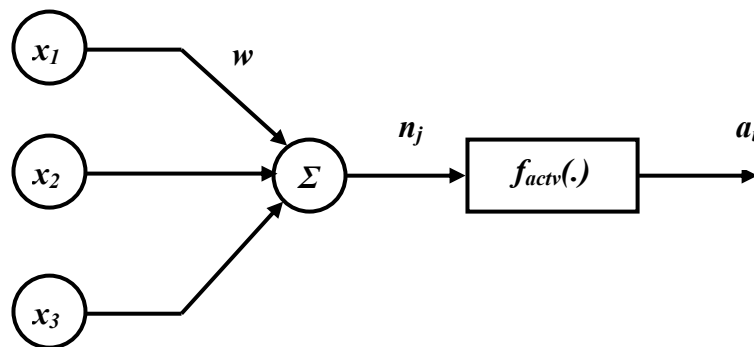
Figure 3.1: Basic model of neuron

From a functional point of view, a unit is simply an active element with some number of inputs and only one output. Equation of the weighted summer is given by:

$$n_j(t) = \sum_{i=0}^{I} w_i x_i(t) \tag{3.1}$$

where: n_j : neuron transfer function

      x_i : the neuron inputs

      w_i : the weight connection

      t : the time variable.

The matrix form of the Equation (3.1) can be written as follow:

$$n_j(t) = WX(t) \tag{3.2}$$

According to Figure 3.1, after the input mapping, the neuron produces an output using an activation function. This activation function transforms the value produced by the input mapping to a value which is suitable for another neuron. The nonlinear function f_{actv} is an activation function gives the signal a_i in the term of the output $n_j(t)$ is given by:

$$a_i = f_{actv}(n_j(t)) \tag{3.3}$$

where: f_{actv} : the activation function

      a_i : the neuron output.

The activation function of a bipolar neuron generates both positive and negative output, while the unipolar ones generate only positive values (Cirstea *et al.*, 2002). Depending on the type of the neuron, the activation function has several forms as given in the following function.

1. Linear:

    the simplest of the activation functions is a linear mapping from input to output defined by:

$$f_{actv}(n_j) = n_j \tag{3.4}$$

The gradient of the linear activation function is given by:

$$\frac{\partial f_{actv}(n_j)}{\partial n_j} = 1 \tag{3.5}$$

2. Sigmoid:

the sigmoid activation function is a bipolar function and defined as:

$$f_{actv}(n_j) = sig(n_j)$$

$$= \frac{1}{1 + \exp^{-n_j}} \tag{3.6}$$

Derivative of the sigmoid activation function is given by (Spooner *et al.*, 2002):

$$\frac{\partial f_{actv}(n_j)}{\partial n_j} = \left(1 - f_{actv}(n_j)\right) f_{actv}(n_j) \tag{3.7}$$

3. Hyperbolic Tangent:

the hyperbolic tangent activation function is a unipolar function and defined as:

$$f_{actv}(n_j) = \tanh(n_j)$$

$$= \frac{1 - \exp^{-n_j}}{1 + \exp^{-n_j}} \tag{3.8}$$

Derivative of the hyperbolic tangent activation function is given by (Spooner *et al.*, 2002):

$$\frac{\partial f_{actv}(n_j)}{\partial n_j} = 1 - \left(f_{actv}(n_j)\right)^2 \tag{3.9}$$

3.3.2   The Network Architecture

The neural network also can be viewed as a weighted directed graph in which artificial neurons are nodes and directed weighted edges represent connections between neurons. Local groups of neuron can be connected in either (Leondes, 2003):

1. A feed-forward architecture and
2. A recurrent architecture.

3.3.2.1 Feed-Forward Neural Network Architecture

Architecture of the feed-forward can be represented by a direct acycli graf as given in Figure 3.2. Each neuron is connected only to neurons in the next layer and there is no connection between neurons in the same layer.
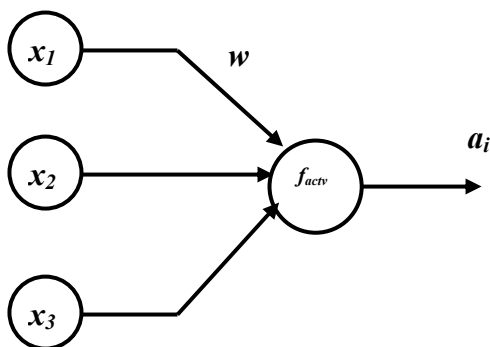
Figure 3.2: A single layer feed-forward neural network

3.3.2.2 Recurrent Neural Network Architecture

The recurrent neural network distinguishes itself from a feedforward neural networks in that it has at least one feedback loop. It so that the output of the neuron can be fed back to the inputs of other neurons in the same or previous layers as shown in Figure 3.3.
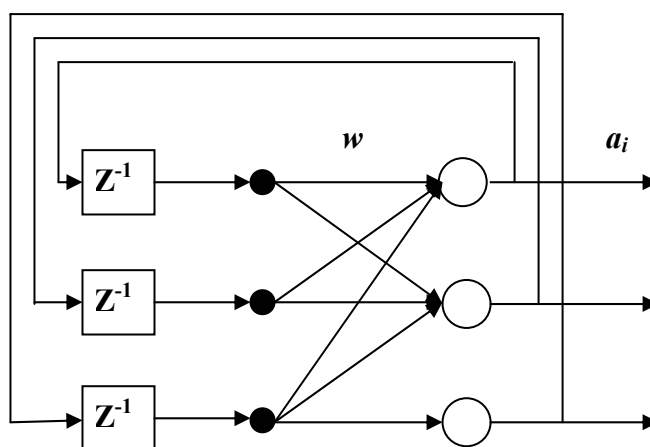
Figure 3.3: A single layer recurrent neural network

The feedback loop presents involve the use of particular braches composed of unit-delay elements denoted by Z^1, which causing the network to display a non-linear dynamic behaviour (Haykin, 1994).

3.3.3 Learning in the Neural Networks

A neural network has to be configured such that the application of a set of inputs produces the desired set of outputs. Various methods to set the strengths of the connections exist. One way is to set the weights explicitly, using by knowledge. Another way is to train the neural network by feeding it teaching patterns and letting it change its weights according to some learning rule. There are two kinds of well known learning rules in neural network training, i.e. supervised learning rule and unsupervised learning rule.

Principle of the supervised neural network system is given in the following section.

3.3.3.1 Supervised Learning Model

An essential ingredient of supervised learning is the availability of an external teacher, as indicated in the arrangement of Figure 3.4 (Haykin, 1994).
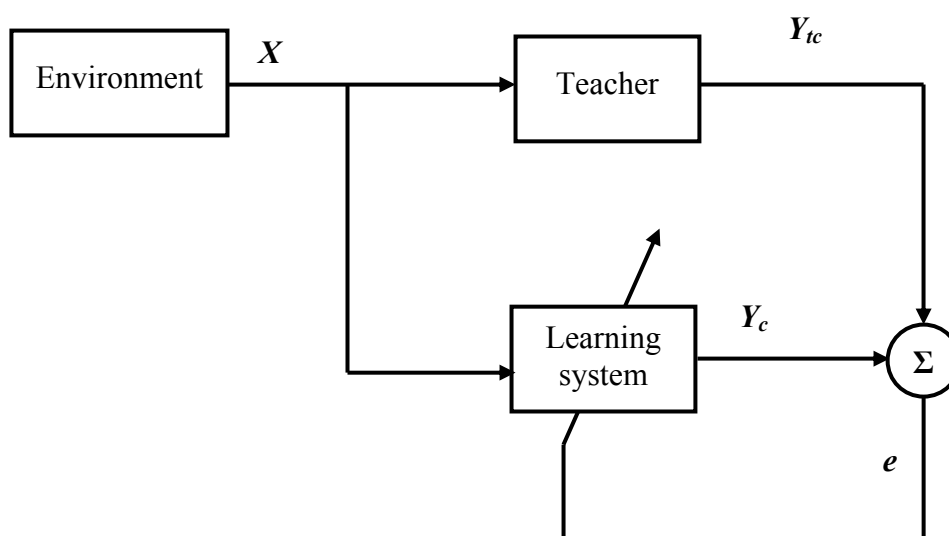
Figure 3.4: Block diagram of supervised learning

The learning feedback or driving force in supervised learning is the error (**e**) between the model's output (**Y_c**) and the system teaching patterns (**Y_{tc}**). Training consists of presenting input and output data to the network. This data is often referred to as the training set. During the training of a network the same set of data is processed many times as the connection weights are ever refined. Then the network parameters are modified according to the particular correction method depending on the learning low algorithm.

Supervised learning can be performed in an off-line or on-line scheme. The function of learning in the neural controller is to automatically adjust the parameters of the controller to provide a satisfactory or desired control response (Lu, 1996, Omatu *et al.*, 1996 and Vas, 1999). As a result of learning, the system response or behaviors can be consistently improved even when the system environment is significantly disturbed.

The off-line learning scheme is also called batch learning. In this scheme, a separate computational facility is used to design the supervised learning system. Once the desired performance is accomplished, the design is frozen, which means that the neural network operates in a static operation.

The on-line learning scheme also called as real-time learning. In the on-line learning the learning procedure is implemented solely within the system itself, not requiring a separate computational facility. During the running process the network parameters of the controller are updated continuously. This mode the updating is performed successively on each partial error function associated with one given pattern in the training data.

3.3.3.2 Neural Networks Performance index

The ultimate propose of the training process in the neural network controller is to minimize the performance index of the network. A criterion commonly used for the performance index is the Mean-Square Error (MSE) criterion. For single data pair that be used in the on-line learning, the performance index function is defined by:

$$F(x) = \frac{1}{2} e^T e \tag{3.10}$$

where: $F()$: the neural network performance index function

e : controller error signal

The error signal of the controller is given by:

$$e = D_c - Y_c \qquad\qquad (3.11)$$

where: Y_c : actual response signal

        D_c : desire response signal

The function of the performance index is also known as error surface neural network function or neural network cost function.

In a linear function model, the general error surface function is given in parabolic function, which means that it is smooth bowl-shape with single minimum value. However in the neural network, the error surface function is much more complex. It is characterized by an unhelpful feature such as local minima point. The local minima point is lower than the surrounding terrain, but above the minimum global.

3.3.3.3 Neural Network Learning Laws

In the learning process there are several schemes that can be used to update the network parameters. The back propagation algorithm developed by Rumelhart et al in 1985, is a first order iterative gradient search algorithm designed to minimize the mean square error between the actual output a multilayer feedforward network and the desired output (Leondes, 2003). This scheme is based on a linear approximation of the neural network performance index given by:

$$F(x + \Delta x) = F(x) + \left(\nabla F(x)\right)^T \Delta x \qquad\qquad (3.12)$$

The weight update is given by:

$$\Delta x = -\alpha \frac{\partial F(x)}{\partial x}$$ (3.13)

Where: α : the learning rate or step size.

The second order learning algorithm is motivated by the desire to accelerate the typical slow convergence associated with the back propagation method (Hagan and Menhaj, 1994). The neural network performance index of the basic second order learning algorithm approximation is given by:

$$F(x + \Delta x) = F(x) + \left(\nabla F(x)\right)^T \Delta x + \frac{1}{2}\Delta x^T \nabla^2 F(x)\Delta x$$ (3.14)

The weight update is given by:

$$\Delta x = -\left(\nabla^2 F(x)\right)^{-1} \nabla F(x)$$ (3.15)

3.3.4   Multi Layer Perceptron

The Multilayer Perceptron (MLP) is a network model in which the neurons are configured in layers, whereby the neurons of a layer are generally all connected with the neurons of the following layer. This network is able to process analogue input patterns and learns in supervised mode, employing the back-propagation algorithm.

In a multilayered neural network, the zero or lower is called input layer consists of input neurons. The last or upper is called output layer which is composed

of output neurons. The remaining, so called hidden or intermediate layers contain hidden neurons.

According to Haykin (1994), a multilayer perceptron has three distinctive characteristics:

- The model of each neuron in the network includes a non-linearity at the output end.
- The network contains one or more layers of hidden neurons that are not part of the input or output of the network.
- The network exhibits a high degree of connectivity, determined by the synapses of the networks.

The Multilayered Perceptron is a natural extension to the single layer perceptrons that were very popular in the 1960's. These multi-layered perceptrons are able to overcome the severe limitation of its single layer predecessor. This plus the availability of several learning algorithms for finding suitable weights and thresholds or biases have made multilayered perceptrons widely popular.

Figure 3.5 shows the multilayer neural network with single hidden layer. The notation employed in the figure can be described which includes: X_i, a_j, Y_k, $W_{i,j}$ and $W_{j,k}$ representing the input unit vector, hidden unit vector, output unit vector, weights (including bias) between input layer and hidden layer, and weights (including bias) between hidden layer and input layer respectively.
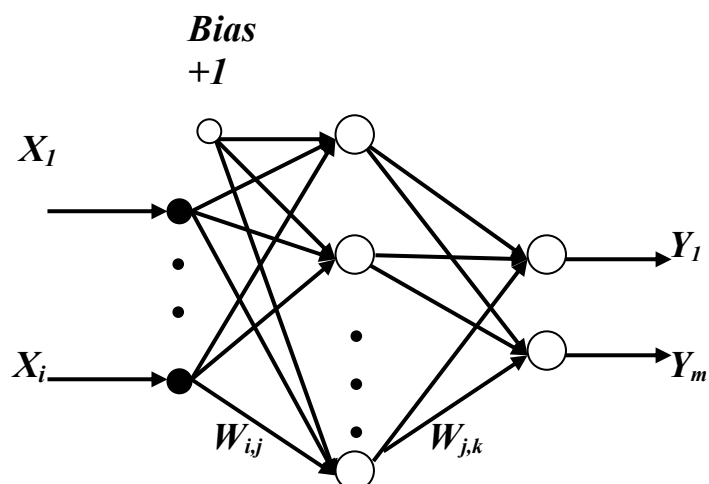
Figure 3.5: Architecture of multi layer perceptron with one hidden layer

The input layer has l neurons that receive real valued in the form of an l-dimensional vector in X^l. This layer also includes an additional bias neuron. Similarly, the hidden layer has p neurons that receive signal from the input layer. A bias neuron has been additionally included in the hidden layer to generate a +1 signal for bias connections of the output layer neurons. The output layer comprises m neurons.

Finally, the network signals that emanate from the last layer of neurons comprise a m-dimensional vector of real numbers. The neural network thus maps a point in X^l (the input) to a point in Y^m (the output).

According to Haykin (1994), a single hidden layer is optimum in the sense of learning time and ease of implementation.

3.3.5   Neural Network Control Scheme

In comparison with other control paradigms, the neural controllers have certain advantages such as they are able to learn in real-time and able to represent almost any nonlinear relationship between control variables and system output (Narendra and Parthasarathy, 1990; Cabrera and Narendra, 1999; Vas, 1999 and Leondes, 2003).

Architecture of the neural controller can be classified into several types such as direct inverse neural network control, direct adaptive neural network control reference model and indirect neural network control reference model (Omatu *et al.,* 1996, Vas, 1999 and Bose, 2001). Figure 3.6 shows the schematic of the direct inverse neural network controller.
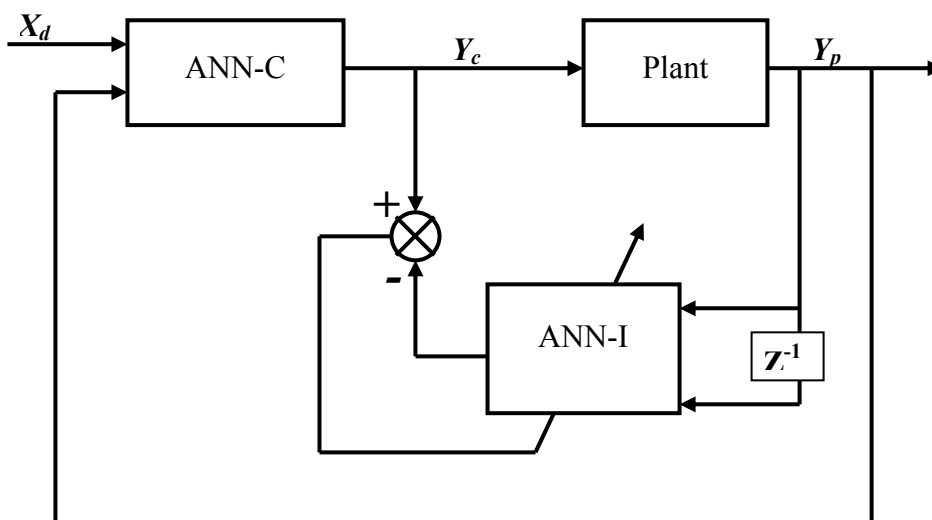
Figure 3.6: Block diagram of the direct inverse neural network control.

The direct inverse neural network controller utilizes the plant inverse model. Initially, the inverse model of the plant is obtained by using an Artificial Neural Network Identifier (ANN-I) and this is simply cascaded with the controller plant. The input of the artificial neural network controller (ANN-C) is the reference signal X_d and also the actual output plant Y_p and the output of the ANN-C is the control action Y_c.

In the direct adaptive neural network control model, the parameters of the controller are directly synthesized from the error between the desired and actual output plant responses. In this model the adaptation mechanism is designed to adjust the approximator causing it to match some unknown nonlinear controller that make the closed-loop system achieve its performance objective. Configuration of the direct adaptive neural control reference model is shown in Figure 3.7.
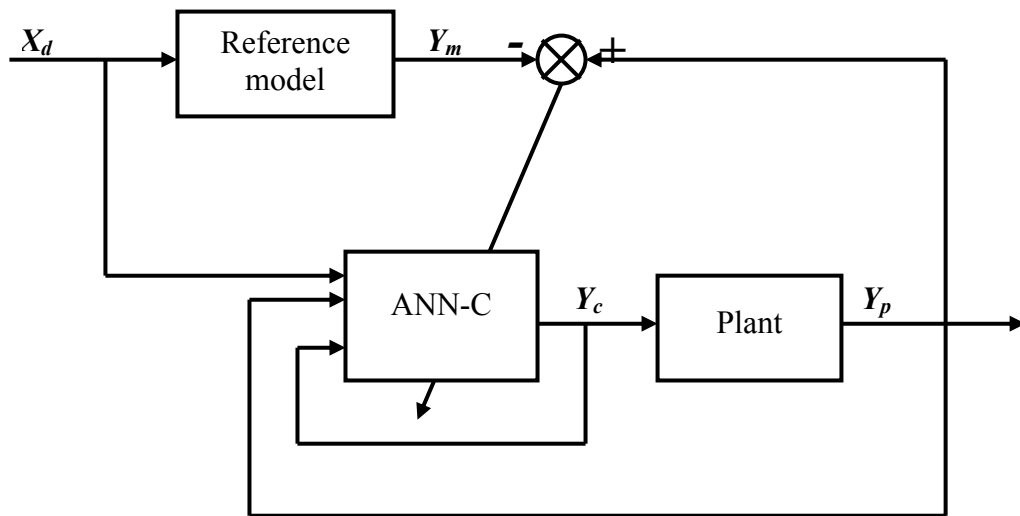
Figure 3.7: Block diagram of the direct adaptive neural control reference model.

The indirect direct adaptive neural control reference model, first an identification scheme is employed to estimate a parametric model of the plant from input-output data, and then the controller parameter are adjusted by assuming that the identified model represents the true pant parameters. Figure 3.8 shows the schematic of the indirect adaptive neural control reference model.
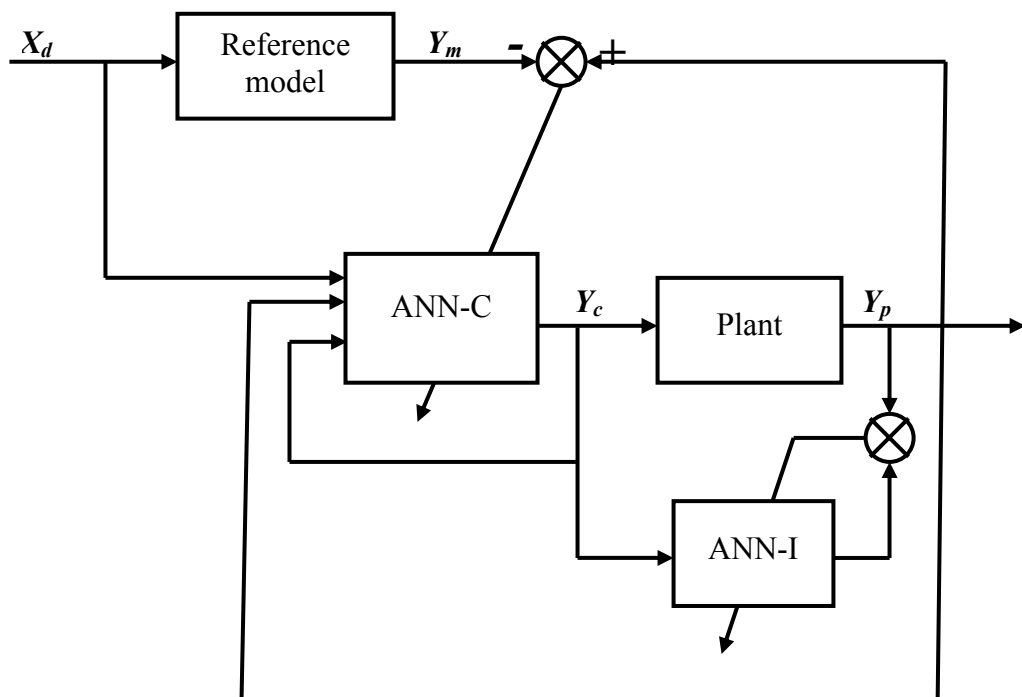
Figure 3.8: Block diagram of the indirect adaptive neural control reference model.

3.4   Development of the Proposed Neural Network Efficiency Optimization Control

Before proceeding to the detail development of the proposed neural network efficiency optimization controller, the practical issues of design and implementation of the ANN controller is described.

3.4.1   Neural Network Controller Design Issue

They are several types of important and practical issues in the design and implementation of the ANN controller. Basically these issues can be grouped in to two categories (Omatu *et al.,* 1996 and Leondes, 2003) i.e.: appropriate design of neural network architecture and the other is related to the improvement of learning efficiency.

3.4.1.1 Appropriate Design of Neural Network Architecture.

Determining the number of neurons in each hidden layer and the number of hidden layers is a critical decision in the design of neural network. As mentioned earlier, the ANN is essentially a nonlinear mapping function *f(x,w)* with *x* as input and *w* as parameter set.

Increasing the number of hidden neurons enhances its ability to approximate input-output data patters, but also increase the number of free parameters. This increases model complexity. In fact a basic issue in designing ANN is proper balance of model complexity and approximation ability.

Unfortunately there is no clear guideline for determining the number of neurons in the hidden layers. However, enough neurons must be provided to enable the network to perform the required mapping function satisfactorily (Haykin,1994).

Haykin (1994) proposed heuristic rule for characterizing the relationship between the number of structural parameters of a neural network, the size of training or validation data set, and desired error goal call as resampling approach. With this approach, several networks of different number of hidden neurons and or different number of hidden layers are created, and trained with same set of data points. The approximation errors are collected. The networks are then tested with a different set of data through cross-validation to obtain generalization error. The best network architecture is determined by comparing and making trade-off between the approximation error and the validation error.

3.4.1.2 Improvement of Learning Efficiency.

For many practical problems, simple backpropagation training takes a very long time due to the nature of gradient descent (Hagan *et al.*, 1995) and (Haykin, 1994). This algorithm is insensitive to the local shape of performance function (error surface) due to a fixed learning rate.

Determination of the learning rate coefficient is a difficult task. A large learning rate often causes the learning steps bouncing between the opposite sides of a deep valley instead of following the contour to reach the bottom (a local minimum). On other hand, a small learning rate results in a very slow convergence on a relatively flat surface.

A nonlinear network usually has many local minima on its error surface. Pure gradient descent search is easily trapped by these local minima. The convergence to a global minimum is not guaranteed. To address these issues and improve the simple backpropagation algorithm, several techniques can be used such as:

- Adaptive learning rate (Bahera *at al.*, 2006)

- Second order optimization method (Hagan and Menhaj, 1994; Wilamowski *et al.*, 1999; Wilamowski *et al.*, 2001; Ampazis and Perantonis, 2002 and Wilamowski, 2003).

3.4.2 The Proposed Neural Network Controller Design

Figure 3.9 shows a block diagram of the conventional scalar control model constant volt per hertz (V/f). In this scheme, the controller generates the slip frequency reference signal $\omega_{sl}{}^*$. The voltage reference signal is generated from a look up table voltage reference signal generator block (Murphy and Turnbull, 1988).
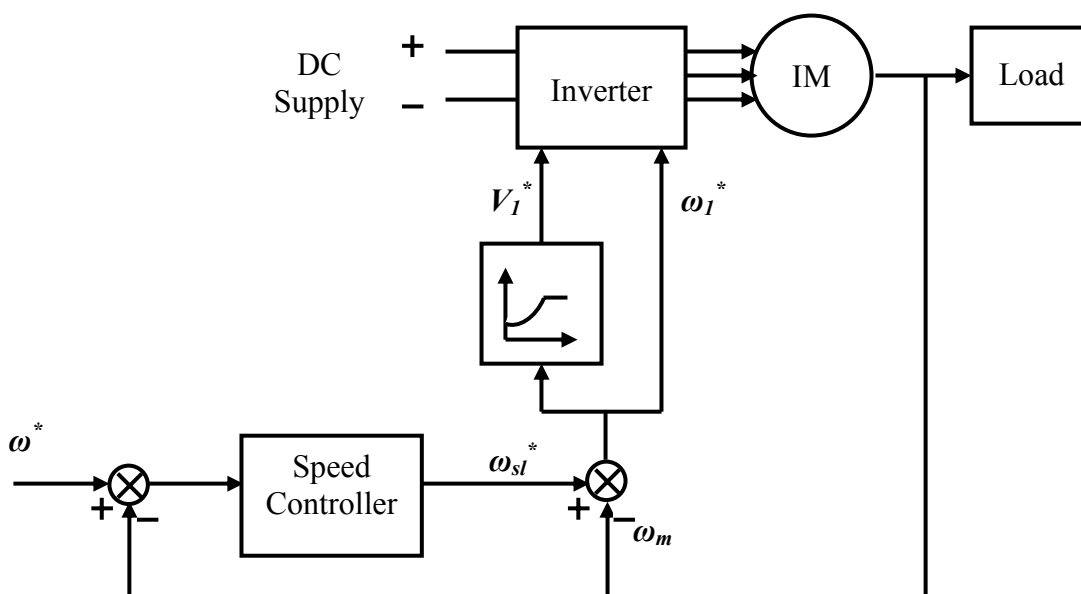
Figure 3.9: The block diagram of scalar constant volt/hertz with slip regulation

In this thesis, a direct feedback adaptive neural network controller for efficiency optimization of the variable speed compressor motor drive is proposed. In this scheme the controller receives the system observed output variables and then provides its control action to the controlled system environment to optimize the control criterion through real-time information processing. The block diagram of the proposed method is shown in figure 3.10.
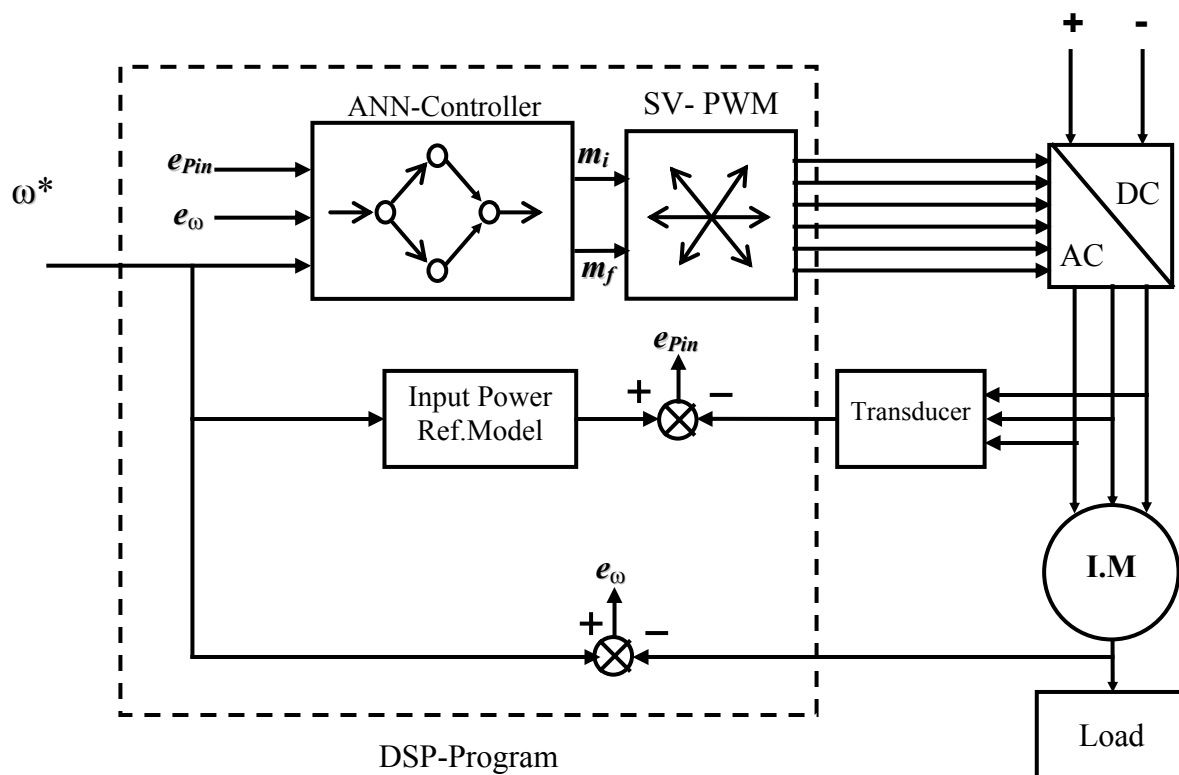
Figure 3.10: The block diagram of the proposed neural network efficiency optimization control

The proposed controller generates both of the voltage and frequency reference signal simultaneously. The difference of this with the methods discussed in chapter 2 is that they only generate the voltage reference signal and the frequency reference signal is generated by the other controller which is assumed ideal. By this strategy the efficiency of the motor drive can be increased and the performance of the speed also can be maintained simultaneously.

To control both of the reference signals simultaneously, a neural network control with multi output and learning algorithm is developed. The controller will receive three input signal i.e. the speed reference signal (w^*), error speed signal (w^* - w) and error input power signal (P_{ref}^* - P_{in}). The output of the controller that consist of stator voltage reference signal or modulation index ($V_s^* = m_i$) and frequency

reference signal or modulation frequency ($f^* = m_f$) is fed to the space vector PWM modulator.

In this scheme the input power reference model (P_{ref}^*) block is determined as follows. With the load torque characteristic of the compressor assumed proportional to the square of the speed as given by:

$$T_{load} = k_L N^2 \qquad (3.16)$$

Where: T_{load} : compressor load torque

   k_L : load torque coefficient

   N : motor speed=compressor speed

The power of the compressor as a mechanical motor load with friction and windage are not considered can be defined as (Shepherd *et al.*, 1995) :

$$P_{load} = T_{load} N \qquad (3.17)$$

$$P_{load} = (k_L N^2)N$$

$$= k_L N^3 \qquad (3.18)$$

where: P_{load} : compressor load power

If efficiency of the motor drive is targeted with the efficiency at nominal speed (η_{nom}) for all speed operation, the input power reference model can be defined as:

$$P_{ref}^* = \frac{P_{load}}{\eta_{nom}} \qquad (3.19)$$

$$P^*_{ref} = \frac{k_L N^3}{\eta_{nom}}$$ (3.20)

Where: P^*_{ref} : the input power motor reference.

η_{nom} : the nominal motor efficient.

3.4.2.1 Neural Network Efficiency Optimization Control Structure

In the present research, a new structure of neural-network efficiency optimization control is developed. The idea is based on the theory of a scalar control constant volt per hertz, where the frequency reference signal output is feedforward to the voltage reference signal generator block that have been described in chapter 2. Referring to this concept, in this network structure one of the output neuron in the last layer will be set as the frequency reference signal and fed back to the network to generate the voltage reference signal.

Basically, to design the neural network controller, the number of inputs and outputs neuron at each layer are equal to the number of input and output signals of the system respectively. Further the number of hidden layers and the total neurons is depended on the complexity of the system and the required training accuracy. Based on the type of the task to be performed, the structure of the proposed neural network controller is shown in Figure 3.11.
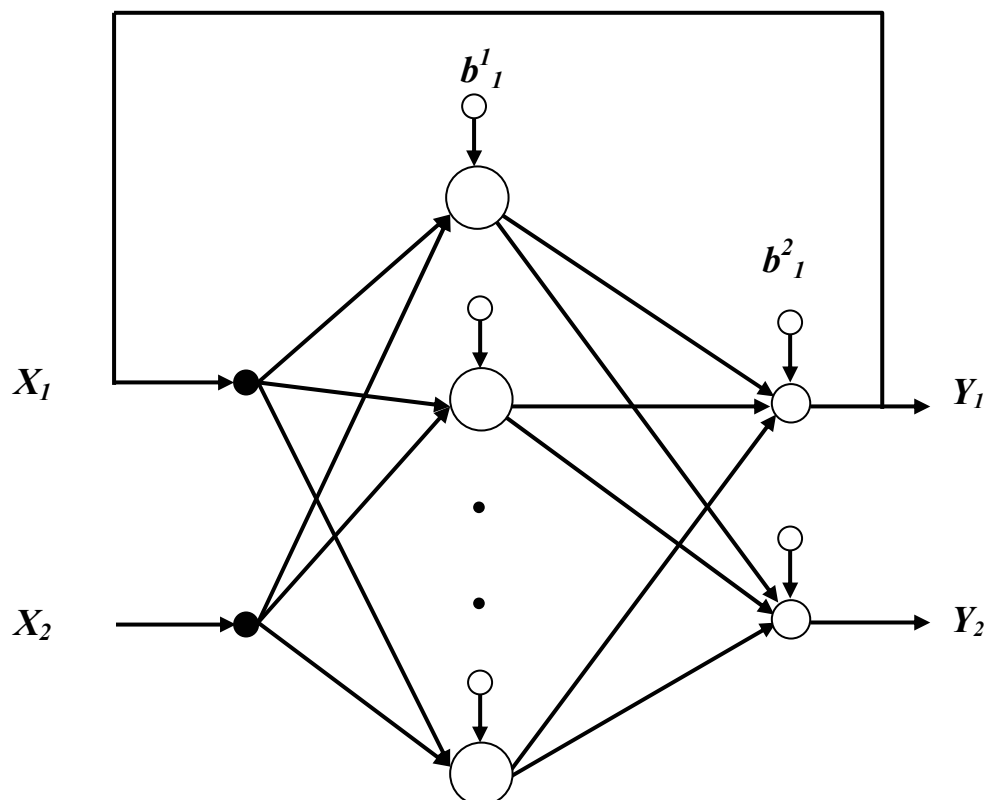
Figure 3.11: Architecture of the neural network efficiency optimization control

The structure of the neural network controller consists of three layers. Based on the neuron number in each layer this structure is known as 2-6-2 network structure. The first layer is the input, which consists of two input signals X_1 and X_2. X_1 received signal from the speed reference or speed command w^*, while X_2 received signal from the output layer Y_1 as a feed back loop or recurrent structure model.

In order to let the neural network interface with the real-world environment, a normalization of the input value is required. With the min-max approach the input signal of the controller is normalized by equation:

$$X_{nor} = \frac{\left(X_{nor}^{max} - X_{nor}^{min}\right)\left(X_{in} - X_{in}^{max}\right)}{\left(X_{in}^{max} - X_{in}^{min}\right)} + X_{in}^{min} \tag{3.21}$$

Where: X_{nor} : normalized input value

X_{in} : input value

X_{nor}^{max} : maximal normalized input value

X_{nor}^{min} : minimal normalized input value

X_{in}^{max} : maximal input value

X_{in}^{min} : manimal input value

By using in-start model, each of the neuron signals in the input layer is feedforward to all neurons in the hidden layer via the weight connections between the input and the hidden layers. The connections weight between neuron i and j in the j_{th} neuron at m_{th} layer respectively are represented by w^m_{ji}.

The second layer also known as hidden layer consists of six neurons a^1_1, a^1_2, .. a^1_6 respectively. Besides receiving signal from input layer, it also receives the bias signal. A transfer function of the neuron in the hidden layer at the j_{th} neuron is defined by:

$$n_j^1 = \sum_{i=1}^{n} w_{j,i}^1 X_i + b_j^1 \tag{3.22}$$

Where: $\boldsymbol{n_j^1}$: neuron transfer function in hidden layer

       X_i : input value that has been normalized

       $\boldsymbol{w_{j,i}^1}$: weight connection parameter value between input layer to hidden layer

       $\boldsymbol{b_j^1}$: bias parameter value in hidden layer

At the hidden layer the tangent hyperbolic activation function (Equation 3.8) are employed. The neuron output function in this layer is given by:

$$a_i^1 = \frac{1 - \exp^{-n_j^1}}{1 + \exp^{-n_j^1}} \tag{3.23}$$

The output layer consist of two neurons, the first neuron is used as a reference signal frequency ($\boldsymbol{Y_1 = f^*}$) and the second neuron is used as a reference signal voltage ($\boldsymbol{Y_2 = V_s^*}$). The activation function employed in this layer is known as the linear activation function (Equation 3.4). The neuron output function in this layer is used as an output variable as given by:

$$n_j^2 = \sum_{i=1}^{n} w_{j,i}^2 a_i^1 + b_j^2 \tag{3.24}$$

$$Y_j = n_j^2 \tag{3.25}$$

In order to let the neural network interface with the real-word environment, a denormalization of the output controller value is required. With the min-max approach the output signal of the controller is denormalized by:

$$Y_{den} = \frac{\left(Y_{den}^{max} - Y_{den}^{min}\right)\left(Y_{out} - Y_{out}^{max}\right)}{\left(Y_{out}^{max} - Y_{out}^{min}\right)} + Y_{out}^{min} \tag{3.26}$$

where: Y_{den} : normalized output value

      Y_{out} : output value

      Y_{den}^{max} : maximal normalized output value

      Y_{den}^{min} : minimal normalized output value

      Y_{out}^{max} : maximal output value

      Y_{out}^{min} : manimal output value

3.4.2.2 Levenberg-Marquardt Optimization

After the neural network architecture is developed, the next stage of the neural network control design is to determine the learning algorithm for updating the network parameters. The learning process will update the network parameter to optimize performance of the network. Generally, to define the network parameters, a sufficient training of the input-output mapping data of the plant is required. By this technique, the neural network controller is able to know the characteristics of the plant, hence the control signal can be defined accurately.

The learning algorithm of the Levenberg-Marquardt for the multilayer network is described as follows.

If the performance index of the network is represented by **F(x)**, where **x** is the scalar parameter of the network, the second order Taylor series expansion at nominal point x^* is given by:

$$F(x) = F(x^*) + \frac{d}{dx} F(x) \Big|_{x=x*} (x - x^*)$$
$$+ \frac{1}{2} \frac{d^2}{dx^2} F(x) \Big|_{x=x*} (x - x^*)^2 \tag{3.27}$$

Because the network parameters consist of many variables, it is more convenient to write in matrix form as given.

$$F(x) = F(x^*) + \nabla F(x)^T \Big|_{x=x*} (x - x^*)$$
$$+ \frac{1}{2} (x - x^*)^T \nabla^2 F(x) \Big|_{x=x*} (x - x^*) \tag{3.28}$$

where $\nabla F(x)$ is the gradient of the performance index, and is defined:

$$\nabla F(x) = \left[\frac{\partial}{\partial x_1} F(x) \frac{\partial}{\partial x_2} F(x) \dots \frac{\partial}{\partial x_n} F(x) \right]^T \tag{3.29}$$

and $\nabla^2 F(x)$ is the Hessian, and is defined as:

$$\nabla^2 F(x) = \begin{bmatrix} \frac{\partial^2}{\partial x_1^2} F(x) \frac{\partial^2}{\partial x_1 \partial x_2} F(x) \dots \frac{\partial^2}{\partial x_1 \partial x_n} F(x) \\ \frac{\partial^2}{\partial x_1 \partial x_2} F(x) \frac{\partial^2}{\partial x_2^2} F(x) \dots \frac{\partial^2}{\partial x_2 \partial x_n} F(x) \\ M \quad\quad M \quad\quad M \\ \frac{\partial^2}{\partial x_1 \partial x_n} F(x) \frac{\partial^2}{\partial x_2 \partial x_n} F(x) \dots \frac{\partial^2}{\partial x_n^n} F(x) \end{bmatrix}^T \tag{3.30}$$

To analyze the gradient and Hessian matrixes of the performance index, the general form of the quadratic function is given:

$$F(x) = \frac{1}{2}x^T Ax + d^T x + c \qquad (3.31)$$

Based on the properties of gradient matrix equation as given by:

$$\nabla(h^T x) = \nabla(x^T h) = h \qquad (3.32)$$

$$\nabla x^T Qx = Qx + Q^T x = 2Qx \qquad (3.33)$$

where: h : a constant vector.

The gradient of Equation (3.31) can be written as follow:

$$\nabla F(x) = Ax + d \qquad (3.34)$$

where A is the Hessian of the $F(x)$ given by:

$$A = \nabla^2 F(x) \qquad (3.35)$$

Therefore for the quadratic function, the Taylor series expansion for x_{k+1} can be defined by:

$$F(x_{k+1}) = F(x_k + \Delta x_k) \approx F(x_k) + g_k^T \Delta x_k + \frac{1}{2}\Delta x_k^T A_k x_k \qquad (3.36)$$

where g_k is the gradient of $F(x_k)$ and can be defined as:

$$g_k \equiv \nabla F(x)\big|_{x=x_k} \qquad (3.37)$$

The gradient of this quadratic function with respect to $\mathbf{\Delta x_k}$ and setting it to zero is given by:

$$g_k + A_k \Delta x_k = 0 \tag{3.38}$$

The equation (3.38) can be solved as follows:

$$\Delta x_k = -A_k^{-1} g_k \tag{3.39}$$

$$x_{k+1} = x_k - A_k^{-1} g_k \tag{3.40}$$

If the **F(x)** in a sum of squares function given by:

$$F(x) = \sum_{i=1}^{N} v_i^2(x) = v^T(x)v(x) \tag{3.41}$$

The gradient for **j_th** element is given by:

$$\left[\nabla F(x)\right]_j = \frac{\partial F(x)}{\partial x_j} = 2\sum_{i=1}^{N} v_i(x)\frac{\partial v_i(x)}{\partial x_j} \tag{3.42}$$

In matrix form the gradient can be rewritten as follows:

$$\nabla F(x) = 2J^T(x)v(x) \tag{3.43}$$

where:

$$J(x) = \begin{bmatrix} \dfrac{\partial v_1(x)}{\partial x_1} & \dfrac{\partial v_1(x)}{\partial x_2} & \Lambda & \dfrac{\partial v_1(x)}{\partial x_n} \\[2ex] \dfrac{\partial v_2(x)}{\partial x_1} & \dfrac{\partial v_2(x)}{\partial x_2} & \Lambda & \dfrac{\partial v_2(x)}{\partial x_n} \\[2ex] M & M & & M \\[2ex] \dfrac{\partial v_N(x)}{\partial x_1} & \dfrac{\partial v_N(x)}{\partial x_2} & \cdots & \dfrac{\partial v_N(x)}{\partial x_N} \end{bmatrix} \tag{3.44}$$

The Hessian for j_{th} element is given by:

$$\left[\nabla^2 F(x)\right]_{k,j} = 2\sum_{i=1}^{N}\left\{\frac{\partial v_i(x)}{\partial x_k}\frac{\partial v_i(x)}{\partial x_j} + v_i(x)\frac{\partial^2 v_i(x)}{\partial x_k \partial x_j}\right\} \tag{3.45}$$

In matrix form, the Equation (3.45) can be expressed by:

$$\nabla^2 F(x) = 2J^T(x)J(x) + 2S(x) \tag{3.46}$$

where:

$$S(x) = \sum_{i=1}^{N} v_i(x)\nabla^2 v_i(x) \tag{3.47}$$

For small value of S(x), the approximation of the Hessian matrix is given by:

$$\nabla^2 F(x) \cong 2J^T(x)J(x) \tag{3.48}$$

From the gradient and Hessian equations, iteration of each element is given by:

$$x_{k+1} = x_k - \left[J^T(x_k)J^T(x_k)\right]^{-1} J^T(x_k)v(x_k) \tag{3.49}$$

Therefore it does not require calculation of the second derivative, however the matrix $H=J^TJ$ may not be invertible. However this can be overcomed by using the following modification to approximate the Hessian matrix (Hagan *et al.,* 1995):

$$G = H + \mu I \tag{3.50}$$

Suppose that the eigenvalues and the eigenvector of the Hessian are $(\lambda_1, \lambda_2, \ldots \lambda_n)$ and $(z_1, z_2, \ldots z_n)$, then

$$\begin{aligned} Gz_i &= (H + \mu I)z_i \\ &= Hz + \mu z_i \\ &= \lambda_i z_i + \mu z_i \\ &= (\lambda_i + \mu)z_i \end{aligned} \tag{3.51}$$

Therefore the eigenvector of G are the same as the eigenvector of the H and the eigenvalues of G is given by:

$$\lambda_i(G) = \lambda_i + \mu \tag{3.52}$$

By this reason matrix G can be made positive definite by increasing μ until $(\lambda_i + \mu)>0$ for all i, and therefore the matrix will be invertible. Then the Equation (3.49) can be rewritten as:

$$x_{k+1} = x_k - \left[J^T(x_k)J^T(x_k) + \mu_k I\right]^{-1} J^T(x_k)v(x_k) \tag{3.53}$$

3.4.2.3 Levenberg-Marquardt Neural Network Optimization

The important step in Levenberg-Marquardt neural network algorithm is the computation of the Jacobian matrix. For two output neuron, the Jacobian matrix J of the neural network is given by:

$$
J = \begin{bmatrix} \dfrac{\partial e_1}{\partial W_{1,1}^1} & \dfrac{\partial e_1}{\partial W_{1,2}^1} & \cdots & \dfrac{\partial e_1}{\partial b_2^2} \\[2ex] \dfrac{\partial e_2}{\partial W_{1,1}^1} & \dfrac{\partial e_2}{\partial W_{1,2}^1} & \cdots & \dfrac{\partial e_2}{\partial b_2^2} \end{bmatrix}
\tag{3.54}
$$

Back propagation derivation of Jacobian matrix weight parameters is described by the following function.

$$
\frac{\partial e_i}{\partial W_{j,i}^m} = \frac{\partial e_i}{\partial n_j^m} \times \frac{\partial n_j^m}{\partial W_{j,i}^m}
\tag{3.55}
$$

Where the first term on the right hand side is defined as the Marquardt sensitivity is given by:

$$
s_j^m = \frac{\partial e_i}{\partial n_j^m}
\tag{3.56}
$$

Derivative of the neuron output function against to the weight parameter is given by:

$$
\frac{\partial n_j^m}{\partial W_{j,i}^m} = a_i^{m-1}
\tag{3.57}
$$

Substitution Equations (3.56) and (3.57) into Equation (6.55) is result in:

$$
\frac{\partial e_k}{\partial W_{j,i}^m} = s_j^m a_i^{m-1}
\tag{3.58}
$$

With same procedure, the back propagation derivation of Jacobian matrix bias parameters is described by the following function.

$$\frac{\partial e_k}{\partial b_j^m} = s_j^m \tag{3.59}$$

The updating neural network parameters can be written by:

$$x_{k+1} = x_k - \left[J^T(x_k) J^T(x_k) + \mu_k I \right]^{-1} J^T(x_k) e(x_k) \tag{3.60}$$

Or

$$\Delta x_k = \left[J^T(x_k) J^T(x_k) + \mu_k I \right]^{-1} J^T(x_k) e(x_k) \tag{3.61}$$

3.4.2.4 Direct Adaptive Neural Network Control Reference Model Algorithm

The algorithm of the proposed on-line learning neural network as direct adaptive neural network control reference model algorithm is given in the following steps:

Step 1: -   Initialization of network parameters i.e.: bias and weight.

Step 2: -   Measured of input data i.e.: input power and rotor speed.
         -    Normalization input data i.e.: input power and rotor speed by using Equation (3.21).

Step 3: -   Calculation of error and incremental error input power and rotor speed
         -    While stopping update condition is true: error fall into the given acceptable error range or error change very little, then go to step 5.

Step 4: -   Calculation of updating neural network parameters by using Equations: (3.54) up to (3.61).

Step 5: -   Calculation of output of the neural network by using Equations: (3.22) up to (3.25).

-   Denormalization output neuron in the output layer using Equation (3.26).

Step 6: -   Repeat by going to step 2.

3.5   Summary

In this chapter, the proposed neural network efficiency optimization control of a variable speed compressor motor drive has been introduced. The basic operation of the neural network control has been described. Development of the proposed controller has been presented. The neural network architecture of a direct feedback neural network controller has been developed. Derivation of the second order Levenberg-Marquardt neural network optimization also has been explained. Finally, the algorithm of the proposed real-time/on-line learning neural network efficiency optimization control has been presented.

CHAPTER 4

EXPERIMENTAL SET-UP OF THE NNEOC VARIABLE SPEED COMPRESSOR MOTOR DRIVE

4.1   Introduction

The set-up and implementation of the proposed neural network efficiency optimization control for variable speed compressor motor drive system is presented in this chapter. The proposed drive system consists of major components namely a DSP-based controller board, gate drive, inverter circuit, sensor and a standard squirrel-cage induction motor along with a dynamometer acting as the compressor load. Figure 4.1 shows the components used in the proposed system.
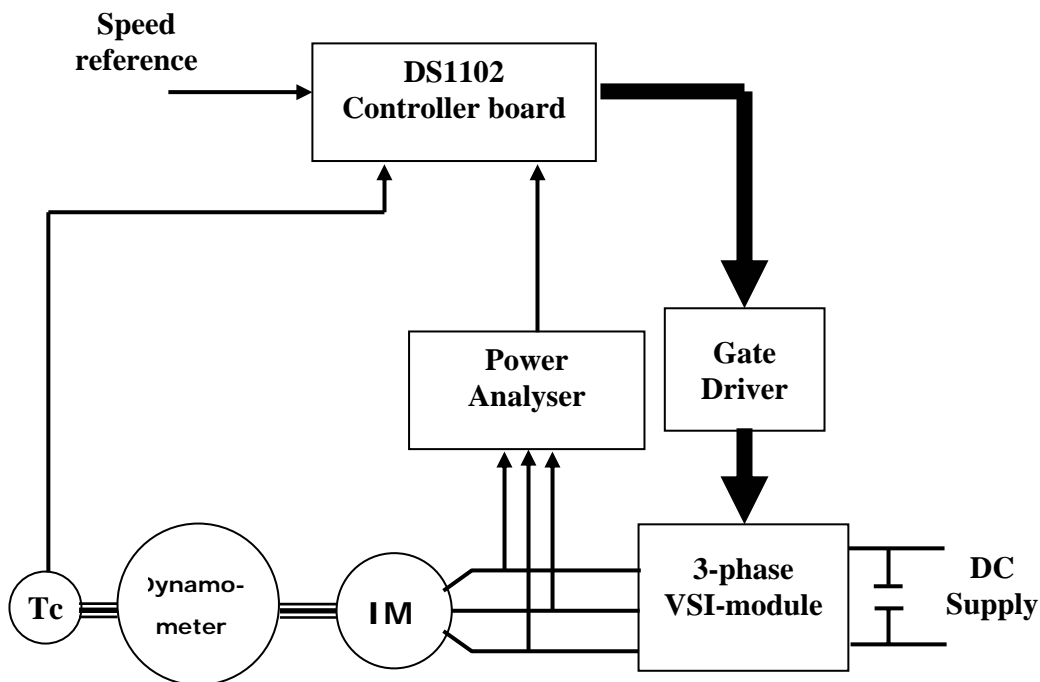
Figure 4.1: Block diagram of the experimental set-up

The neural network model and its controls are implemented through the DSP controller board. In the prototype of the drive system, the rotor mechanical speed is sensed by DC generator speed sensor and the torque by the torque sensor fitted to the dynamometer, while the input power is sensed by current and voltage sensor fitted to the universal power analyser.

In the following sections, each hardware components are described in more detail. Figure 4.2 shows a photograph of the experimental set-up of the proposed controller of the variable speed compressor motor drive system.
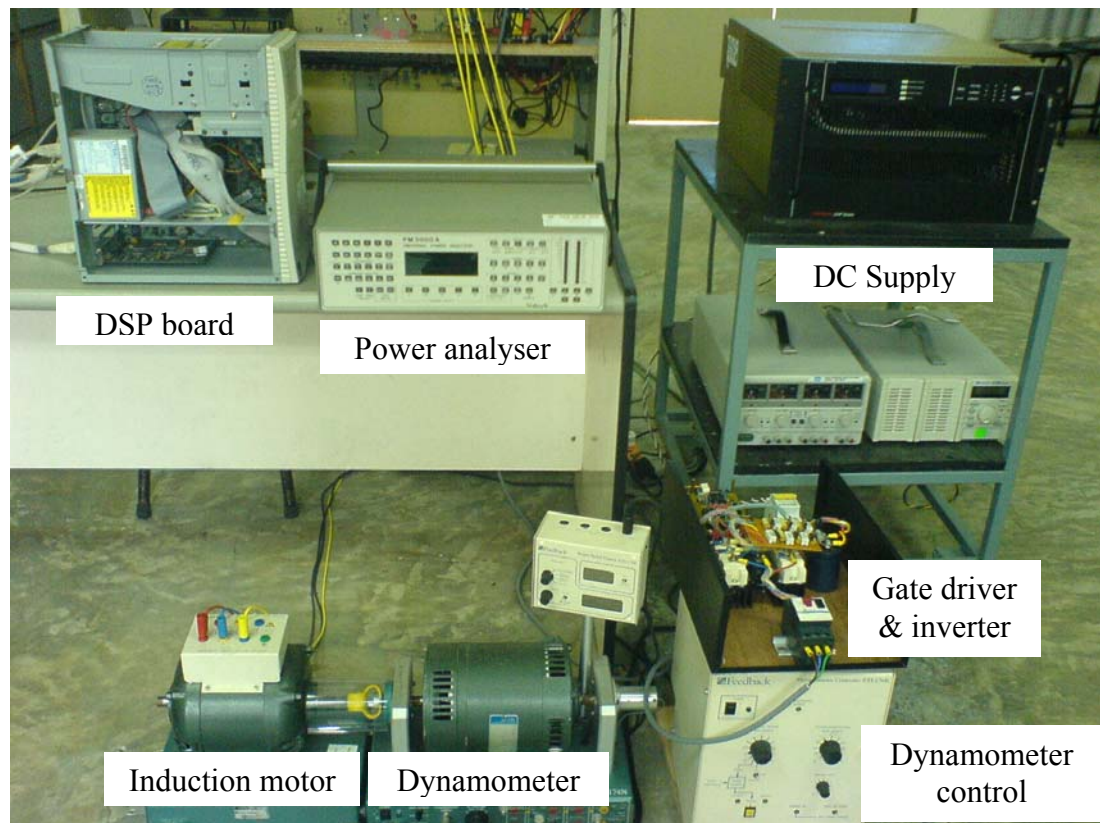
Figure 4.2: The experimental set-up

4.2   DS1102 Controller Board

The single board system of the DS1102 DSP controller board is shown in Figure 4.3 (dSPACE GmbH, 1996). As the term reveal, this board is designed to build a complete real-time control system with just one board. The controller board includes a fast digital signal processor and I/O components for a variety of applications in the rapid control prototyping, development of digital high-speed multivariable controlling and real-time simulations.

The DS1102 board is a standard 16-bit PC/AT card that can be slotted straight in to the PC using ISA bus. The DS1102 controller board consists of a TMS320C31 floating point digital signal processor as a main processor and a TMS320C14 as a co-processor. The board is manufactured by *dSPACE digital processing and control engineering*, GmbH, Germany.

The board provides a fast instruction cycle time for numeric intensive algorithms. The board interfaces to the host (a standard PC) via a standard PC AT interface bus. The block diagram and the data sheet of the DS1102 controller are given in **Appendix A**. Some of the features contained on the board are:

- TMS320C31 floating-point DSP
- Slave-DSP TMS320P14
- Four 12-bit Digital to Analogue Converter (DAC)
- Two 16-bit Analogue to Digital Converter (ADC)
- Two 12-bit ADC
- Twenty six digital input-output (I/O)

Some of the major tasks performed by the DS1102 controller board are to develop the proposed controller which includes:

- *Signal normalization* :

    To interface the input signals from the output device such as the speed and input power sensor to the neural network controller program, it is required to normalize the entire input signal.

- *Neural network controller*:

    In this program the input voltages from the speed and power sensors that fed to the ADC channel on the controller board are processed to obtain the speed and input power of the motor.

- *Real-time learning neural network algorithm*:

To update the neural network parameters, the real-time learning technique is performed entirely in software.

- *Space Vector PWM:*

Computed results of the controller are then employed to determine the IGBT switching state using the Space Vector PWM (SVPWM) signal generator technique.

Implementation of the reference speed using analog signal method is however easily subjected to disturbance from noise. Thus, to avoid this problem the reference speed of the drive system is developed in the Control Desk instrument panel program Release 3.3, which is included with DS1102 controller board. This program provides graphical output and interactive modification of variables on the DS1102 board. Layout of the proposed controller is shown in Figure 4.3.
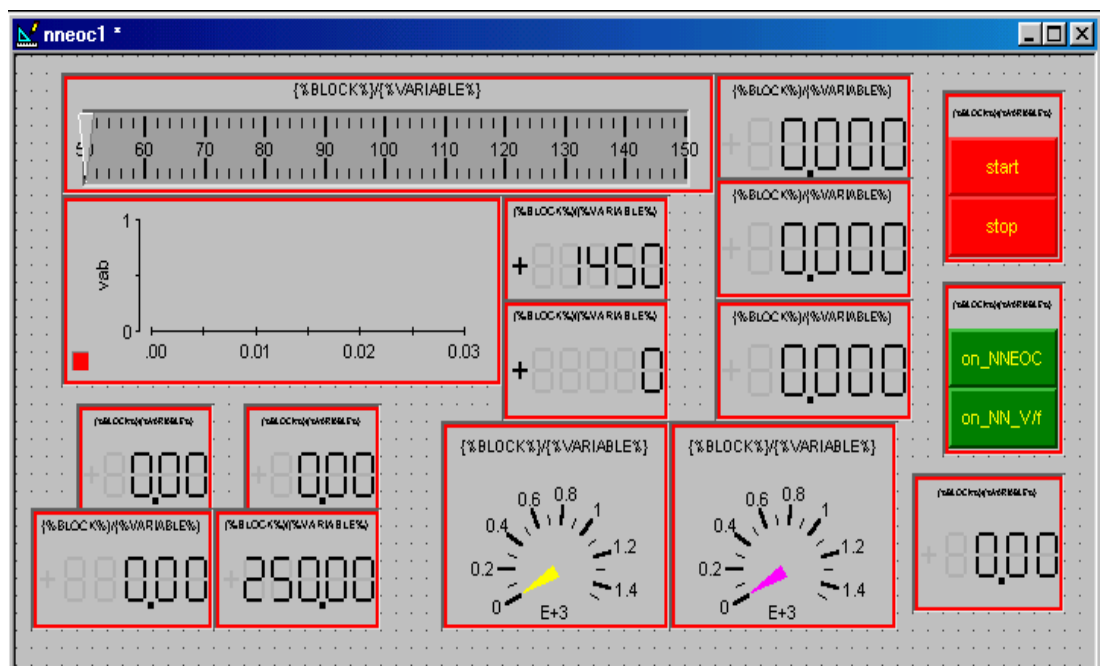
Figure 4.3: Layout of the proposed controller in the Control Desk program

4.3   Power Analyser

The power analyser is used to measure and record the input power of the induction motor drive via analog output connector. It is manufactured by Voltech with part number PM3000ACE (Voltech, 1996). The block diagram of the PM300ACE is given in **Appendix B**.

4.4   Power Circuit and Gate Driver

The power supply module for the drive system is made up of three units of SEMITRANS IGBT modules rated at 1200V and 50A. It is manufactured by Semikron with part number SKM 50 GB 123 D. The datasheet of this IGBT is given in **APPENDIX C**. Each module consists of top and bottom IGBT for one leg or arm of inverter. The schematic of the VSI module is shown in Figure 4.4.
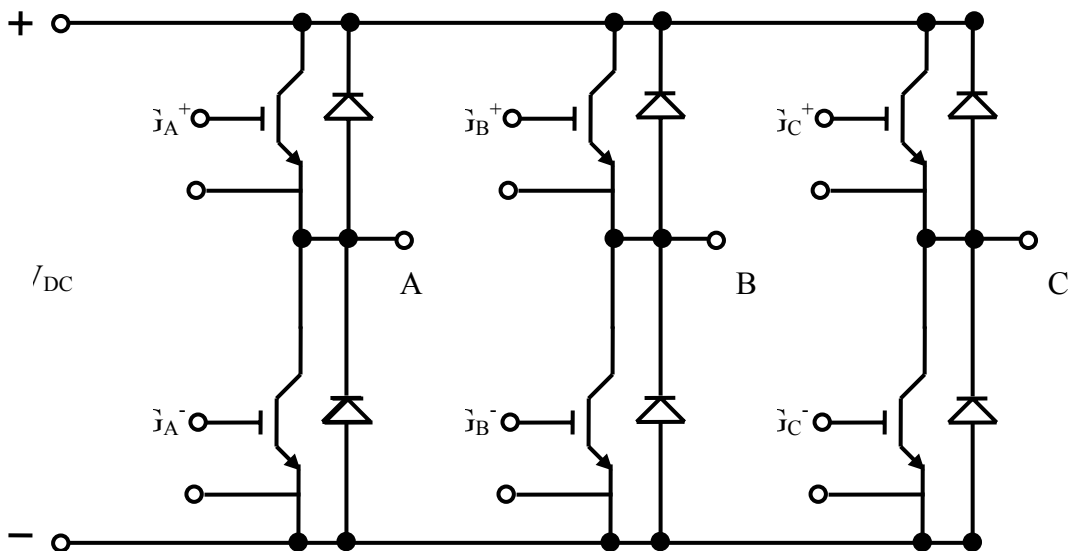
Figure 4.4: Schematic of the IGBT module

The VSI module receives DC link voltage from a DC power supply unit. To protect the IGBT module, a RCD snubber is installed for each the IGBT device. The circuit of the RCD snubber is shown in Figure 4.5.
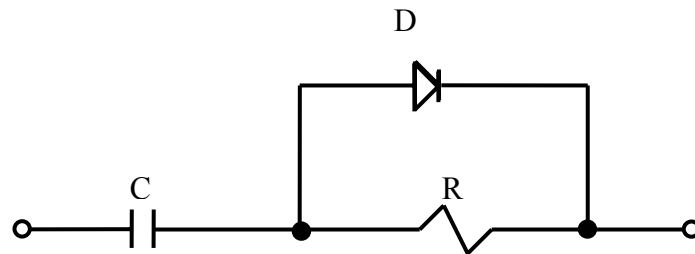
Figure 4.5: RCD snubber circuit

The gate drives receive the signal from DS1102 controller board and amplify them to the correct level to drive the IGBT devices. The power supply gate drivers are generated from the low-side power supply and transferred and isolated through power transformers. Beside that the gate drivers also isolate the signal controller using optocoupler HCPL-A3120 from the DS1102 controller board to the IGBT module. Figure 4.6 shows the schematic of DC-DC isolation and signal isolation of the gate driver circuit.

Figure 4.6 (a): Schematic of DC-DC isolation of the gate driver circuit

Figure 4.6 (b): Schematic of signal isolation of the gate driver circuit

Figure 4.7 shows the gate drivers, snubber and voltage source inverter.
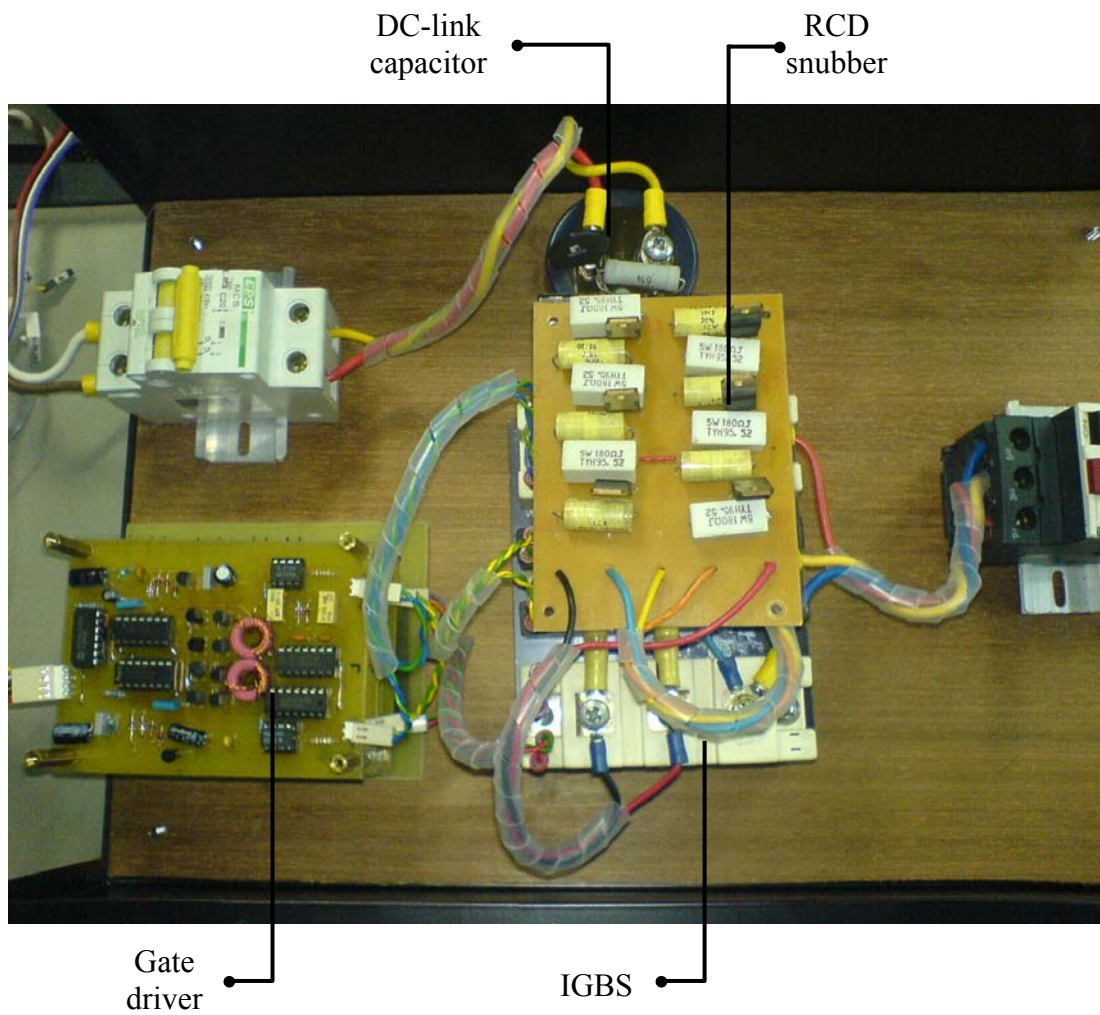
Figure 4.7: Gate driver and voltage source inverter

4.5 Induction Motor

The induction motor used in the experiment is manufactured by *Feedback Inc*. It has stator windings in which are connected in delta and a squirrel cage rotor. It is rated at 120V, 0.25hp, 50 Hz and with rated speed of 1400 rpm. Block rotor and no load test are performed to determine the motor's parameters. The parameters of the induction motor used in the experiments are given in Tabel 4.1.

Table 4.1: Induction motor parameters

Stator resistance, R_s	5.2 Ω
Rotor resistance, R_r	4.0 Ω
Stator self inductance, L_s	0.347 H
Rotor self inductance, L_r	0.347 H
Mutual inductance, L_m	0.336 H
Combined inertia, J	0.000153 kg-m^2

Figure 4.8 show the photograph of the three phase induction motor.

Figure 4.8: Induction motor 0.25 hp

4.6   Dynamometer

The dynamometer used as the load is manufactured by *Feedback Inc.* model ETL-174N. The dynamometer is operated through a controller model ELT-174 R.

The tachogenerator as a speed sensor is fitted to the dynamometer. Output voltage of the tachogenerator is fedback to the dynamometer controller to adjust the torque of the dynamometer. This dynamometer controller provides two types of load function i.e. constant torque and torque that is proportional to speed. Photograph of the dynamometer and dynamometer controller are shown in Figure 4.9.

Figure 4.9: Dynamometer and the dynamometer controller

4.7   Summary

This chapter has presented the major components used in the experimental set-up. These include:

- The controller board DS1102
- 3-phase VSI and gate drivers
- Induction motor and dynamometer

The tasks performed by the controller board have been discussed. The parameters and specifications of the VSI, gate drivers and the induction motor have also been explained.

CHAPTER V

SIMULATION AND EXPERIMENTAL RESULTS AND DISCUSSION

5.1   Introduction

This chapter presents the simulation and experimental results and discuss on the proposed method towards the achievement of the research objective. The chapter begins by looking at the simulation results of the proposed controller. In the simulation, the effect of on-line/real-time learning control scheme to the robustness of the neural networks controller against the motor parameter variation is investigated.

In order to verify the efficiency improvement of the neural network efficiency optimization control, the developed controller is compared with the neural network constant volt per hertz method. The proposed Neural Network Efficiency Optimization Controller (NNEOC) is then applied to the experimental set-up. In this set-up, the comparison between the proposed controller and Neural Network Constant Volt per Hertz (NNV/f) is verified. This chapter also presents the advantages of the proposed controller in efficiency optimization control area, and some of its limitations. The chapter ends by presenting a summary of the results.

5.2 Simulation Results

Simulation of the efficiency optimization of the proposed control scheme is carried out using various block developed to represent the actual system using the MATLAB/SIMULINK program. The Simulink block consists of three major blocks, i.e. the three phase induction motor and compressor load block, three phase space vector PWM inverter block and the controller block. These blocks are designed in the S-function block by employing Borland C++ program.

Based on the proposed control scheme as shown in Figure 3.10, development of the Simulink blocks of a variable speed compressor motor drive system is shown in Figure 5.1.
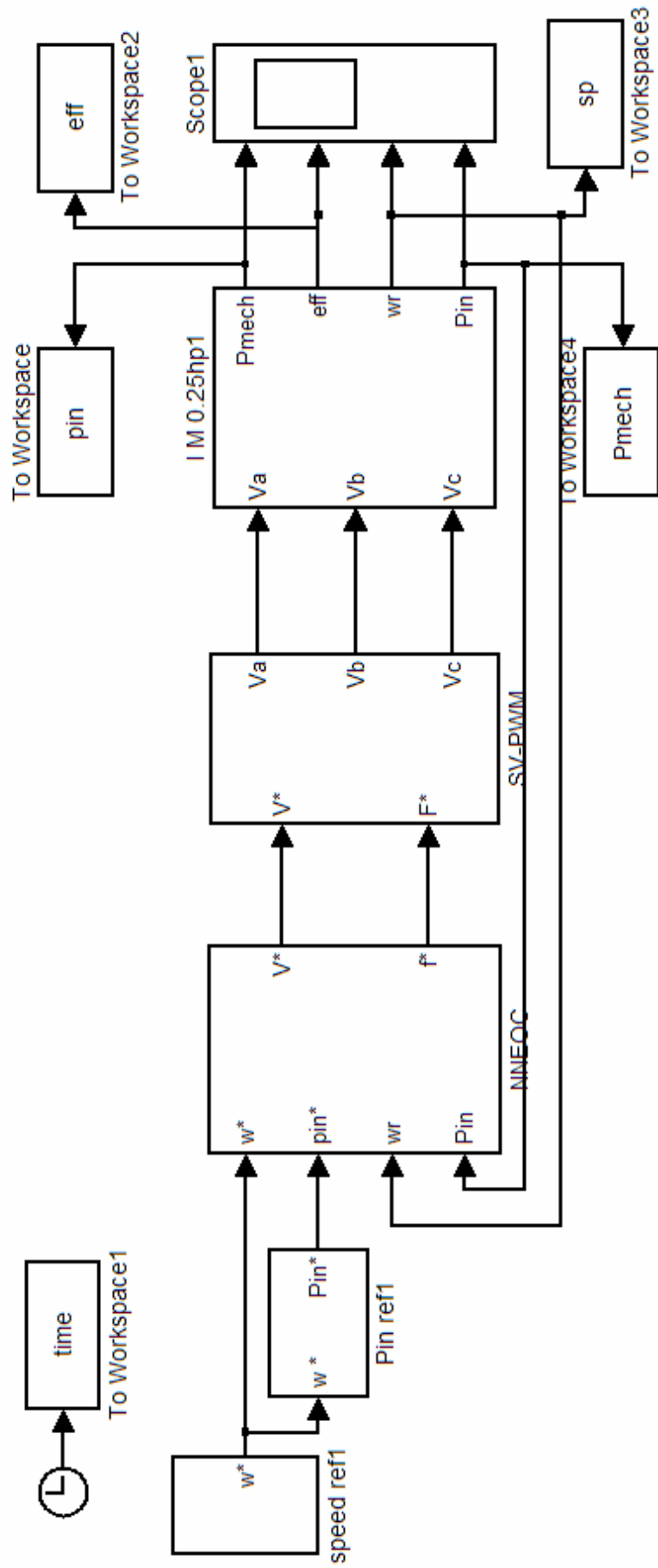
Figure 5.1: Simulink block of the efficiency optimization control for a variable speed compressor motor drive system

Based on the neural network and learning algorithm equations that have been described in the section 3.4, a detail Simulink block of the proposed neural network efficiency controller is shown in Figure 5.2.
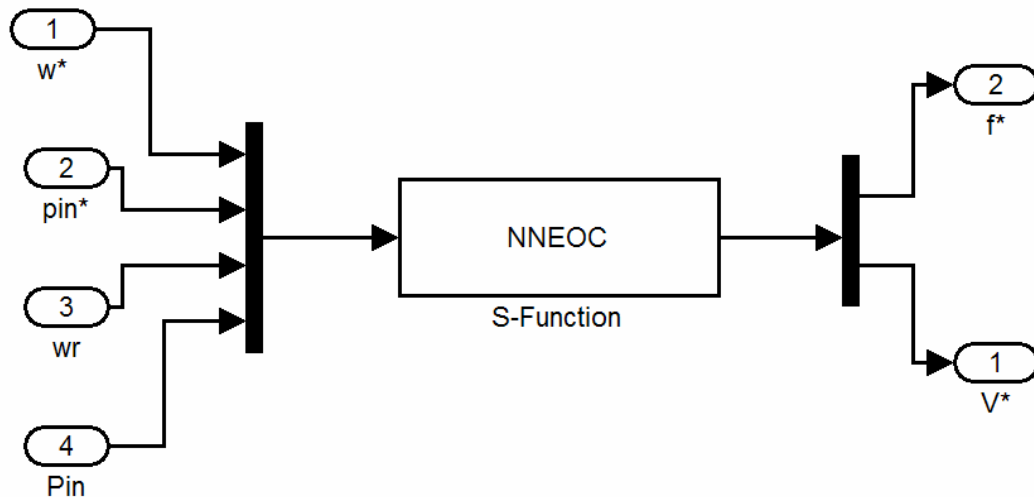
Figure 5.2: Simulink block of the neural network efficiency optimization controller

Detail simulation blocks and S-function program of the induction motor, compressor load and space vector PWM are given in APPENDIX D.

5.2.1   Control Performance Against Motor Parameter Variations

It has been described in the Chapter 2 that, the induction motor parameters value is not constant, but these parameters vary with temperature and magnetic saturation. To simulate the induction motor with parameter variation, particularly on the resistance variation due to temperature variation, a temperature Simulink block is added and fed into the induction motor block. The stator and rotor resistances variation on this simulation are determined by equation 2.3 and 2.7.

To illustrate the robustness of the proposed motor drive controller against the parameter deviation, a parallel block of the proposed controller with on-line and off-line learning scheme at same reference speed command and same load condition was developed. Figure 5.3 show the development of the Simulink block with parallel controller.
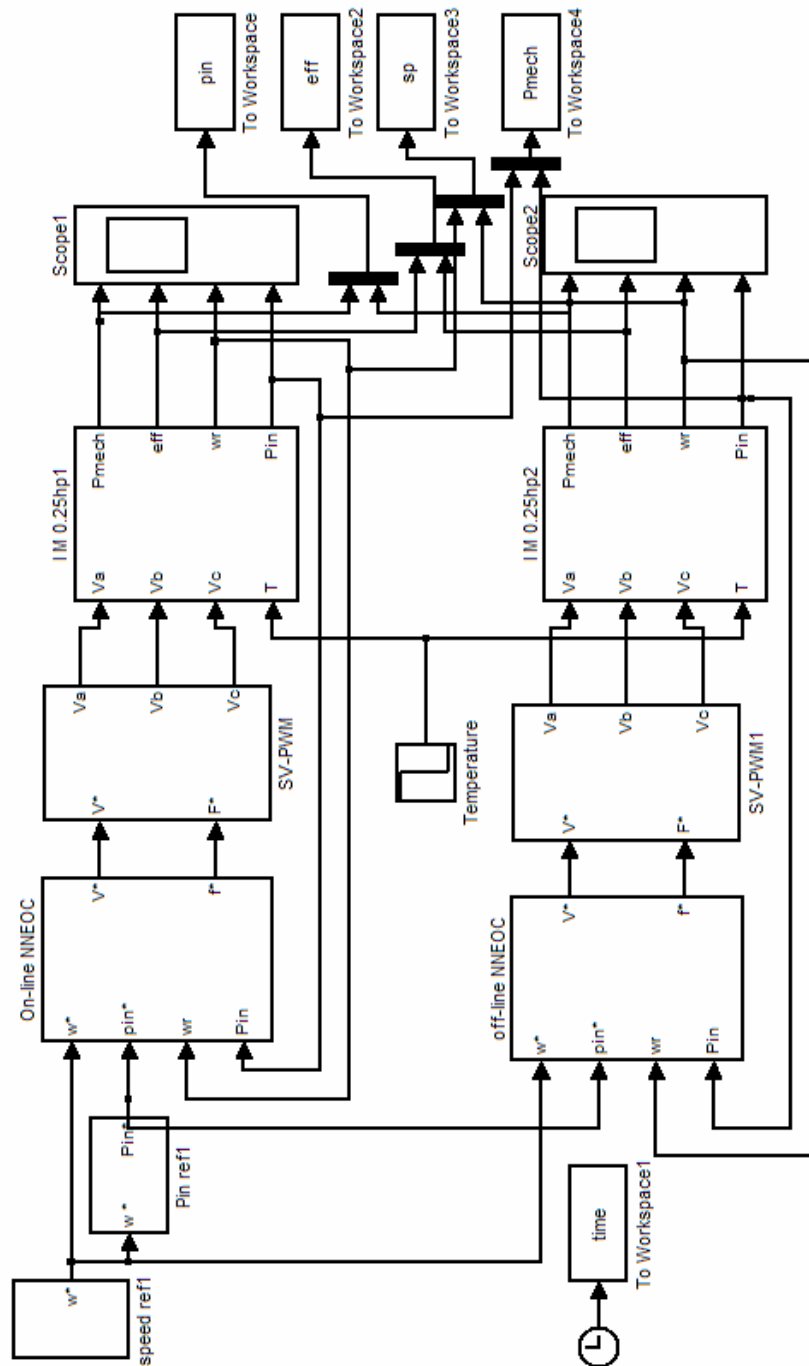
Figure 5.3: Simulink block of the on-line and off-line neural network efficiency optimization controller for same speed reference

For this purpose the stator and rotor resistance of the motor are changed with the increase in temperature from the ambient (20^0C) to a maximum (105^0C) for A class isolation (Boldea and Nasar, 1997). At the start of the plot, the motor was operated under ambient temperature and after that at 5 second the temperature is increased up to the maximum value.

Response of the rotor speed when temperature is changed to maximum value at reference speed 1000, 800 and 600 rpm are shown in Figure 5.4a, 5.4b and 5.4c respectively.
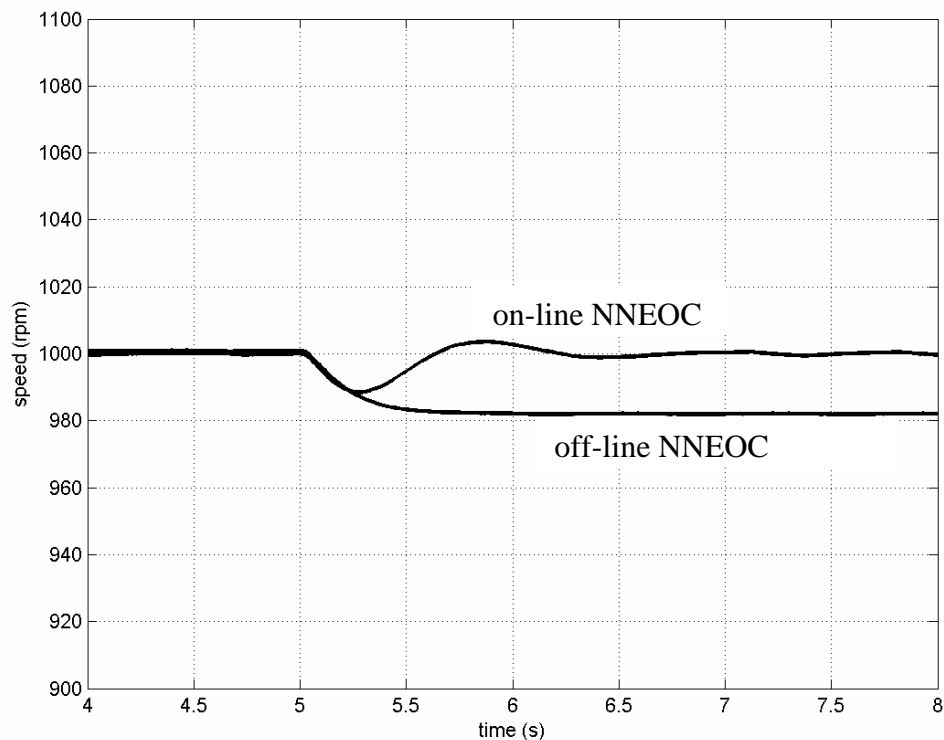
(a)

Figure 5.4: Simulation results, response of the rotor speed when the temperature is switched from 20^0C to maximum 105^0C at **(a)** a speed reference command of 1000 rpm, **(b)** a speed reference command of 800 rpm and **(c)** a speed reference command of 600 rpm.
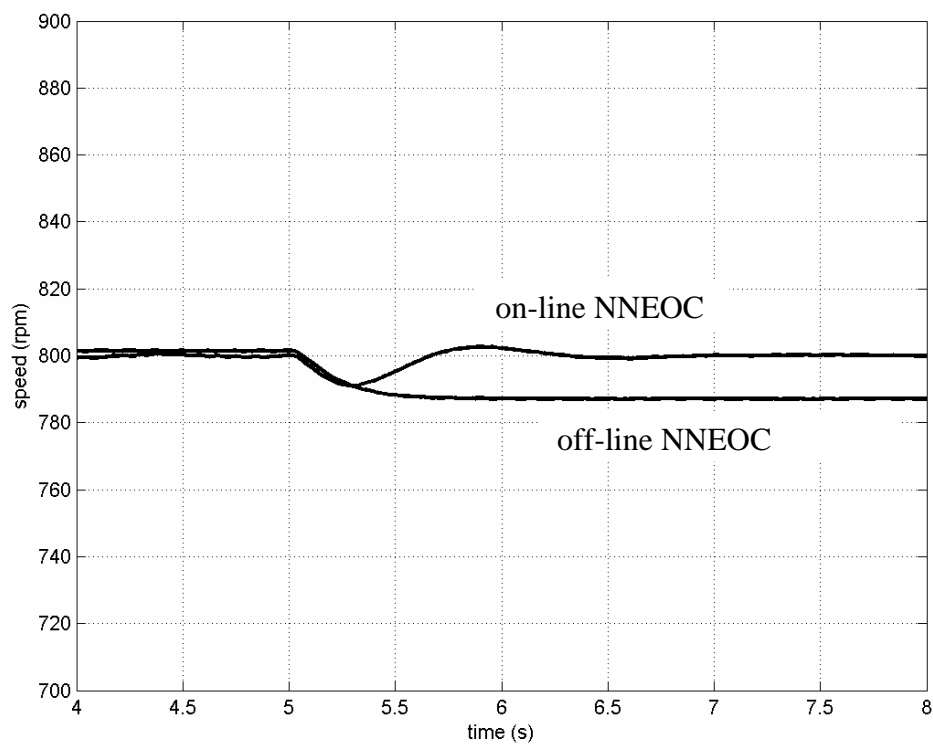
(b)
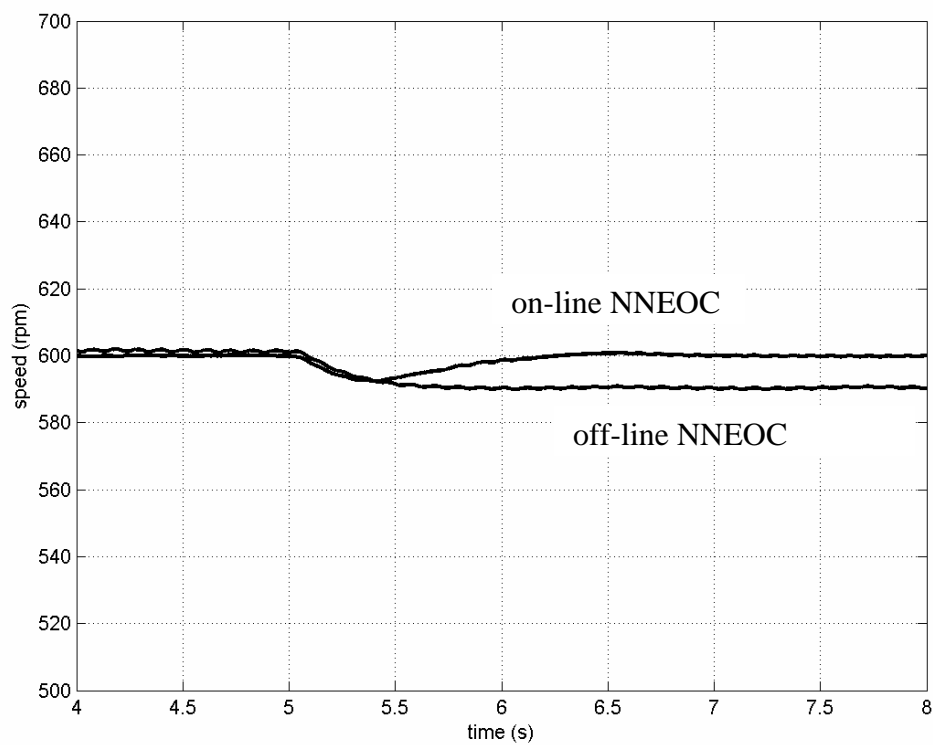
(c)

Figure 5.4: (continued).

The simulations results in Figure 5.4 (a), (b) and (c) show that, increasing the resistances due to the temperature variation causes disturbance to the rotor speed. However by using the proposed on-line learning scheme, the deviation of the rotor speed can be compensated and return to the original speed reference command.

It should be emphasized that, by using the proposed on-line learning scheme, the controller is more robust against the resistance parameters variation.

5.2.2   Efficiency Improvement of the Neural Network Efficiency Controller

To investigate the efficiency improvement of the proposed controller, two Simulink controller blocks of the proposed controller and neural network constant volt per hertz are developed in parallel. In order to switch the controller from the proposed controller to neural network constant volt per hertz or vice versa, a switch selector block is added and fed to the controller. Simulink block of the parallel controller is shown in Figure 5.5.
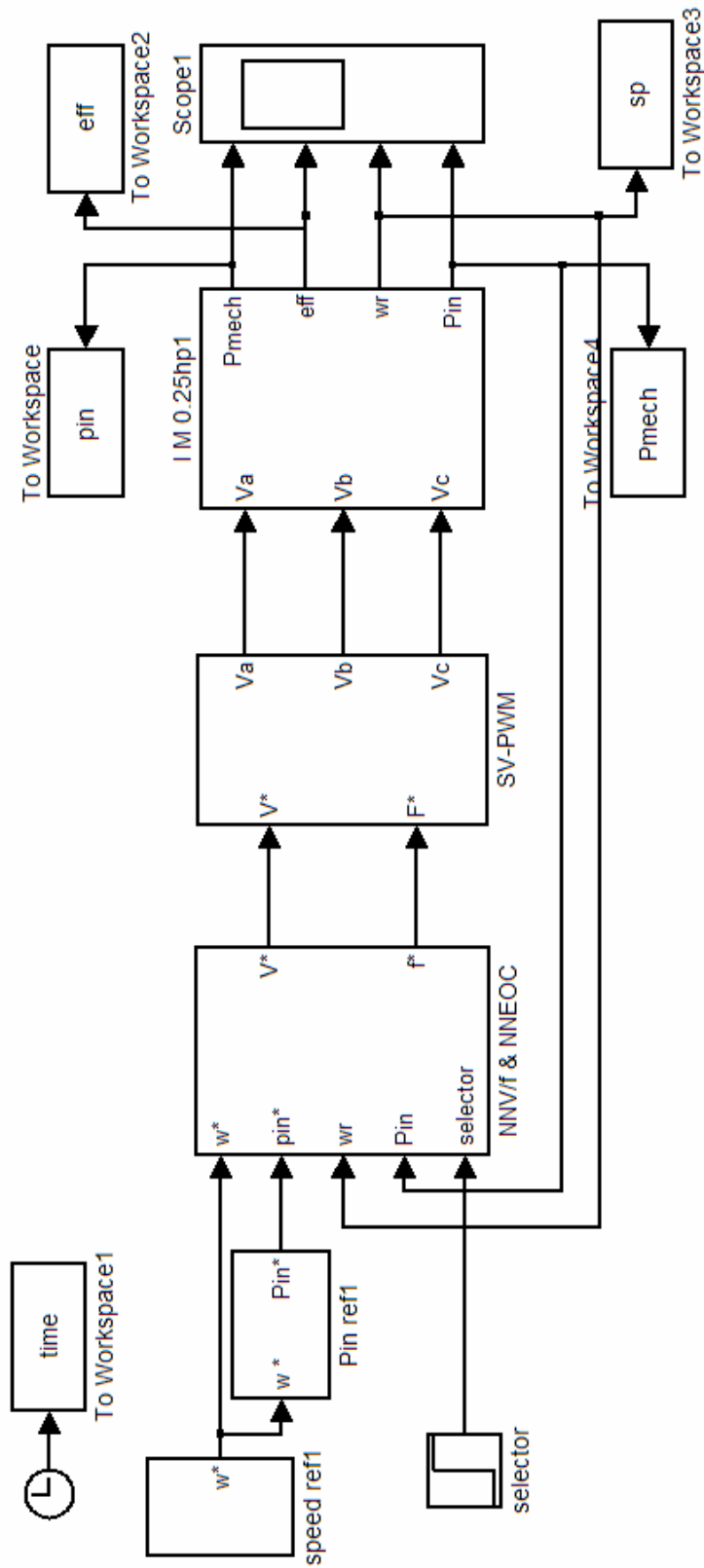
Figure 5.5: Simulink block to investigate efficiency improvement between NNEOC and NNV/f scheme

At the start of the plot, the variable speed compressor motor drive system was operated by neural network constant volt per hertz, after the system is stable at 3 second the controller is switched to the proposed controller. Figure 5.6 shows the response of the input power, rotor speed and stator voltage of the motor when the control is switched from the neural network constant volt per hertz to the proposed controller at speed reference command of 500 rpm.
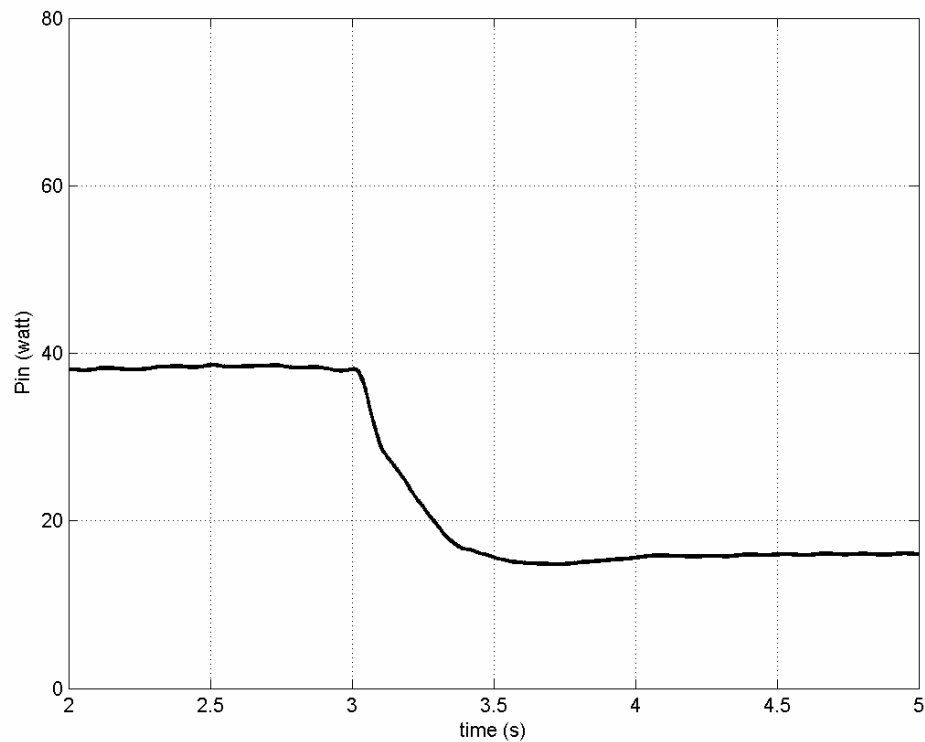
(a)

Figure 5.6: Simulation results **(a)** input power consumption of the motor **(b)** speed of the motor **(c)** stator voltage of the motor when the controller is switched from NNV/f to proposed method at t=3 second for the same speed (500 rpm) and load (0.163 Nm) condition
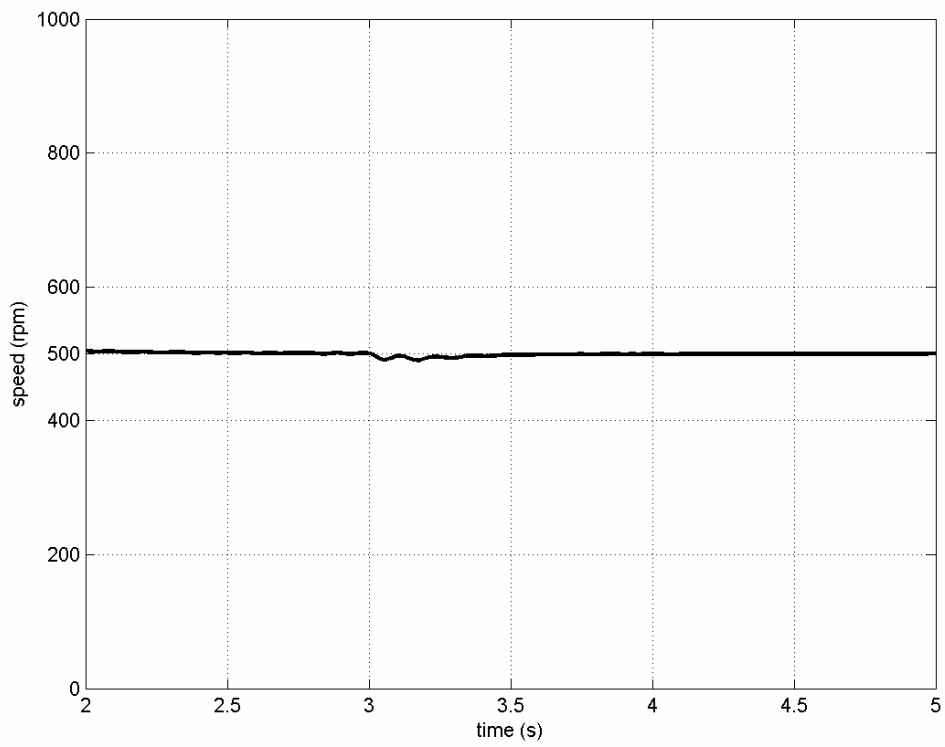
(b)
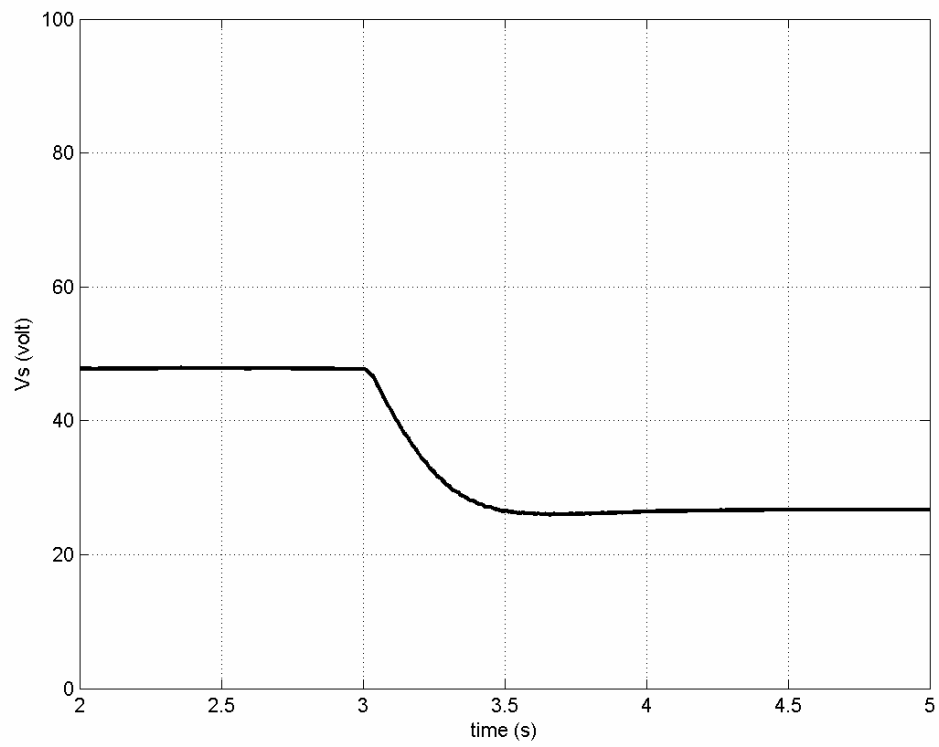
(c)

Figure 5.6: (continued)

Other simulation result for the same test at a speed reference command of 600 rpm is shown in Figure 5.7.
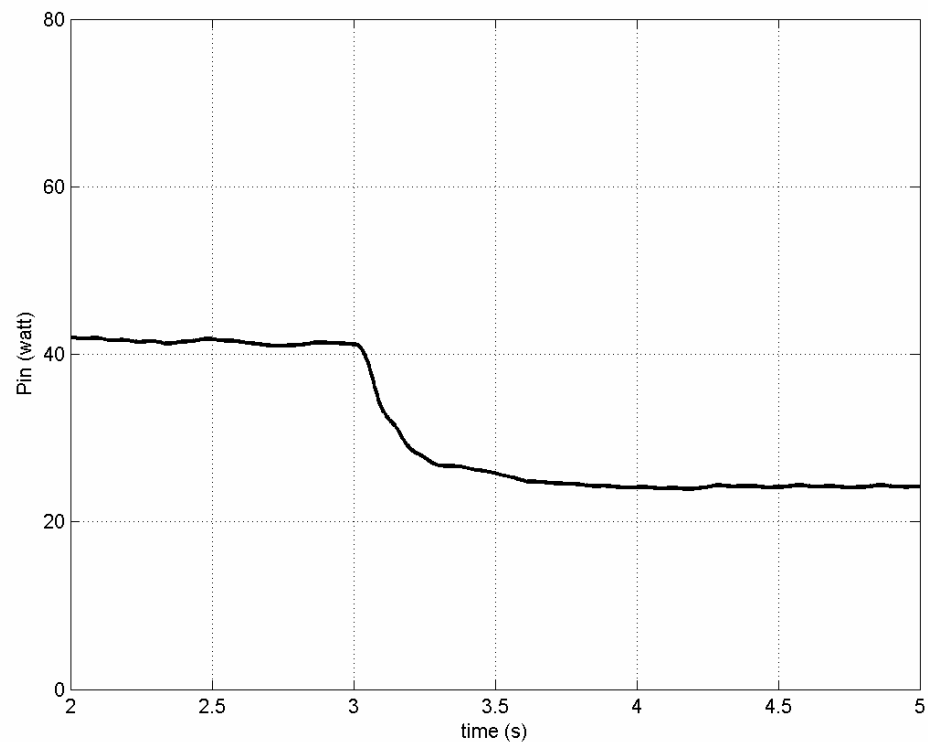
(a)

Figure 5.7: Simulation results **(a)** input power consumption of the motor **(b) s**peed of the motor **(c)** stator voltage of the motor when the controller is switched from the neural network constant volt per hertz to proposed method at t=3 second for the same speed (600 rpm) and load (0.235Nm) condition
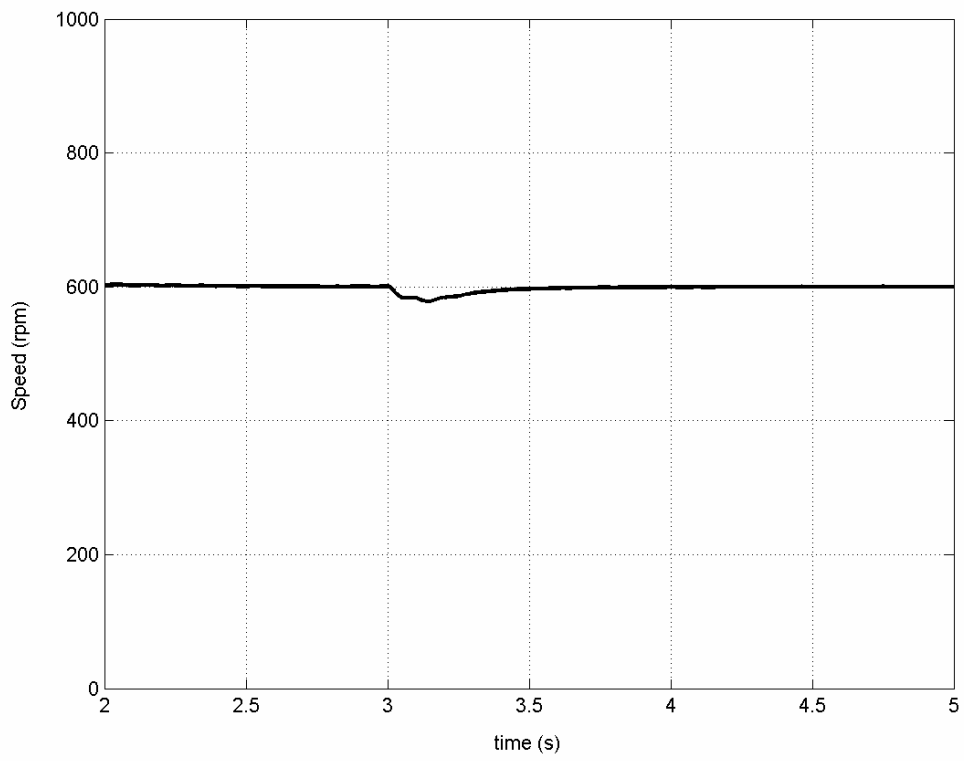
(b)
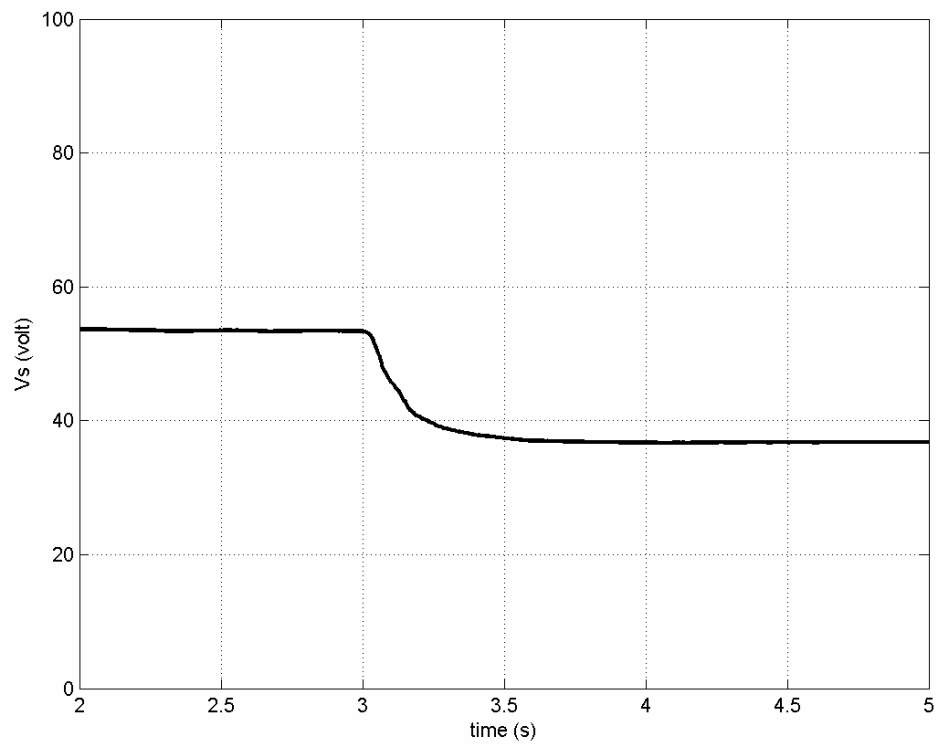
(c)

Figure 5.7: (continued)

5.3   Experimental Results

Based on the experimental set-up that has been described in the chapter 4, both of the on-line learning schemes proposed controller and neural network constant volt per hertz control are developed in the DSP controller board. The speed reference command and switching selector command to choose between the proposed controller and neural network constant volt per hertz are developed as an interactive variable via Dspace Control Desk program. The source codes of the developed programs of the DSP are given in APPENDIX E.

In this experiment, to verify the efficiency improvement of the proposed controller, the same procedures that have been done in the simulation test in section 5.2.2 is developed. Initially, the motor is run at reference speed command by using neural network constant volt per hertz, and maintaining the same load condition the controller was changed to the proposed controller.

Figure 5.8 show responses of the rotor speed, electromagnetic torque, stator voltage and input power motor when the controller is switched from the neural network constant volt per hertz to the proposed controller at a speed reference command of 500 rpm.
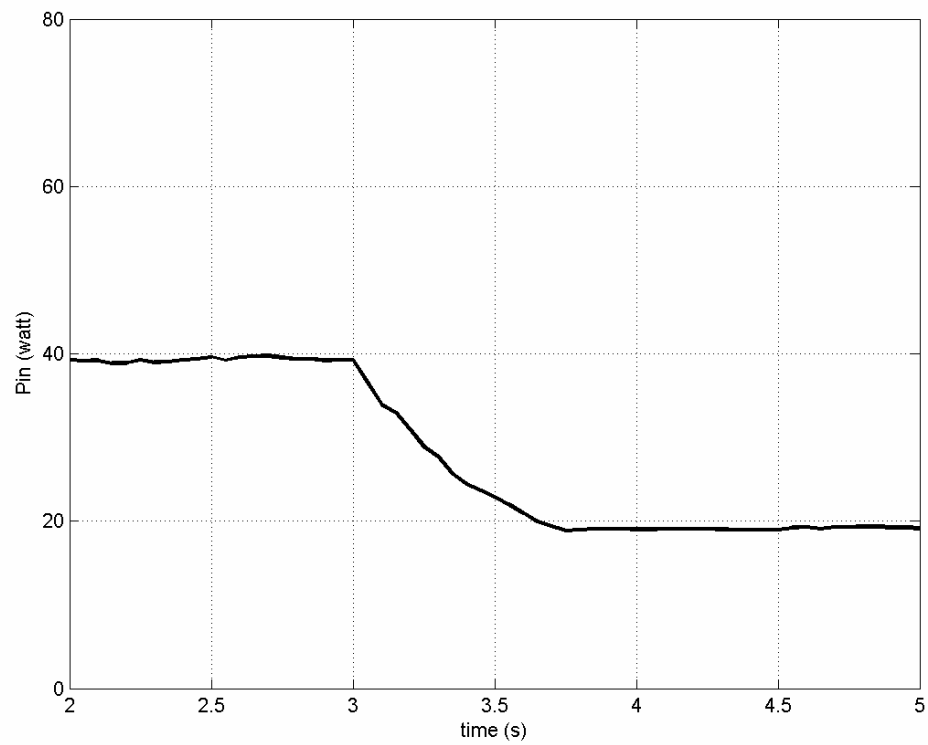
(a)

Figure 5.8: Experimental results **(a)** input power consumption of the motor **(b)** speed of the motor **(c)** stator voltage of the motor when the controller is switched from the neural network constant volt per hertz to proposed method at t=3 second for the same speed (500 rpm) and load (0.163 Nm) condition
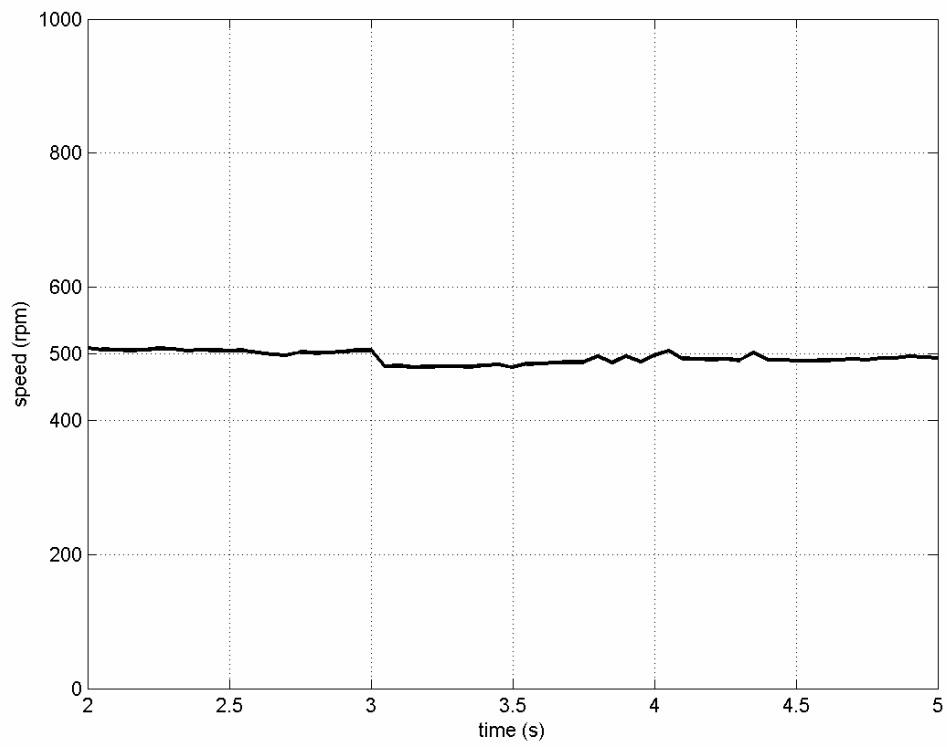
(b)
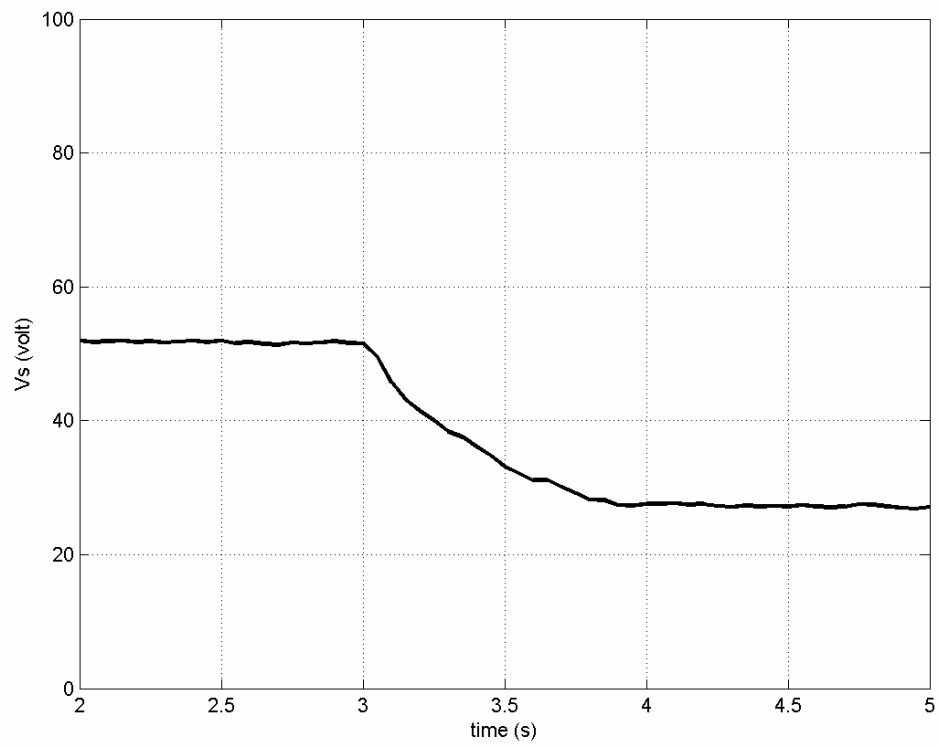
(c)

Figure 5.8: (continued)

Other experimental result for the same test at a speed reference command of 600 rpm is shown in Figure 5.9.
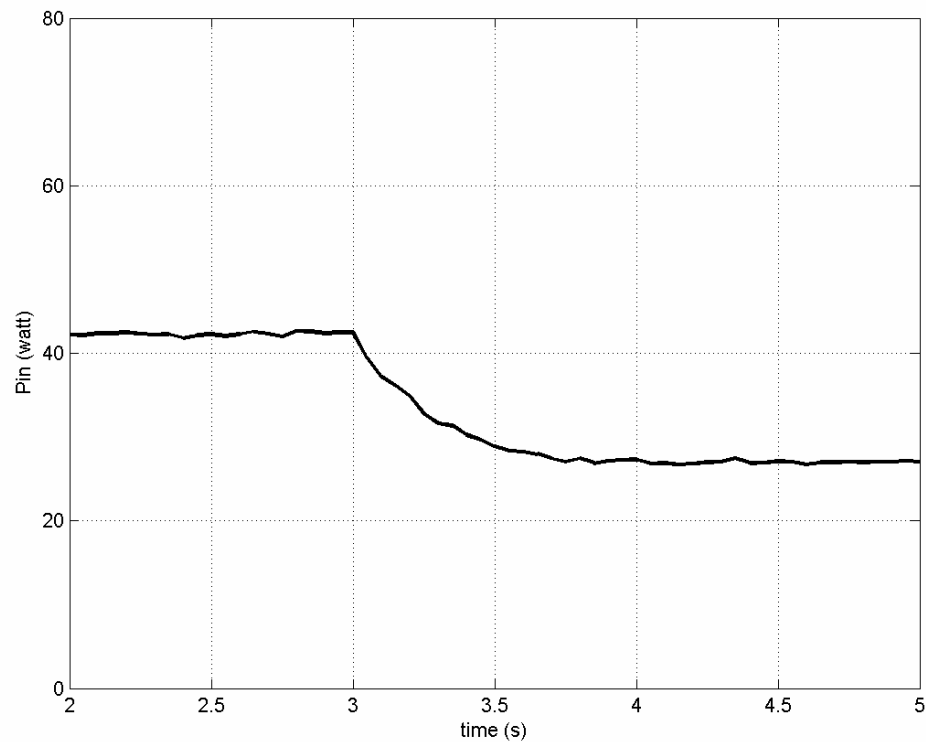
(a)

Figure 5.9: Experimental results **(a)** input power consumption of the motor **(b)** speed of the motor **(c)** stator voltage of the motor when the controller is switched from the neural network constant volt per hertz to proposed method at t=3 second for the same speed (600 rpm) and load (0.235Nm) condition
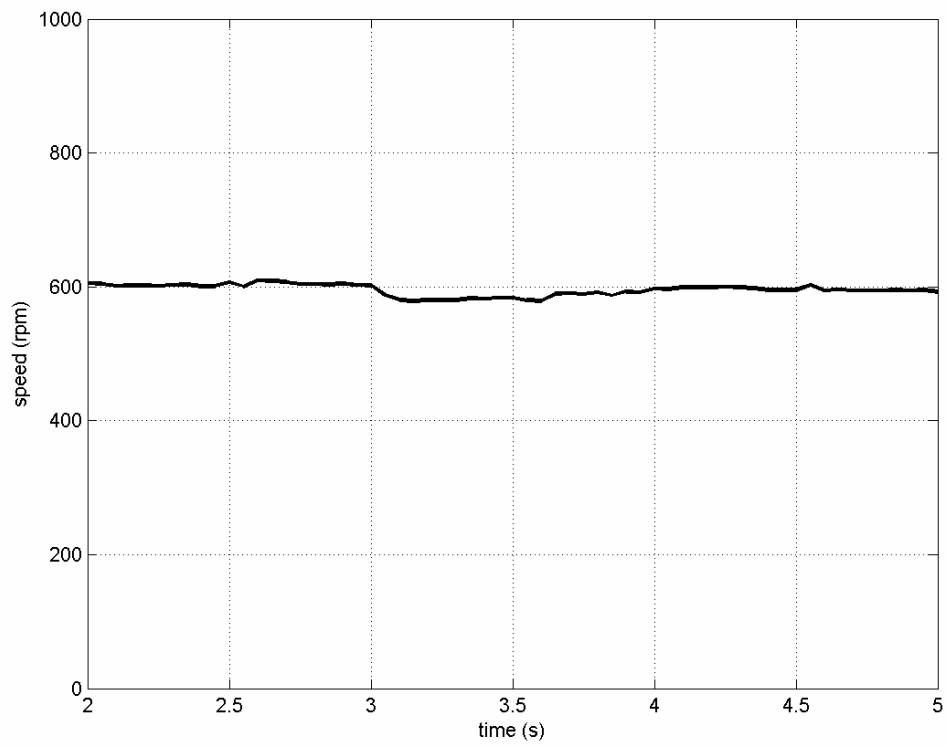
(b)
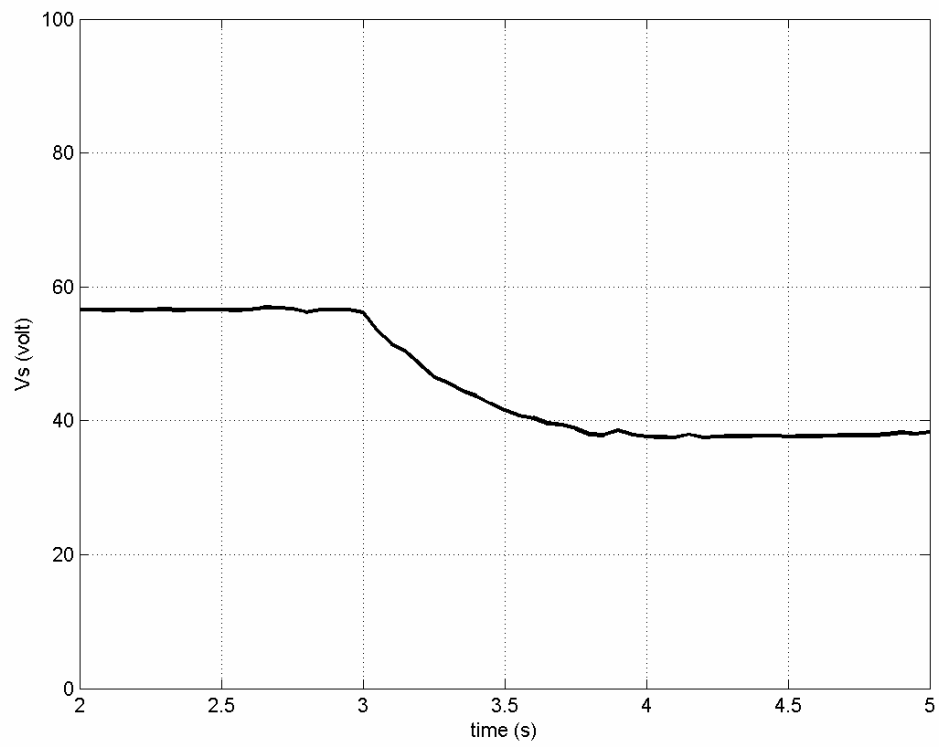
(c)

Figure 5.9: (continued)

The experimental results show that, by using the proposed controller, the input power consumption and stator voltage reduce, and the speed of the motor can be maintained constant in accordance to the speed reference command. Comparison of the efficiency between proposed controller and neural network constant volt per hertz is for several speed operations is given in Figure 5.10.
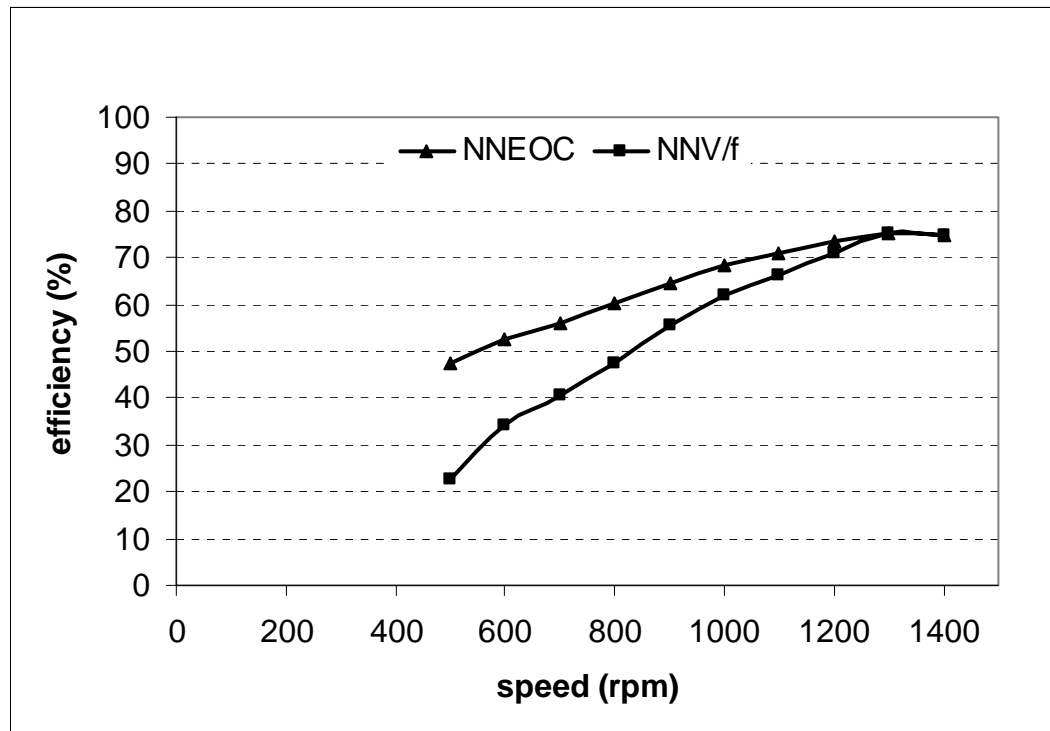
Figure 5.10: Comparison of the efficiency between the proposed controller and neural network constant volt per hertz

5.4   Summary

In this Chapter, verification of the proposed efficiency optimization control for variable speed compressor motor drive has been presented. The robustness of the on-line learning scheme neural network efficiency optimization against motor parameters variation has been tested by simulation, particularly based on the temperature variation. It was found that the proposed on-line learning scheme is more robust to the stator and rotor resistance deviation.

Comparison of the efficiency between the proposed controller and the neural network constant volt per hertz has been verified by using simulation and experimental set-up. It was found that, by using the proposed controller the efficiency of the motor can be increased. In addition, at the same time the rotor speed can be maintained constant according to the speed reference command.

CHAPTER VI

CONCLUSSION AND FUTURE WORK

6.1   Conclusions

This report has presented the theoretical and practical improvement on efficiency optimization of variable speed compressor motor drives. The major issue related to the basic methods of the efficiency optimization control which is based on mathematic derivation and power input measurement have been discussed.

Previous research works conducted in these areas were briefly reviewed. This includes the model loss control and search control methods control scheme to optimize the motor flux as well as to increase the efficiency. The various artificial intelligent techniques for efficiency optimizations were briefly reviewed.

Improvement on efficiency optimization control on the scalar control method of a variable speed compressor motor drive has been proposed in this thesis. Development of the neural network control to optimize the efficiency of the compressor motor at low speed operation has been presented.

The adaptive neural network controller has been proposed by on-line learning scheme. Simulations on the neural network efficiency controller with on-line and without on-line learning scheme have been conducted to investigate the robustness of the proposed controller. It is shown that the on-line learning technique improves the robustness of the controller.

To increase the efficiency of the compressor motor drive particularly at low speed and load operation, a neural network efficiency optimization control to optimize stator voltage and frequency has been proposed.

Simulation and experiments on the variable speed compressor motor drive system with neural network efficiency optimization control and neural network constant volt per hertz scheme have been conducted to verify the efficiency improvement of the proposed controller. The results obtained clearly show that the efficiency at low speed is significantly increased.

6.2   Future Work

Several recommendations of future work are listed as follows:

a. Currently the proposed controller intended to improve the efficiency optimization of the compressor motor drive load model, of which the typical load does not require high dynamic response. Therefore for other types of load that need high dynamic response, the vector control of neural network efficiency control can be considered.

b. In this proposed efficiency optimization, the development was based on the motor flux level optimization. Currently in this thesis three phase sinwave generator symmetric space vector PWM was employed. Incorporating to the overall losses on the motor drive system, it is also important to minimize the losses of drive system by development of the optimal space vector PWM technique.

APPENDIX A

DS1102 CONTROLLER BOARD

A.1 DS1102 Block Diagram
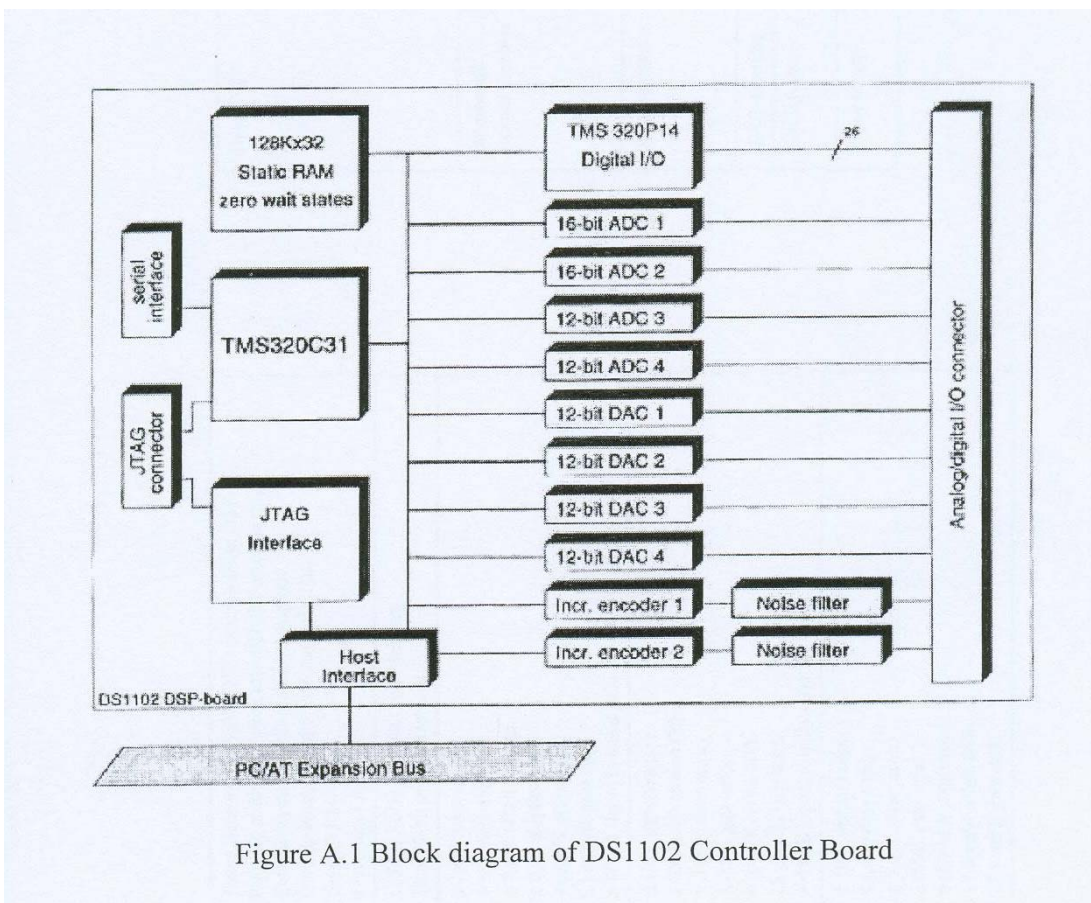
Figure A.1 Block diagram of DS1102 Controller Board

Figure A.1 Block diagram of DS1102 controller board

Slave-DSP	Texas Instruments TMS320P14 DSP. 25 MHz clock rate, 160 ns cycle time. 32-bit arithmetic unit. 4K x 16-bit on-chip PROM containing firmware. 4K x 16-bit external program RAM. 256 x 16-bit on-chip data RAM. Bit-selectable 16-bit I/O port. 6 high precision PWM outputs. Event manager with capture inputs and compare outputs.
Incremental encoder interface	Three RS422 differential inputs per channel. Fourfold pulse multiplication. 8.3 MHz maximum count frequency. Three stage digital pulse filter. 24-bit loadable position counter. 5 V / 200 mA sensor supply voltage.
Host-interface	Four 16-bit and three 8-bit I/O ports in the 64K host I/O space. Memory and I/O are accessible by the host even while the DSP is running. DSP-host and host-DSP interrupts.
JTAG-interface	On board test bus controller and emulator connector.
Physical size	160 mm x 107 mm x 20 mm. Requires one half length PC-slot.
Power supply	+ 5 V ± 10 %, 2A. ± 12 V ± 5 %, 100mA.

Processor	Texas Instruments TMS320C31 floating-point DSP. Running at 60 MHz clock rate and 33.3 ns cycle time. Two 32-bit on-chip timers/event counters. On-chip bidirectional 15 MBaud serial link. On-chip DMA. 4 interrupt lines.
Memory	128K x 32-bit zero wait state memory. 2K x 32-bit on-chip memory.
16-bit ADCs	± 10 V input range. 4 µs conversion time. ± 5 mV offset voltage. ± 0.25 % gain error. 4 ppm/K offset drift. 25 ppm/K gain drift. > 80 dB signal to noise ratio.
12-bit ADCs	± 10 V input range. 1.25 µs conversion time. ± 5 mV offset error. ± 0.5% gain error. 4 ppm/K offset drift. 25 ppm/K gain drift. > 65 dB signal to noise ratio.
DACs	± 10 V output range. 4 µs settling time. ± 5 mV offset error. ± 0.5% gain error. 5 mA output current. 13 ppm/K offset drift. 25 ppm/K gain drift.

APPENDIX B

IGBT DATA SHEETS

B.   Data sheet of IGBT

SEMIKRON

SEMITRANS® M IGBT Modules

SKM 50 GB 123 D
SKM 50 GAL 123 D

Absolute Maximum Ratings		Values	Units
Symbol	Conditions [1]	... 123 D	
V_{CES}		1200	V
V_{CGR}	$R_{GE} = 20\ k\Omega$	1200	V
I_C	$T_{case} = 25/80\ °C$	50 / 40	A
I_{CM}	$T_{case} = 25/80\ °C;\ t_p = 1\ ms$	100 / 80	A
V_{GES}		± 20	V
P_{tot}	per IGBT, $T_{case} = 25\ °C$	310	W
$T_j, (T_{stg})$		− 40 . . . +150 (125)	°C
V_{isol}	AC, 1 min.	2 500	V
humidity	DIN 40 040	Class F	
climate	DIN IEC 68 T.1	40/125/56	
Diodes			
$I_F = I_C$	$T_{case} = 25/80\ °C$	50 / 40	A
$I_{FM} = I_{CM}$	$T_{case} = 25/80\ °C;\ t_p = 1\ ms$	100 / 80	A
I_{FSM}	$t_p = 10\ ms;\ sin.;\ T_j = 150\ °C$	550	A
I^2t	$t_p = 10\ ms;\ T_j = 150\ °C$	1500	A^2s

Characteristics		min.	typ.	max.	Units
Symbol	Conditions [1]				
$V_{(BR)CES}$	$V_{GE} = 0,\ I_C = 1\ mA$	$\geq V_{CES}$	–	–	V
$V_{GE(th)}$	$V_{GE} = V_{CE},\ I_C = 2\ mA$	4,5	5,5	6,5	V
I_{CES}	$V_{GE} = 0$ $T_j = 25\ °C$	–	0,3	1	mA
	$V_{CE} = V_{CES}$ $T_j = 125\ °C$	–	3	–	mA
I_{GES}	$V_{GE} = 20\ V,\ V_{CE} = 0$	–	–	200	nA
V_{CEsat}	$I_C = 40\ A$ $V_{GE} = 15\ V;$	–	2,5(3,1)	3(3,7)	V
V_{CEsat}	$I_C = 50\ A$ $T_j = 25\ (125)\ °C$	–	2,7(3,5)	–	V
g_{fs}	$V_{CE} = 20\ V,\ I_C = 40\ A$	–	30	–	S
C_{CHC}	per IGBT	–	–	350	pF
C_{ies}	$V_{GE} = 0$	–	3300	4000	pF
C_{oes}	$V_{CE} = 25\ V$	–	500	600	pF
C_{res}	$f = 1\ MHz$	–	220	300	pF
L_{CE}		–	–	30	nH
$t_{d(on)}$	$V_{CC} = 600\ V$	–	70	–	ns
t_r	$V_{GE} = + 15\ V / - 15\ V$ [3]	–	60	–	ns
$t_{d(off)}$	$I_C = 40\ A,\ ind.\ load$	–	400	–	ns
t_f	$R_{Gon} = R_{Goff} = 27\ \Omega$	–	45	–	ns
E_{on} [5]	$T_j = 125\ °C$	–	7	–	mWs
E_{off} [5]		–	4,5	–	mWs
Diodes [6]					
$V_F = V_{EC}$	$I_F = 40\ A$ $V_{GE} = 0\ V;$	–	1,85(1,6)	2,2	V
$V_F = V_{EC}$	$I_F = 50\ A$ $T_j = 25\ (125)\ °C$	–	2,0(1,8)	–	V
V_{TO}	$T_j = 125\ °C$	–	–	1,2	V
r_T	$T_j = 125\ °C$	–	–	22	$m\Omega$
I_{RRM}	$I_F = 40\ A;\ T_j = 25\ (125)\ °C$ [2]	–	23(35)	–	A
Q_{rr}	$I_F = 40\ A;\ T_j = 25\ (125)\ °C$ [2]	–	2,3(7)	–	μC
Thermal Characteristics					
R_{thjc}	per IGBT	–	–	0,4	°C/W
R_{thjc}	per diode	–	–	0,7	°C/W
R_{thch}	per module	–	–	0,05	°C/W

SEMITRANS 2

GB   GAL

Features
- MOS input (voltage controlled)
- N channel, Homogeneous Si
- Low inductance case
- Very low tail current with low temperature dependence
- High short circuit capability, self limiting to 6 $\times$ I_{cnom}
- Latch-up free
- Fast & soft inverse CAL diodes [8]
- Isolated copper baseplate using DCB Direct Copper Bonding Technology
- Large clearance (10 mm) and creepage distances (20 mm).

Typical Applications: → B 6 - 85
- Three phase inverter drives
- Switching (not for linear use)

[1] $T_{case} = 25\ °C$, unless otherwise specified
[2] $I_F = - I_C,\ V_R = 600\ V$, − di$_F$/dt = 800 A/μs. $V_{GE} = 0\ V$
[3] Use $V_{GEoff} = -5\ ...\ -15\ V$
[5] See fig. 2 + 3; $R_{Goff} = 27\ \Omega$
[8] CAL = Controlled Axial Lifetime Technology

Case and mech. data → B 6 - 86
SEMITRANS 2

APPENDIX C

PM3000ACE POWER ANALYSER

C.   Block diagram of PM3000ACE
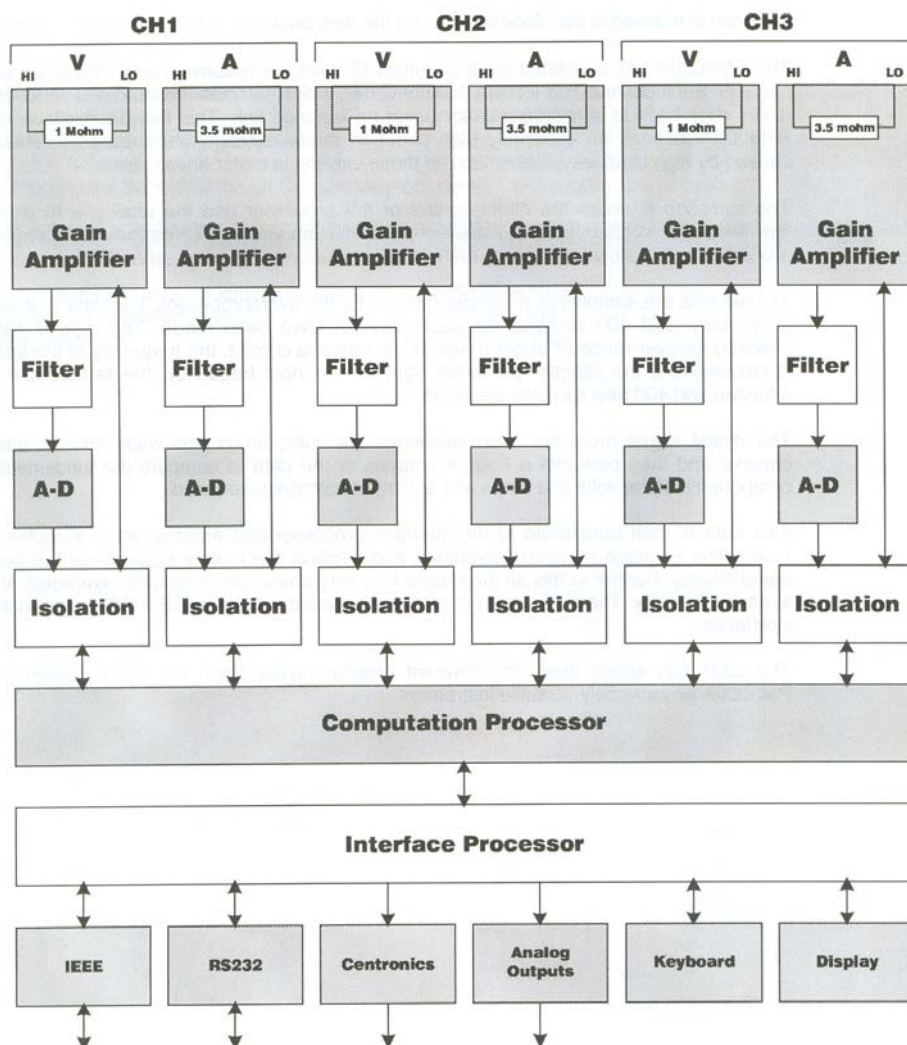
APPENDIX D

SIMULATION OF NEURAL NETWORK EFFICENCY OPTIMIZATION CONTROL

Equations of the induction motor, space vector PWM –voltage source inverter and neural network controller models are represented using the S-function and SIMULINK blocks. The S-function is written using C language and compiled as a MEX-file using *mex* utility (Mathwork, 1997).

D.1 Simulink Block of Induction Motor

The induction machine model used for the simulation is developed by equations (Wade *et al.*, 1994 and Nik-Idris, 2000):

$$V_{qs} = \frac{2}{3}V_{as} - \frac{1}{3}V_{bs} - \frac{1}{3}V_{cs} \tag{D.1}$$

$$V_{ds} = -\frac{1}{\sqrt{3}}V_{bs} + \frac{1}{\sqrt{3}}V_{cs} \tag{D.2}$$

$$\begin{bmatrix} \dot{i}_{sd} \\ \dot{i}_{sq} \\ \dot{i}_{rd} \\ \dot{i}_{rq} \end{bmatrix} = \frac{1}{L_m^2 - L_r L_s} \begin{bmatrix} R_s L_r & -\omega_r L_m^2 & & -\omega_r L_m L_s \\ \omega_r L_m^2 & R_s L_r & \omega_r L_m L_s & -R_r L_m \\ & \omega_r L_m L_s & R_r L_s & \omega_r L_m L_s \\ -\omega_r L_m L_s & R_s L_m & -\omega_r L_m L_s & R_s L_r \end{bmatrix} \begin{bmatrix} i_{sd} \\ i_{sq} \\ i_{rd} \\ i_{rq} \end{bmatrix} + \frac{1}{L_m^2 - L_r L_s} \begin{bmatrix} -L_r & 0 \\ 0 & L_r \\ L_m & 0 \\ 0 & L_m \end{bmatrix} \begin{bmatrix} V_{sd} \\ V_{sq} \end{bmatrix} \tag{D.3}$$

$$T_e = \frac{2}{3}\frac{p}{3} L_m \left(i_{rd} i_{sq} - i_{rq} i_{sd} \right) \qquad \text{(D.4)}$$

$$J \frac{d\omega_m}{dt} = J \frac{2}{p}\frac{d\omega_r}{dt} \qquad \text{(D.5)}$$

$$= T_e - T_{load} - \omega_r B \qquad \text{(D.6)}$$

The inputs to the induction motor Simulink block are the stator voltage and the rotor speed. The outputs are the stator rotor currents and electromagnetic torque. In this simulation the input power, mechanical power and efficiency also be calculated. The Simulink block of the induction motor is given in Figure D.1.
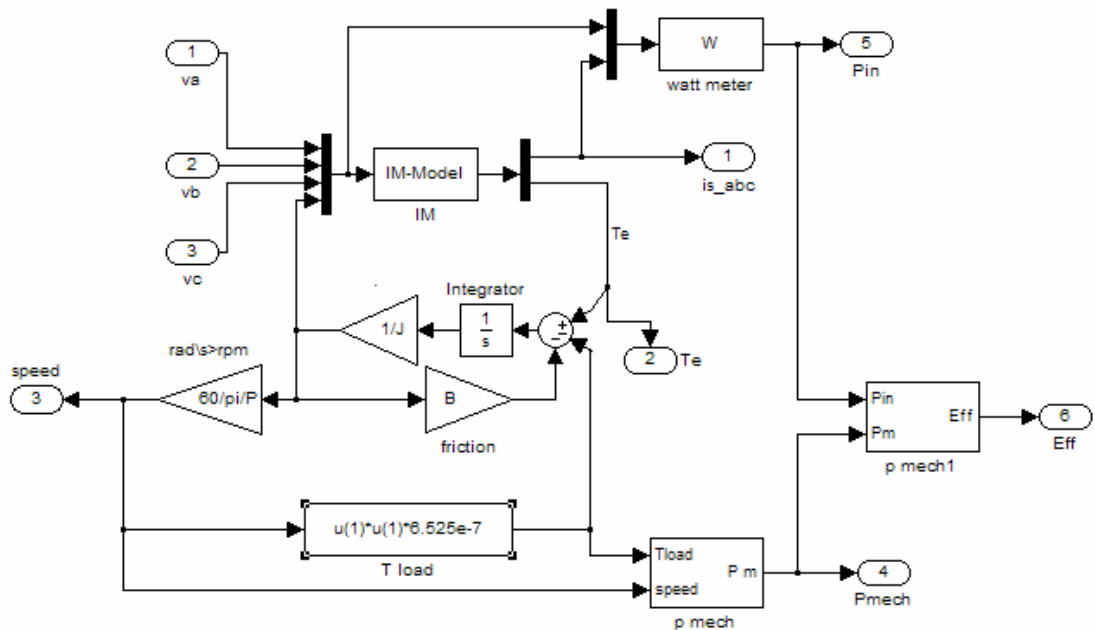
Figure D.1: Induction motor Simulink block

D.2   Simulink Block of Space Vector PWM

The representation of rotating vector in complex plane is shown in Figure D.2.
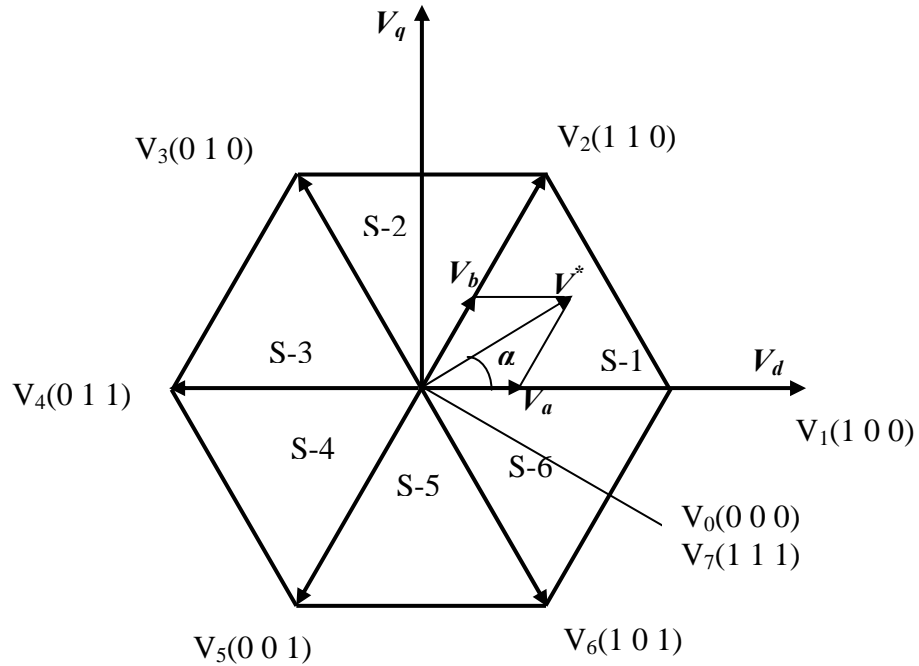
Figure D.2: Inverter state and switching plane

The required time duration can be calculated by following equation (Zhou and Wang, 2002):

Sector 1:

$$t_a = \frac{\sqrt{3}}{2} mT_s \cos(\alpha + \frac{\pi}{6}) \tag{D.7}$$

$$t_b = \frac{\sqrt{3}}{2} mT_s \cos(\alpha + \frac{3\pi}{2}) \tag{D.8}$$

Sector 2:

$$t_a = \frac{\sqrt{3}}{2} mT_s \cos(\alpha + \frac{11\pi}{6})$$

(D.9)

$$t_b = \frac{\sqrt{3}}{2} mT_s \cos(\alpha + \frac{7\pi}{6})$$

(D.10)

Sector 3:

$$t_a = \frac{\sqrt{3}}{2} mT_s \cos(\alpha + \frac{3\pi}{2})$$

(D.11)

$$t_b = \frac{\sqrt{3}}{2} mT_s \cos(\alpha + \frac{5\pi}{6})$$

(D.12)

Sector 4:

$$t_a = \frac{\sqrt{3}}{2} mT_s \cos(\alpha + \frac{7\pi}{6})$$

(D.13)

$$t_b = \frac{\sqrt{3}}{2} mT_s \cos(\alpha + \frac{\pi}{2})$$

(D.14)

Sector 5:

$$t_a = \frac{\sqrt{3}}{2} mT_s \cos(\alpha + \frac{5\pi}{6})$$

(D.15)

$$t_b = \frac{\sqrt{3}}{2} mT_s \cos(\alpha + \frac{\pi}{6})$$

(D.16)

Sector 6:

$$t_a = \frac{\sqrt{3}}{2} m T_s \cos(\alpha + \frac{\pi}{2})$$

(D.17)

$$t_b = \frac{\sqrt{3}}{2} m T_s \cos(\alpha + \frac{11\pi}{6})$$

(D.18)

$$t_0 + t_7 = T_s - t_a - t_b$$

(D.19)

The construction of the symmetrical pulse pattern for each switching period is shown in Figure D.3.

$t_0/2$	$t_a/2$	$t_b/2$	$t_0/2$	$t_0/2$	$t_b/2$	$t_a/2$	$t_0/2$
0	1	1	1	1	1	1	0
t_0	t_a	t_b	t_0	t_0	t_b	t_a	t_0
t_0	t_a	t_b	t_0	t_0	t_b	t_a	t_0
t_0	t_a	t_b	t_0	t_0	t_b	t_a	t_0
t_1	t_2	t_3	t_4		t_5	t_6	t_7

Figure D.3: Symmetrical switching state period for sector 1.

The switching sequence in Figure D.3 related to equations D.7-D.19 is given by:

$$t_1 = t_7 = \frac{t_0}{4} \tag{D.20}$$

$$t_2 = t_6 = \frac{t_a}{2} \tag{D.21}$$

$$t_3 = t_5 = \frac{t_b}{2} \tag{D.22}$$

The inputs to the space vector PWM Simulink block are the modulation index (voltage reference) and modulation frequency (frequency reference) signals. The outputs are the IGBT switching signal state. Then these signals are fed to voltage source inverter. The Simulink block of the space vector PWM and VSI are given in Figure D.4.
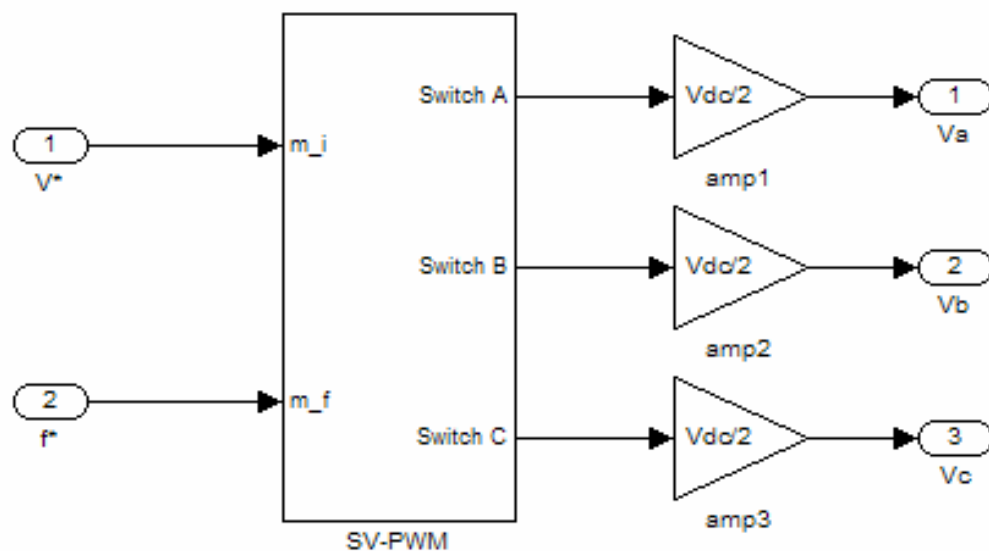
Figure D.4: Space Vector PWM and VSI Simulink block

Line to line fundamental voltage in rms is given by:

$$V_{ab} = \frac{\sqrt{3}}{\sqrt{2}} \frac{4}{\pi} \frac{V_{dc}}{2}$$

D.3 Simulink Block of Neural Network Controller

The neural network efficiency optimization controller used for the simulation is based on equations (2.22) - (2.60). Figure D.5 shows the Simulink block of the controller.
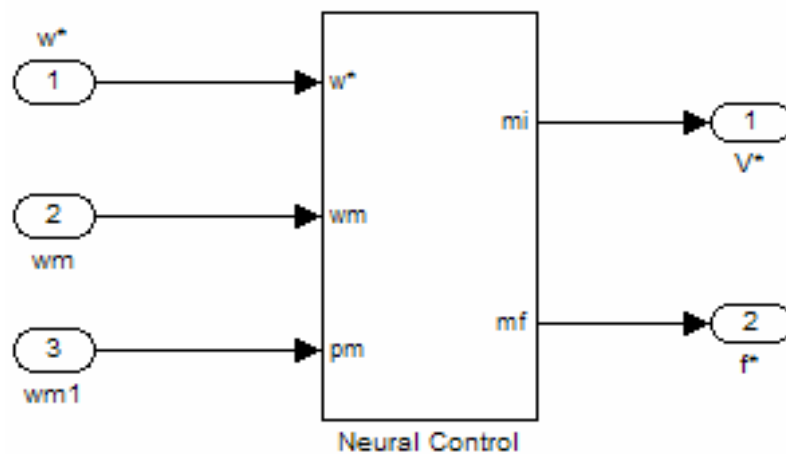
Figure D.5: Neural network controller Simulink block

APPENDIX E

SOURCE CODE LISTINGS

DSP source code listing for space vector pulse width modulation of the inverter

```
/*=====NNEOC.c ===================================/
* 1.  Space Vector PWM and                            *
* 2.  Neural Network Efficiency Controller            *
*     Using Levenberg Marquardt Algorithm             *
* Writen by Wahyu Mulyo Utomo                         *
*====================================================*/

#include <brtenv.h>
#include <math.h>
#define pi 3.141592654
#define DT 0.000150
#define DT2 0.01
#define input(u)  \
 ds1102_ad_start(); \
 in1=ds1102_ad(1);  \
 in2=ds1102_ad(2);    \
 in3=ds1102_ad(3);
```

```
#define output(y) \
 ds1102_da(1,ou1); \
 ds1102_da(2,ou2); \
 ds1102_da(3,ou3);


float exec_time;


int dcamin3a=0;
float dcamin3=0;


int spin1a=0;
float spin1=0;
float in1=5;
float in2=0;
float in3=0;
float ou1=0;
float ou2=0;
float ou3=0;


/* -------------------------------------------------- */
/* 1.  Softstart and Reference Variable --------------- */


int power_input();
        int signal_port=0;
        int on=2;
        int start=2;
        int control=0;
        float sp_on=300;
        int time_on=1;
        float sp_off=1450;
        int time_off=1;


int speed_ref();
   int sp_ref=1450;
```

```
    int sp_runref=145;
   float sp_nom=1450;
   float sp_min=500;
         int five=0;
         int six=0;
         int sev=0;
         int eig=0;
         int nine=0;
         int ten=0;
         int fteen=0;
   float sp_in=500;
         int up=0;
         int dw=0;


float inisnn();
float softst();
float run();
float svpwm();
float run_pin();


float softst()
{
if (sp_on<sp_nom){
        sp_on=sp_on+0.15;}


else {sp_on=sp_on;}
        mf=sp_on/sp_nom;
        mi=mf;
        annmf=mf;
        pinann=mi;
        sp_ref=sp_on;
        if (sp_ref>=sp_nom) {
                sp_ref=sp_nom;}
```

```
return;
}


int power_input()
{
  if (on==1){
  start=1;
  time_off=1;
  sp_off=sp_on;        }


  if (on==0){
  start=0;
       time_on=1;
  sp_on=300;   }
return;
}

float run()
{
       sp_ref=sp_runref*10;
              xin=sp_ref/30;
       mtrsp=rpm_rotor/30;
       errsp=(xin-mtrsp);


   if (annmf>0.25){
                     if (annmf>=1){
                            if (errsp<0){
                            learning();  }
       }
       else {
                     learning();}
      }
    else {
```

```
                        if (errsp>0){
                        learning();  }
                }
                neural_net();
return;
}


float run_pin()
{
        pin_ref();
        pin_sensor();
    scale_pin();

    if (pinann>0.25){
                        if (pinann>=1){
                                if (pinerr<0){
        learn_pin();  }}
        else {
                        learn_pin();}}
    else {
                        if (pinerr>0){
                        learn_pin(); }}

                nn_pin();
return;
}


float speed_sensor()
{
        rpm_rotor=rpminc;


return;
}
```

```
float speed_sensor();
        int rpm_rotor=1000;
        float mtrsp=0;
  int rpminc=0;
  int spinc1=0;
  float spinc2=0;
  int vinc=0;
  float rpmincft=0;
  int soinc=0;




/* -------------------------------------------------- */
/* 2. Space Vector - PWM  ---------------------------- */


        float mi=0;
        float mf=0;
  float freq=0;
  float period=0;


int counter();
        int q=0;


float sin_waves();
        int n=0;
        float w=0;
        float va=0;
        float vb=0;
  float vc=0;
        float vd=0;
  float vq=0;


float ampl_theta ();
        float amp=0;
  float ang=0;
```

```
int sector ();
        int sec=0;

float time_abnul();
        float ta=0;
   float tb=0;
   float tnul=0;
        float tcycle=0;
        float dtcycle=0;
        float tmax=0.0;
        float tabgain=0.7846;

int gate_abc ();
        float t_one=0;
        float t_two=0;
   float t_three=0;
        float t_four=0;
        float t_five=0;
   float t_six=0;
        float t_mdl1=0;
        float t_mdl2=0;
        float t_mdl3=0;
        int ga=0;
        int gb=0;
        int gc=0;
        int swA=0;
        int swB=0;
        int swC=0;

int enabl=0;
float vab=0;
float vbc=0;
float vca=0;
```

```c
int out;
int emergency=0;
int reset=0;


/* -------------------------------------------------- */
int counter()
{
        static int q=0;
  q++;
        if (q>(1/(mf*DT*50)))
    {q=0;}
  return(q);
}


/* ----------- Sine Wave Generations ------------------ */
float sine_waves ()
{
  freq=mf*50;
  period=1/freq;
  w=2*pi*mf*50;
  n=counter();
  va=mi*sin(n*w*DT);
  vb=mi*sin(n*w*DT-(120*pi/180));
  vc=mi*sin(n*w*DT+(120*pi/180));
  vd=(va-0.5*vb-0.5*vc)*2/3;
  vq=(vb-vc)/sqrt(3);

return;
}
```

```
/* ----------- Amplitude & Angle References ---------- */


float ampl_theta ()      {
amp=sqrt(vd*vd+vq*vq);


  if (vd>=0 && vq>=0){
               ang=atan(vq/vd);                          }
  else if (vd<0 && vq>=0){
     ang=pi+atan(vq/vd);                }
  else if (vd<0 && vq<=0){
               ang=-pi+atan(vq/vd);          }
  else{
               ang=atan(vq/vd);              }


return;
  }



/* ----------- Sector References --------------------- */


int sector ()      {
  if (ang>=0 && ang<=1.047){
  sec=3;
  ta=tabgain*mi*tmax*cos((3*pi/2)+ang);
  tb=tabgain*mi*tmax*cos((5*pi/6)+ang);   }
  else if (ang>1.047 && ang<=2.0944){
  sec=1;
  tb=tabgain*mi*tmax*cos((pi/6)+ang);
  ta=tabgain*mi*tmax*cos((3*pi/2)+ang); }
  else if (ang>2.0944 && ang<=3.1416){
  sec=5;
  ta=tabgain*mi*tmax*cos((5*pi/6)+ang);
  tb=tabgain*mi*tmax*cos((pi/6)+ang);  }
  else if (ang>-3.1416 && ang<=-2.0944){
```

```
    sec=4;
    tb=tabgain*mi*tmax*cos((7*pi/6)+ang);
    ta=tabgain*mi*tmax*cos((pi/2)+ang);    }
    else if (ang>-2.0944 && ang<=-1.047){
    sec=6;
    ta=tabgain*mi*tmax*cos((pi/2)+ang);
    tb=tabgain*mi*tmax*cos((11*pi/6)+ang);    }
    else{
    sec=2;
            tb=tabgain*mi*tmax*cos((11*pi/6)+ang);
    ta=tabgain*mi*tmax*cos((7*pi/2)+ang);
    }
return;
}


/* ----------- ta-tb-tnul generation ------------------ */

float time_abnul ()
{   tmax=1;
    dtcycle=0.102;
    tcycle=tcycle+dtcycle;
    if (tcycle>=tmax){
    tcycle=0;   }

    tnul=(tmax-ta-tb);
    if (tnul<0){
    tnul=0;}

return;
}
```

```
/* ----------- Gate generation ----------------------- */

int gate_abc () {
t_one=tnul/4;
t_two=(tnul/4)+(ta/2);
t_three=(tnul/4)+((ta+tb)/2);
t_four=(3*tnul/4)+((ta+tb)/2);
t_five=(3*tnul/4)+tb+((ta)/2);
t_six=(3*tnul/4)+ta+tb ;

if (tcycle<t_one || tcycle>t_six ){
  ga=0;
  gb=0;
  gc=0;   }

else {

if (sec==3){
  if (tcycle<t_two){
  ga=1;
  gb=0;
  gc=0;   }
  else if (tcycle<t_three){
  ga=1;
  gb=1;
  gc=0;   }
  else if (tcycle<t_four){
  ga=1;
  gb=1;
  gc=1;   }
  else if (tcycle<t_five){
  ga=1;
  gb=1;
  gc=0;   }
```

```
            else {
           ga=1;
           gb=0;
           gc=0;   }
 }

 if (sec==1){
             if (tcycle<t_two){
           ga=0;
           gb=1;
           gc=0;   }
           else if (tcycle<t_three){
           ga=1;
           gb=1;
           gc=0;   }
           else if (tcycle<t_four){
           ga=1;
           gb=1;
           gc=1;   }
           else if (tcycle<t_five){
           ga=1;
           gb=1;
           gc=0;   }
           else  {
           ga=0;
           gb=1;
           gc=0;   }
 }
 if (sec==5){
             if (tcycle<t_two){
           ga=0;
           gb=1;
           gc=0;   }
           else if (tcycle<t_three){
```

```
ga=0;

gb=1;

gc=1;   }

else if (tcycle<t_four){

ga=1;

gb=1;

gc=1;   }

else if (tcycle<t_five){

ga=0;

gb=1;

gc=1;   }

else {

ga=0;

gb=1;

gc=0;   }

}

if (sec==4){

        if (tcycle<t_two){

ga=0;

gb=0;

gc=1;   }

else if (tcycle<t_three){

ga=0;

gb=1;

gc=1;   }

else if (tcycle<t_four){

ga=1;

gb=1;

gc=1;   }

else if (tcycle<t_five){

ga=0;

gb=1;

gc=1;   }

else {
```

```
    ga=0;
    gb=0;
    gc=1;   }
  }
  if (sec==6){
    if (tcycle<t_two){
    ga=0;
    gb=0;
    gc=1;   }
    else if (tcycle<t_three){
    ga=1;
    gb=0;
    gc=1;   }
    else if (tcycle<t_four){
    ga=1;
    gb=1;
    gc=1;   }
    else if (tcycle<t_five){
    ga=1;
    gb=0;
    gc=1;   }
    else {
    ga=0;
    gb=0;
    gc=1;   }
  }

  if (sec==2){
    if (tcycle<t_two){
    ga=1;
    gb=0;
    gc=0;   }
    else if (tcycle<t_three){
    ga=1;
```

```
  gb=0;
  gc=1;   }
  else if (tcycle<t_four){
  ga=1;
  gb=1;
  gc=1;   }
  else if (tcycle<t_five){
  ga=1;
  gb=0;
  gc=1;   }
  else {
  ga=1;
  gb=0;
  gc=0;   }
}
}
return;
}




/* -------------------------------------------------- */
/* 3. Neural Network Controller ----------------------- */

float learning();
        float errsp=0;

        float dwasi=0;
        float dwbsi=0;
        float dwcsi=0;
        float dbasi=0;
        float dbbsi=0;
        float dbcsi=0;
```

```
        float dwasiold=0;
        float dwbsiold=0;
        float dwcsiold=0;

        float dbasiold=0;
        float dbbsiold=0;
        float dbcsiold=0;

        float erdwasi=0;
        float erdwbsi=0;
        float erdwcsi=0;
        float erdbsi=0;

float neural_net();
        float xin=0;
        float annmf=0.25;

        float wasi=0.0066;
        float wbsi=0.0044;
        float wcsi=0.0055;
        float walo=0.4043;
        float wblo=0.302;
        float wclo=0.353;
        float wate=0.384;
        float wbte=0.293;
        float wcte=0.34;

        float ba=0.0958;
        float bb=0.0958;
        float bc=0.0958;

float    pin_ref();
   float pinrunref=250;
   float pinref=250;
```

```
float pin_sensor();
    float pinin=0;
    float pinflt=0;
    int   pinint=0;
    float pinin2=0;


float scale_pin();
    float refpin=0;
    float pin=0;
    float pinerr=0;


float learn_pin();
            float efdwa=0;
            float efdwb=0;
            float efdwc=0;
            float efdba=0;
            float efdbb=0;
            float efdbc=0;


            float efdwao=0;
            float efdwbo=0;
            float efdwco=0;
            float efdbao=0;
            float efdbbo=0;
            float efdbco=0;


            float eferdwa=0;
            float eferdwb=0;
            float eferdwc=0;
            float eferdb=0;
```

```
float nn_pin();
        float pinann=0.25;


        float efwa1=0.4591;
        float efwb1=0.3682;
        float efwc1=0.2982;
        float efwa2=0;
        float efwb2=0;
        float efwc2=0;
        float efwa3=0;
        float efwb3=0;
        float efwc3=0;


        float efba=-0.08276;
        float efbb=-0.07485;
        float efbc=-0.06485;


float inisnn () {
        wasi=0.266;
        wbsi=0.2666;
        wcsi=0.2676;
        walo=0;
        wblo=0;
        wclo=0;
        wate=0;
        wbte=0;
        wcte=0;


        ba=0.07934;
        bb=0.08899;
        bc=0.09897;
```

```
        dwasi=0;
        dwbsi=0;
        dwcsi=0;
        dbasi=0;
        dbbsi=0;
        dbcsi=0;

   dwasiold=0;  // delta wa_old
        dwbsiold=0;
        dwcsiold=0;

        dbasiold=0;
        dbbsiold=0;
        dbcsiold=0;

   erdwasi=0;   // error delta (dwa-dwaol)
        erdwbsi=0;
        erdwcsi=0;
        erdbsi=0;

return;
}



float pin_sensor()
{
        pinin2=pinin;
return;
}
```

```
float pin_ref()
{
 pinrunref=(0.000215*sp_ref-0.18)*sp_ref+57;
  pinref=pinrunref;


return;
}


float scale_pin()
{
                refpin=pinref*0.0054;
        pin=pinin2*0.0054;
    efxin=pin
        pinerr=(refpin-pin);
return;
}



float learning()
{
        dwasi=(-errsp*(1-mtrsp*mtrsp)*wasi*alfa);
        dwbsi=(-errsp*(1-mtrsp*mtrsp)*wbsi*alfa);
        dwcsi=(-errsp*(1-mtrsp*mtrsp)*wcsi*alfa);

   dbsi=(-errsp*(1-mtrsp*mtrsp)*alfa);

   erdwasi=dwasi-dwasiold;
   erdwbsi=dwbsi-dwbsiold;
   erdwcsi=dwcsi-dwcsiold;

   dwasiold=dwasi;
   dwbsiold=dwbsi;
   dwcsiold=dwcsi;
   wasi=wasi+dwasi;
```

```
  wbsi=wbsi+dwbsi;

  wcsi=wcsi+dwcsi;


  ba=ba+dbsi;

  bb=bb+dbsi;

  bc=bc+dbsi;

return;

 }




/* ------------------------------------------------ */

/* 4. Levenberg Marquardt Learning  ------------------- */


float neural_net()

{

  walo=xin*wasi+ba;

  wblo=xin*wbsi+bb;

  wclo=xin*wcsi+bc;


  wate=(1-exp(-2*walo)/ (1+exp(-2*walo));

  wbte=(1-exp(-2*wblo)/ (1+exp(-2*wblo));

  wcte=(1-exp(-2*wclo)/ (1+exp(-2*wclo));


  annmf=wate+wbte+wcte;


      if (annmf<=0.25){

              annmf=0.25;

   }

      if (annmf>=1){

      annmf=1.0;

   }

return;

 }
```

```
float learn_pin()
{
        ej1=(1-efwa3*efwa3)*efxin;
        ej2=(1-efwb3*efwb3)*efxin;
        ej3=(1-efwc3*efwc3)*efxin;
        ej4=(1-efwa3*efwa3);
        ej5=(1-efwb3*efwb3);
        ej6=(1-efwc3*efwc3);

        eujjt=efalf+ej1*ej1+ej2*ej2+ej3*ej3+ej4*ej4+ej5*ej5+ej6*ej6;

        ejtj1=((eujjt-ej1*ej1)+ej2*ej2+ej3*ej3+ej4*ej4+ej5*ej5+ej6*ej6)*ej1;
        ejtj2=(ej1*ej1+(eujjt-ej2*ej2)+ej3*ej3+ej4*ej4+ej5*ej5+ej6*ej6)*ej2;
        ejtj3=(ej1*ej1+ej2*ej2+(eujjt-ej3*ej3)+ej4*ej4+ej5*ej5+ej6*ej6)*ej3;
        ejtj4=(ej1*ej1+ej2*ej2+ej3*ej3+(eujjt-ej4*ej4)+ej5*ej5+ej6*ej6)*ej4;
        ejtj5=(ej1*ej1+ej2*ej2+ej3*ej3+ej4*ej4+(eujjt-ej5*ej5)+ej6*ej6)*ej5;
        ejtj6=(ej1*ej1+ej2*ej2+ej3*ej3+ej4*ej4+ej5*ej5+(eujjt-ej6*ej6))*ej6;

        efdwa=(ejtj1*pinerr)/(efalf*eujjt);
        efdwb=(ejtj2*pinerr)/(efalf*eujjt);
        efdwc=(ejtj3*pinerr)/(efalf*eujjt);

        efdba=(ejtj1*pinerr)/(efalf*eujjt);
        efdbb=(ejtj2*pinerr)/(efalf*eujjt);
        efdbc=(ejtj3*pinerr)/(efalf*eujjt);

    efwa1=efwa1+efdwa;
    efwb1=efwb1+efdwb;
    efwc1=efwc1+efdwc;

    efba=efba+efdba;
    efbb=efbb+efdbb;
    efbc=efbc+efdbc;
```

```
    eferdwa=efdwa-efdwao;
    eferdwb=efdwb-efdwbo;
    eferdwc=efdwc-efdwco;


    efdwao=efdwa;
    efdwbo=efdwb;
    efdwco=efdwc;

return;
}



float nn_pin()
{
    efwa2=efxin*efwa1+efba;
    efwb2=efxin*efwb1+efbb;
    efwc2=efxin*efwc1+efbc;


    efwa3=(1-exp(-efwa2)/ (1+exp(-efwa2));
    efwb3=(1-exp(-efwb2)/ (1+exp(-efwb2));
    efwc3=(1-exp(-efwc2)/ (1+exp(-efwc2));


    pinann=efwa3+efwb3+efwc3;

        if (pinann<=0.25){
                pinann=0.25;
    }
        if (pinann>=1){
        pinann=1.0;
    }
return;
}
```

```
/* ------------------------------------------------- */
/* --- Sub-Main_t1 Program --------------------------- */

void sv_gen1 ()
{
power_input();
speed_sensor();
pin_sensor();

if (start==1){
        if (control==0){
        softst();
    sp_runref=145;
    pinrunref=250;
    pinref=250;         }


        if (control==1){
    run();
    run_pin();
                mf=annmf;
        mi=pinann;
  }


        if (control==2){
    run();
                mf=annmf;
        mi=mf;
  }


}
```

```
if (start==0){
   sp_on=300;
   control=0;
        sp_runref=145;
        sp_off=sp_ref;
        sp_ref=sp_nom;
   mf=0.24;
        mi=0.24;
        inisnn ();}
return;
}




/* -------------------------------------------------- */
/* --- Sub-Main_t0 Program --------------------------- */

float svpwm()
{
        sine_waves ();
        ampl_theta();
   sector();
        time_abnul();
   gate_abc ();
        enabl=1;


return;
}

void sv_gen ()
{
        if ((mf>=0.25)&&(mi>=0.25))
   {
   svpwm ();
   }
```

```
else {
  ga=0;
  gb=0;
  gc=0;
       enabl=0;}


  vab=ga-gb;
  vbc=gc-gb;
  vca=gc-ga;

return;
}



/* -------------------------------------------------- */
/* --- Main_t0 Program ------------------------------ */


void isr_t0()                          /*timer0 interrupt service routine*/
{
  out=(ga*1)+(gb*2)+(gc*4);                /*output switching gates*/
  ds1102_p14_pin_io_write(out);



       isr_t0_begin();                  /*overload check*/
  host_service(1,0);                    /*call TRACE service*/
  tic0_start();               /*start execution time measurement*/


       sv_gen();


  exec_time=tic0_read();                /*calculate execution time*/
  isr_t0_end();               /*end of interrupt service routine*/
}
```

```
/* ------------------------------------------------- */
/* --- Main_t1 Program ----------------------------- */

void isr_t1()                              /*timer1 interrupt service routine*/
{
        isr_t1_begin();                    /*overload check*/
    host_service(1,0);                     /*call TRACE service*/

    input(u);
    pinflt=12.35*in3;
        pinint=pinflt*100;
    pinin=pinint;

    rpmincft=15.81*in1;
    rpminc=rpmincft*1000;

    output(ou1);
    output(ou2);

    ou1=mf/2;                                    /*output NN Speed controller*/
    ou2=mi/2;

        sv_gen1();

    isr_t1_end();                          /*end of interrupt service routine*/
}

void main ()
{
        init();
    ds1102_p14_pin_io_init(0xffff);
    msg_info_set(MSG_SM_RTLIB, 0, "System started.");

    isr_t0_start(DT);
```

```
isr_t1_start(DT2);

while (1)
{
     while (msg_last_error_number()==DS1102_NO_ERROR)
  {
     host_service (0,0);
  }
  isr_t0_disable();
  isr_t1_disable();

  while (msg_last_error_number()!=DS1102_NO_ERROR)
  {
     host_service (0,0);
  }
  isr_t0_enable();
 }
}
```

LIST OF PUBLICATION

1. Utomo, W.M., and Mohd Yatim. A.H. (2003). Efficiency Optimization of Induction Motor Drive for Air Conditioning Compressor Load Using Neural Network. Seminar on Artificial Intelligent Application in Industry (AIAI 2003). Kuala Lumpur, Malaysia. June 24-25.

2. Utomo, W.M., and Mohd Yatim. A.H. (2004). On Line Optimal Control of Variable Speed Compressor Motor Drive System Using Neural Control Model. Proceeding on the Second National Power and Energy Conference (PECon) 2004. Kuala Lumpur, Malaysia. 29 and 30 November 2004.

3. Utomo, W.M., and Mohd Yatim. A.H. (2005), Neuro Fuzzy On-Line Optimal Energy Control Variable speed compressor motor drive system. Proceeding on the Sixth International Conference on Power Electronics and Drive Systems (PEDS 2005), Kuala Lumpur, Malaysia, 28 Nov - 1 Dec 2005.

4. Utomo, W.M., and Mohd Yatim. A.H. (2006), Efficiency Optimization of Variable Speed Induction Motor Drive Using Real Time Neural Network. International Review of Electrical Engineering, (Accepted paper, reference number IREE 02-07).

5. Utomo, W.M., and Mohd Yatim. A.H. (2006), Online Neural Network Based Efficiency Optimization of a Variable Speed Compressor Motor Drive. International Journal of Knowledge-Based and Intelligent Engineering Systems, (Accepted paper, reference number KESJj06-038).

6. Utomo, W.M., and Mohd Yatim. A.H. (2006), Efficiency Optimization of Variable Speed Induction Motor Drive Using Online Backpropagation. Proceeding on the First International Power and Energy Conference (PECon 2006), Kuala Lumpur, Malaysia, 28 and 29 November 2006

REFERENCES

Abdin, E.S.; Ghoneem, A.S.; Diab H.M.M. and Desaz S.A. (2003). Efficiency Optimization of a Vector Controlled Induction Motor Drive an Artificial Neural Network. *Proceedings of IEEE-IECON Conference.* 2543-2548.

Abrahamsen, F.; Blaabjerg, F.; Pedersen, J.K. and Grabowski, P.Z. (1998). On the Energy Optimized Control of Standard and High Efficiency Induction Motors in CT and HVAC Application. *IEEE Transaction on Industrial Application.* 34(4): 822-831.

Abrahamsen, F. (2000). *Energy Optimal Control of Induction Motor Drives*. Institute of Energy Technology, Aalborg University. PhD Thesis.

Abrahamsen, F.; Blaabjerg, F.; Pedersen, J.K.; Pedersen, J.K. and Thoegersen, P.B. (2001). Efficiency-Optimized Control of Medium-Size Induction Motor Drives. *IEEE Transaction on Industrial Application.* 37(6): 1761-1767.

Ampazis, N. and Perantonis, S.J. (2002). Two Highly Efficient Second-Order Algorithms for Training Feedforward Networks. *IEEE Transactions on Neural Networks*. 13(5): 1064-1073.

Astrom, K.J. and Wittenmark, B. (1995). *Adaptive Control.* USA, Addison-Wesley Longman Publishing Co Inc.

Bahera, L.; Kumar, S. and Awhan, P. (2006). On Adaptive Learning Rate that Guarantees Convergence in Feedforward Networks. *IEEE Transaction on Neural Networks.* 17(5): 1116-1125.

Bernal, F. F.; Cerrada, A. G. and Faure, R. (2000). Model-based loss minimization for DC and AC vector-controlled motors including core saturation. *IEEE Transaction on Industrial Application.* 36: 755–763.

Blanusa, B. and Vukasovic, N. (2003). An Improved Search Based Algorithm for Efficiency Optimization in the Induction Motor Drives. *Proceeding of ETRAN Conference.* XLVII(1): 417-420.

Boldea, I. and Nasar, S.A. (2002). *The Induction Machine Handbook.* Florida, CRC Press.

Bose, B. K. (1982). Adjustable Speed AC Drives-A Technology Status Review. *Proceeding of IEEE.* 70(2): 116-139.

Bose, B. K.; Patel, N. R. and Rajashekara, K. (1997). A Neuro-Fuzzy-based On-line Efficiency Optimization Control of a Stator Flux-Oriented Direct Vector-Controlled Induction Motor Drive. *IEEE Transaction on Industrial Application.* 44(2):270–273.

Bose, B.K. (1997). High Performance Control and Estimation in AC Drives. *Proceeding of IEEE-IECON.* 2: 377-385.

Bose, B. K. (2000). Energy, Environment, and Advances in Power Electronics. *IEEE Transaction on Power Electronics.* 15(4):668–701.

Bose, B. K. (2001). *Modern Power Electronics and AC Drives.* NJ, Prentice Hall PTR.

Cabrera, J.B.D. and Narendra, K.S. (1999). Issues in the Application of Neural Networks for Tracking Based on Inverse Control. *IEEE Transactions on Automatic Control.* 44(11): 2007-2027.

Callcut, V; Chapman, D.; Heathcote, M. and Parr, R. (1997). *Electrical Energy Efficiency*. CDA Publishing.

Chakraborty, C. and Hori, Y. (2003). Fast Efficiency Optimization for the Indirect Vector-Controlled Induction Motor Drives. *IEEE Transaction on Industrial Application.* 39(4): 1070-1076.

Chakraborty, C.; Uchida, T. and Hori, Y. (2002). Fast Search Controllers for Efficiency Maximization of Induction Motor Drives Based on DC Link Power Measurement. *Proceedings of IEEE-Power Conversion Conference.* 2: 402-408.

Chen, S. and Yeh, S-N. (1992). Optimal Efficiency Analysis of Induction Motor By Variable-Voltage and Variable Frequency. *IEEE Transactions on Energy Conversion.* 7(3): 537-543.

Chen, S.L. and Tsay, M.T. (2004). The Electricity Saving by Using Probabilistic Neural Network for Room Air Conditioners. *Proceedings of IEEE-TENCON Conference.* 3: 516-519.

Choy, I.; Kwon, S.H.; Choi, J.Y.; Kim, J.W., and Kim, K.B. (1996). On-Line Efficiency Optimization Control of a Slip Angular Frequency Controlled Induction Motor Drive Using Neural Networks. *Proceeding of IEEE-IECON Conference.* 13: 1216-1221.

Cirstea, M.N.; Dinu, A.; Khor, J.G. and McCormick, M. (2002). *Neural and Fuzzy Logic Control of Drives and Power Systems*. Great Britain, Newnes Publications.

Cleland, J.G.; McCormick, V.E. and Turner, M.W. (1995). Design of an Efficiency Optimization Controller for Inverter-fed AC Induction Motors. *IEEE -Industry Applications Conference*. 1: 16 -21.

Cleland, J.G. and Turner, M.W. (1996). Fuzzy Logic Control of Electric Motors and Motor Drives: Feasibility Study. *Environmental Protection Agency*. 175: 1-5.

Couto, C.M. and Martin, J.S. (1994). Control of a Voltage Source Inverter Fed Induction Motor with On-Line Efficiency Optimization. *Proceeding of IEEE-Industrial Technology Conference*. 528–532.

Dabala, K. (2001). Analysis of Mechanical Losses in Three-Phase Squirrel-Cage Induction Motor. *Proceeding of IEEE-ICEMS Conference.* 1:39-42.

Domijan, A.; Hanhock, O. and Maytrott, C. (1992). A Study and Evaluation of Power Electronic Based Adjustable Speed Motor Drives for Air Conditioners and Heat Pumps whit an Example Utility Case Study of the Florida Power and Light Company. *IEEE Transactions on Energy Conversion*. 7(3): 396-404.

dSPACE GmbH. (1996). *Floating Point Control Board*. User's Guide.

Emadi, A. (2005). *Handbook of Automotive Power Electronics and Motor Drives.* NW, CRC Press.

Famouri, P. and Cathey, J. L. (1991). Loss minimization control of an induction motor drive. *IEEE Transactions on Industrial Application*. 27(1): 32–37.

Garcia, G.; Luiz; J.; Stephan, R. and Watanabe, E. (1994). An Efficient Controller for an Adjustable Speed Induction Motor Drive. *IEEE Transactions on Industrial Electronics*. 41(5): 533-539.

Grigsby, L.L. (2001). *The Electric Power Engineering Handbook.* NW, CRC-IEEE Press.

Gupta, M.M. and Sinha, N.K. (1996). *Intelligent Control Systems Theory and Applications.* Piscataway, NJ, IEEE Press.

Hagan, M.T. and Menhaj, M.B. (1994). Training Feedforward Networks with the Marquardt Algorithm. *IEEE Transaction on Neural Networks.* 5(6): 989-993.

Hagan, M.T.; Demuth, H.B. and Beale, M. (1995). *Neural Network Design.* Boston, PWS Publishing Company.

Hasan, K.M.; Zhang, L. and Singh, B. (1997). Neural Network Aided Energy Efficiency Control for a Field Orientation Induction Motor Drive. *Proceedings of IEEE-IECON Conference*. 13: 488-492.

Haykin, S. (1994). *Neural Network, A Comprehensive Foundation*. New York, Macmillan College Publishing Company.

Huang, T.C. and El-Sharkawi, M.A. (1996). Induction Motor Efficiency Maximizer using Multi-Layer Fuzzy Control. *Proceedings of IEEE-Intelligent System Applications to Power Systems Conference*. 109-113.

IEEE Std 112. (2004). *IEEE Standard Test Procedure for Polyphase Induction Motors and Generators*. New York, IEEE Power Engineering Society.

Johnson, F.X.; Brown, R.E.; Hanford, J.W.; Sanstad A.H. and Koomey, J.G. (1994). *Residential HVAC Data, Assumptions and Methodology for End-Use Forecasting with EPRI-REEPS 2.1.* USA, Lawrence Berkeley Laboratory.

Kioskederis, I. and Margaris, N.. (1996). Loss Minimization in Induction Motor Adjustable Speed Drives. *IEEE Transactions on Industrial Electronics.* 43(1): 226-231.

Kioskederis, I. and Margaris, N.. (1996). Loss Minimization in Scalar Control Induction Motor Drives with Search Controllers. *IEEE Transactions on Power Electronics.* 11(2): 213-220.

Leidhold, R. and Garcia, G. (1998). Losses Minimization in a Variable Speed Field-Oriented Controlled Induction Generator. *Proceedings of IEEE-IECON Conference.*2: 865-870

Leondes, C.T (2003). *Intelligent Systems: Fuzzy Systems, Neural Networks and Expert System*. Florida, CRC.

Loewen, J.M.; Levine, M.D. and Busch, J.F. (1992). *Audits in ASEAN-USAID Building Energy Conservation.* USA, Lawrence Berkeley Laboratory.

Lu Z.Y. (1996). *Industrial Intelligent Control*. England, John Willey and Son Ltd.

Mathwork Inc. (1997). *Simulink User's Guide*. Massachusetts, USA.

Mills, P.M.; Zomaya, A.Y. and Tode, M.O. (1996). *Neuro Adaptive Process Control*. England, John Willey and Son Ltd.

Mohan, N., Undeland, T., and Robbins, W. (1995). *Power Electronics: Converters, Applications, and Design*. New York, John Wiley & Sons.

Moreno-Equitaz, J.; Cipolla, M. and Paracaula, J. (1997). Fuzzy Logig Based Improvements in Efficiency Optimization of Induction Motor Drives. *Proceedings of FUZZ-IEEE*. 219-224.

Murphy, J.M.D. and Turnbull, F.G. (1988). *Power Electronic Control of AC Motors*. NY, Pergamon Press.

Narendra, K.S. and Annaswamy, A.M.(1989). *Stable Adaptive Systems*. NJ, Prentice-Hall Publisher.

Narendra, K.S. and Parthasarathy, K. (1990). Identification and Control of Dynamical Systems Using Neural Networks. *IEEE Transactions on Neural Networks*. 1(1): 4-27.

Nik Idris, N.R. (2000). *Improved Performance of Direct Torque Control of Induction Machines*. Department of Energy Conversion, Universiti Teknologi Malaysia. PhD Thesis.

Ohnishi, T.; Miyazaki, H. and Okitsu, H. (1988). High Efficiency Drive of an Induction Motor by Means of V/F Ratio Control. *Proceeding of IEEE-IECON Conference.* 3: 780-785.

Omatu, S.; Khalid, M. and Yusof, R. (1996). *Neuro-Control and Its Applications.* UK, Springer-Verlag London Limited.

Pryymak, B.; Moreno-Eguilaz, J.M. and Petracaula, J. (2005). An Efficient Energy Controller for Induction Motor Drive With Compensation of Temperature Using Neural Networks. *Proceedings of EPE*. 1-10.

Rashid, M. H. (1993). *Power Electronics, Circuits, Devices, and Applications*. NJ, Prentice-Hall Publisher.

Rice, D. E. (1988). A Suggested Energy-Savings Evaluation Method for AC Adjustable-Speed Drive Applications. *IEEE Transaction on Industrial Application*. 244(6): 1107-1117.

Sen, P.C. (1990). Electric Motor Drives and Control-Past, Present and Future. *IEEE Transactions on Industrial Electronics*. 37(6): 562-575.

Sen, P.C.; Namudiri, C.S. and Nandam, P.K. (1996). Evaluation of Control Techniques for Industrial Drives. *Proceedings of Power Electronics, Drives and Energy Systems for Industrial Growth Conference*. 2: 869-875.

Sen, P.K. and Landa, H.A.(1990). Derating of Induction Motors Due to Waveform Distortion. *IEEE Transactions on Industrial Application*. 26(6): 1102-1107.

Shepherd, W.; Hulley, L.N. and Liang, D.T.W. (1995). *Power Electronics and Motor Control*. UK, Cambridge University Press.

Skvarenina, T.L. (2002). *The Power Electronics Handbook*. Florida, CRC Press.

Sousa, G.C.D.; Bose, B.K.; and Cleland, J.G. (1992). Loss Modeling of Converter Induction Machine System For Variable Speed Drive. *Proceeding of IEEE-IECON*. 114-120.

Sousa, G.C.D.; Bose, B.K.; and Cleland, J.G. (1995). Fuzzy Logic Based On-line Efficiency Optimization Control of an Indirect Vector-Controlled Induction Motor Drive", *IEEE Transactions on Industrial Electronics*. 42(2): 192-198.

Spooner, J.T.; Maggiore, M.; Ordonez, R. and Passino, K.M. (2002). *Stable Adaptive Control and Estimation for Nonlinear Systems: Neural and Fuzzy Approximator Techniques.* USA, John Wiley and Sons, Inc Publication.

Stebbins, W.L. (1994). Are You Certain You Understand the Economics for Applying ASD Systems to Centrifugal loads? *Proceeding of IEEE-Textile, Fiber and Film Industry Technical Conference.* 1-8.

Sul, S. K. and Park, M. H. (1988). A Novel Technique for Optimal Efficiency Control of a Current Source Inverter fed Induction Motor. *IEEE Transactions on Power Electronics.* 3: 192–199.

Ta, C.M. and Hori, Y. (2001). Convergence Improvement of Efficiency Optimization Control of Induction Motor Drives. *IEEE Transaction on Industrial Application.* 37(6): 1746-1753.

Trzynadlowski A.M. and Legowski S. (1994). Minimum-Loss Vector PWM Strategy for Three Phase-Inverter. *IEEE Transactions on Industrial Electronics*, vol. 9(1):26-34.

Umans, S.D. (2004). AC Induction Motor Efficiency. *Proceedings of Electrical Electronics Insulation Conference.* 19:9-107.

Valentine, R. (1998). *Motor Control Electronics Handbook.* New York, McGraw-Hill.

Vas, P. (1999). *Artificial-Intelligent-Based Electrical Machines and Drives.* New York, Oxford University Press.

Voltech Instruments. (1996). *Power Analyzer PM3000ACE.* User's Guide.

Vukosavic, S.N. and Levi E. (2003). Robust DSP-Based Efficiency Optimization of a Variable Speed Induction Motor Drive. *IEEE Transactions on Industrial Electronics*. 50(3): 560-570.

Wade, S.; Dunnigan, M.W. and Williams, B. M. (1994). Simulation of Induction Machine Vector Control and Parameters Identification. *Proceeding of IEEE-Power Electronics and Variable Speed Drives*. 339: 42-47.

Wasynczuk, 0.; Sudhoff, S. D.; Corzine, K. A.; Tichenor, J.L.; Krause, P. C. ; Hamen, I. G. and Taylor, L. M.. (1998). A Maximum Torque per Ampere Control Strategy for Induction Motor Drives. *IEEE Transactions on Energy Conversion*. 13(2): 163-169.

Widrow B. and Lehr M.A. (1990), 30 years of adaptive neural networks: perception, madaline and backpropagation. *Proceedings of the IEEE*, 78: 1441-1457.

Wilamowski, B.M. (2003). Neural Network Architecture. *Proceeding of IEEE-Industrial Technology Conference*. 1: 1–12.

Wilamowski, B.M.; Chen, Y. and Malimowski, A. (1999). Efficiency Algorithm for Training Neural Networks with one Hidden Layers. *Proceeding of IEEE-IJCNN Conference*. 3:1725–1728.

Wilamowski, B.M.; Iplikci, S.; Kaynak, O. and Efe, M.O. (2001). An Algorithm for Fast Convergence in Training Neural Networks. *Proceeding of IEEE-IJCNN Conference*. 1778–1782.

Zhang, L. and Hasan, K.M. (1999). Energy Saving in Electric Motor Drives using Neural Networks. *Proceedings of IEEE-Electrical Machines and Drives Conference*.9: 356-360.

Zhou, K. and Wang, D. (2002). Relationship Between Space Vector Modulation and Three Phase Carrier based PWM: A Comprehensive Analysis. *IEEE Transactions on Industrial Electronics.* 49(1): 186-195.

Zidani, F.; Said, M.S.N; Abdessemed, R.; Diallo, D. and Benbouzid, M.E.H. (2002). A Fuzzy Technique for Loss Minimization in Scalar Controlled Induction Motor." *Electric Power Components and System-Taylor & Francis.* 30(6): 625-635.

UNIVERSITI TEKNOLOGI MALAYSIA
Research Management Centre

PRELIMINARY IP SCREENING & TECHNOLOGY ASSESSMENT FORM
(To be completed by Project Leader submission of Final Report to RMC or whenever IP protection arrangement is required)

1. **PROJECT TITLE IDENTIFICATION** :

   To Develop an Efficient Variable Speed Compressor Motor System

   Vote No: | 74535 |

2. **PROJECT LEADER** :

   Name : Prof. Dr. Abdul Halim Mohd Yatim

   Address: Fakulti Kejuruteraan Elektrik , Universiti Teknologi Malaysia
   Skudai, Johor Baru 81310

   Tel   : 07-5535202   Fax : 07-5566272   e-mail : halim@ieee.org

3. **DIRECT OUTPUT OF PROJECT** *(Please tick where applicable)*

Scientific Research	Applied Research	Product/Process Development
☐ Algorithm	☑ Method/Technique	☐ Product / Component
☐ Structure	☑ Demonstration / Prototype	☐ Process
☐ Data		☐ Software
☐ Other, please specify	☐ Other, please specify	☐ Other, please specify
_____	_____	_____
_____	_____	_____
_____	_____	_____

4. **INTELLECTUAL PROPERTY** *(Please tick where applicable)*

   ☐ Not patentable ☐ Technology protected by patents

   ☐ Patent search required ☐ Patent pending

   ☐ Patent search completed and clean ☐ Monograph available

   ☐ Invention remains confidential ☐ Inventor technology champion

   ☐ No publications pending ☐ Inventor team player

   ☐ No prior claims to the technology ☑ Industrial partner identified

5. LIST OF EQUIPMENT BOUGHT USING THIS VOT

1. Dynamometer

2. DC Suppy

3. Computer

4. Laser Jet Printer

5. Power Semiconductor Device

6. Electronic Components

7. Mechanical Components and Tools

6. STATEMENT OF ACCOUNT

a)   APPROVED FUNDING   RM : 400,000

b)   TOTAL SPENDING   RM : 400,000

c)   BALANCE   RM : 0

7. TECHNICAL DESCRIPTION AND PERSPECTIVE

Please tick an executive summary of the new technology product, process, etc., describing how it works. Include brief analysis that compares it with competitive technology and signals the one that it may replace. Identify potential technology user group and the strategic means for exploitation.

a)   Technology Description

This project includes the modelling, simulation and development of a variable speed compressor motor drive. This project proposes a method that improves the efficiency of the variable speed induction motor for driving compressor load by controlling the motor flux. A digital signal processor (DSP) based on online learning neural network efficiency optimization control is developed. The controller is designed to generate optimum flux by controlling both the stator voltage and frequency. The simulation is verified by experimental test. The results obtained clearly show that the efficiency at low speed is significantly increased. The project has also produced 1 PhD graduate and also involved a number of final year undergraduate students.

b)   Market Potential

For the future, the energy cost will raise and the people were looking for the product with high efficiency. Therefore this product very potential, because compared to the existing product efficiency of this research product is significantly increased.

c)   Commercialisation Strategies

A Number of local variable speed compressor motor drive manufactures are aware of this project and they interested to proceed further for commercialisation aspect.

8.   RESEARCH PERFORMANCE EVALUATION

a)   FACULTY RESEARCH COORDINATOR

Research Status	( )	( )	( )	( )	( )	( )
Spending	( )	( )	( )	( )	( )	( )
Overall Status	( )	( )	( )	( )	( )	( )
	Excellent	Very Good	Good	Satisfactory	Fair	Weak

Comment/Recommendations:

_____
_____
_____
_____
_____
_____

…………………………………………   Name : ……………………………………

Signature and stamp of   Date   : ……………………………………
JKPP Chairman

b)   RMC EVALUATION

Research Status   ( )   ( )   ( )   ( )   ( )   ( )
Spending   ( )   ( )   ( )   ( )   ( )   ( )
Overall Status   ( )   ( )   ( )   ( )   ( )   ( )
                  Excellent Very Good Good Satisfactory Fair   Weak

Comments:-

_____

_____

_____

_____

_____

_____

Recommendations:

☐   Needs further research

☐   Patent application recommended

☐   Market without patent

☐   No tangible product. Report to be filed as reference

…………………………………..   Name : ………………………………………
Signature and Stamp of Dean /   Date : ………………………………………
Deputy Dean
Research Management Centre

End of Project Report

<table>
<tr><td>

A.   **Project number :**

Project title: To Develop An Efficient Variable Speed Compressor Motor System

Project leader: Prof. Dr. Abdul Halim Mohd Yatim

Tel: 07-5535202   **Fax:** 07-5566272

</td></tr>
<tr><td>

B.   **Summary for the MPKSN Report** (for publication in the Annual MPKSN Report, please summarise the project objectives, significant results achieved, research approach and team strucure)

This project includes the modelling, simulation and development of a variable speed compressor motor drive. This project proposes a method that improves the efficiency of the variable speed induction motor for driving compressor load by controlling the motor flux. A digital signal processor (DSP) based on online learning neural network efficiency optimization control is developed. The controller is designed to generate optimum flux by controlling both the stator voltage and frequency. The simulation is verified by experimental test. The results obtained clearly show that the efficiency at low speed is significantly increased. The project has also produced 1 PhD graduate and also involved a number of final year undergraduate students.

</td></tr>
</table>

C. **Objectives achievement**

- **Original project objectives** (Please state the specific project objectives as described in Section ll of the Application Form)

  To develop an efficient variable speed compressor motor drive.

- **Objectives Achieved** (Please state the extent to which the project objectives were achieved)

  The project objectives have been met whereby a small scale laboratory working prototype was tested and working satisfactorily.

- **Objectives not achieved** (Please identify the objectives that were not achieved and give reasons)

  None

D. **Technology Transfer/Commercialisation Approach** (Please describe the approach planned to transfer/commercialise the results of the project)

Technology and expertise obtained from the outputs of the project can be transferred through collaboration work with the variable speed compressor motor drive industries. Such industries in Malaysia should take this opportunity as part of their strategies in facing future energy saving product competition. Thus collaboration is also needed with other organizations or industries that are focus on the application of variable speed compressor drive such as air conditioning or refrigeration manufacturing.

E. Benefits of the Project (Please identify the actual benefits arising from the project as defined in Section lll of the Application Form. For examples of outputs, organisational outcomes and sectoral/national impacts, please refer to Section lll of the Guidelines for the Application of R&D Funding under IRPA)

- **Outputs of the project and potential beneficiaries** (Please describe as specifically as possible the outputs achieved and provide an assessment of their significance to users)

The following outputs should be achieved by the project:
- A new conceptual design of a variable speed compressor motor drive with high efficiency for low speed operation.

- A New control technique that improve the efficiency of the variable speed compressor motor drive and maintain the speed output of the motors according to the speed reference command.

- The direct beneficiaries of the project are the efficient variable speed compressor motor drive system.

- **Organisational Outcomes** (Please describe as specifically as possible the organisational benefits arising from the project and provide an assessment of their significance)

Contributions of the project on the level of the research organization are highlighted as follows:
- 1 PhD degree and 1 research staff with new specialization
- Royalties from consultation work that can be offered by the researchers based on the technology, experience and expertise obtained from the project.
- Better facilities which include new equipments and staffs with practical expertise and experience in Energy Conversion Department, UTM as a result of the hardware development of the controller.
  The Energy Conversion Department, UTM get recognition as a local center with expertise and experience in the development of efficient variable speed compressor motor drive, where the variable speed compressor industries can opt to refer to, instead of depending on foreign expertise.

- **National Impacts** (If known at this point in time, please describes specifically as possible the potential sectoral/national benefits arising from the project and provide an assessment of their significance)

Contribution of the project on the national level:

- In modern countries like Japan, U.S.A and Europe active moving towards commercialization of efficient variable speed compressor motor drive, output of the project can definitely be a stepping stone for Malaysia towards linkages with these foreign research institutions as a platform in exchanging ideas and experience.

F.   Assessment of project structure

- **Project Team** (Please provide an assessment of how the project team performed and highlight any significant departures from plan in either structure or actual man-days utilised)

There is no problem of manpower as the researcher is a PhD candidate.

- **Collaborations** (Please describe the nature of collaborations with other research organisations and/or industry)

Technical drive was also granted from Compressor Laboratory of Mechanical Faculty, UTM in term of ideas and suggestions

G.   Assessment of Research Approach (Please highlight the main steps actually performed and indicate any major departure from the planned approach or any major difficulty encountered)

Research approach follows as planned

H.   Assessment of the Project Schedule (Please make any relevant comment regarding the actual duration of the project and highlight any significant variation from plan)

The project schedule duration was extended due to the long process of purchasing of components and equipment especially from overseas whereby approval was need from the relevant authorities.

I. **Assessment of Project Costs** (Please comment on the appropriateness of the original budget and highlight any major departure from the planned budget)

No departure from planned budget

J. **Additional Project Funding Obtained** (In case of involvement of other funding sources, please indicate the source and total funding provided)

Nil

K. **Other Remarks** (Please include any other comment which you feel is relevant for the evaluation of this project)

Date : **Signature :**

Benefit Report

1.   Description of the Project

A. **Project identification**	
1. **Project number : 03-02-06-0031-PR0023/11-02**	
2. **Project title : To Develop An Efficient Variable Speed Compressor Motor System**	
3. **Project leader : Prof. Dr. Abdul Halim Mohd Yatim**	

B.   Type of research

Indicate the type of research of the project (Please see definitions in the Guidelines for completing the Application Form)

☐ Scientific research (fundamental research)

☐ Technology development (applied research)

☑ Product/process development (design and engineering)

☐ Social/policy research

C.   Objectives of the project

1.   Socio-economic objectives

Which socio-economic objectives are adressed by the project? (Please indentify the sector, SEO Category and SEO Group under which the project falls. Refer to the Malaysian R&D Classification System brochure for the SEO Group code)

Sector: Energy, Mineral and Geo Science

SEO Category: Energy Resources (S 20400)

 SEO Group and Code: Preparation and supply of Energy Source Materials (S 20403)

2.   Fields of research

Which are the two main FOR Categories, FOR Groups, and FOR Areas of your project? (Please refer to the Malaysia R&D Classification System brochure for the FOR Group Code)

a.   Primary field of research

FOR Category: F10700 Engineering Sciences

FOR Group and Code: F10710 Mechanisation and Design Engineering

FOR Area: Other Mechanisation and Design Engineering

b.   Secondary field of research

FOR Category: F10600 Applied Sciences and Technologies

FOR Group and Code: F10602 Manufacturing and Process Technologies and Engineering

FOR Area: Other Manufacturing and Process Technologies and Engineering

D.   Project duration

What was the duration of the project?

    60 Months

E.   Project manpower

How many man-months did the project involve?

    27 Man-months

F.   Project costs

What were the total project expenses of the project?

RM 400,000

G.   Project funding

Which were the funding sources for the project?

Funding sources	Total Allocation (RM)
IRPA	RM400,000
_____	_____
_____	_____
_____	_____

ll.   **Direct Outputs of the Project**

A.   **Technical contribution of the project**

1.   **What was the achieved direct output of the project :**

For scientific (fundamental) research projects?

☐   Algorithm

☐   Structure

☐   Data

☐   Other, please specify : _____

For technology development (applied research) projects :

☑   Method/technique

☑   Demonstrator/prototype

☐   Other, please specify : _____

For product/process development (design and engineering) projects:

☐   Product/component

☐   Process

☐   Software

☐   Other, please specify : _____

2.   **How would you characterise the quality of this output?**

☐   Significant breakthrough

☑   Major improvement

☐   Minor improvement

B. Contribution of the project to knowledge

1. How has the output of the project been documented?

- [✓] Detailed project report

- [ ] Product/process specification documents

- [ ] Other, please specify : _____

2. Did the project create an intellectual property stock?

- [ ] Patent obtained

- [ ] Patent pending

- [ ] Patent application will be filed

- [ ] Copyright

3. What publications are available?

- [✓] Articles (s) in scientific publications   How Many: 6

- [✓] Papers(s) delivered at conferences/seminars   How Many: 6

- [ ] Book

- [ ] Other, please specify : _____

4. How significant are citations of the results?

- [ ] Citations in national publications   How Many:

- [✓] Citations in international publications   How Many: 2

- [ ] None yet

- [ ] Not known

lll.   Organisational Outcomes of the Project

A.   Contribution of the project to expertise development

1.   How did the project contribute to expertise?

    [✓] PhD degrees   How Many: 1

    [ ] MSc degrees   How Many: _____

    [✓] Research staff with new specialty   How Many: 1

    [ ] Other, please specify: _____

2.   How significant is this expertise?

    [✓] One of the key areas of priority for Malaysia

    [ ] An important area, but not a priority one

B.   Economic contribution of the project?

1.   How has the economic contribution of the project materialised?

    [✓] Sales of manufactured product/equipment

    [ ] Royalties from licensing

    [ ] Cost savings

    [ ] Time savings

    [ ] Other, please specify : _____

2.   How important is this economic contribution ?

    [ ] High economic contribution   Value: RM_____

    [✓] Medium economic contribution   Value: RM_____

    [ ] Low economic contribution   Value: RM_____

3. **When has this economic contribution materialised?**

☐ Already materialised

☐ Within months of project completion

☐ Within three years of project completion

☑ Expected in three years or more

☐ Unknown

C **Infrastructural contribution of the project**

1. **What infrastructural contribution has the project had?**

☑ New equipment   Value: RM 194,880

☐ New/improved facility   Investment :   RM _____

☐ New information networks

☐ Other, please specify: _____

2. **How significant is this infrastructural contribution for the organisation?**

☐ Not significant/does not leverage other projects

☐ Moderately significant

☑ Very significant/significantly leverages other projects

D. **Contribution of the project to the organisation's reputation**

1. **How has the project contributed to increasing the reputation of the organisation**

☐ Recognition as a Centre of Excellence

☐ National award

☐ International award

☐ Demand for advisory services

☐ Invitations to give speeches on conferences

☑ Visits from other organisations

☐ Other, please specify: _____

2. How important is the project's contribution to the organisation's reputation ?

☐ Not significant

☑ Moderately significant

☐ Very significant

1V. National Impacts of the Project

A. **Contribution of the project to organisational linkages**

1. **Which kinds of linkages did the project create?**

[ ] Domestic industry linkages

[ ] International industry linkages

[✓] Linkages with domestic research institutions, universities

[ ] Linkages with international research institutions, universities

2. **What is the nature of the linkages?**

[ ] Staff exchanges

[ ] Inter-organisational project team

[ ] Research contract with a commercial client

[✓] Informal consultation

[ ] Other, please specify: _____

B. **Social-economic contribution of the project**

1. **Who are the direct customer/beneficiaries of the project output?**

Customers/beneficiaries: Number:

_____   _____

_____   _____

_____   _____

2. **How has/will the socio-economic contribution of the project materialised ?**

[ ] Improvements in health

[ ] Improvements in safety

[ ] Improvements in the environment

[✓] Improvements in energy consumption/supply

[ ] Improvements in international relations

[ ] Other, please specify: _____

3. **How important is this socio-economic contribution?**

☐ High social contribution

☑ Medium social contribution

☐ Low social contribution

4. **When has/will this social contribution materialised?**

☐ Already materialised

☐ Within three years of project completion

☑ Expected in three years or more

☐ Unknown

Date: **Signature:**

UNIVERSITI TEKNOLOGI MALAYSIA
Invention Disclosure

This form contains disclosure of invention or copyrightable material and should be submitted in confidence to The Secretariat, Intellectual Property Committee, Research Management Centre (RMC), Universiti Teknologi Malaysia, 81310 UTM Skudai.

1. Type of Material :   Invention ☑   Copyright ☐

2. Title of Invention or Copyright :

   AN EFFICIENT VARIABLE SPEED COMPRESSOR MOTOR DRIVE.

3. Inventor(s) Approximate

	Full Name	Department/Institute/Centre/Unit	% Contribution
3.1 Principal	**Prof. Dr. Abdul Halim Mohd Yatim**	**ENCON/FKE**	**70%**
3.2 Associates	**Wahyu Mulyo Utomo**	**ENCON/FKE**	**30%**
3.3 Others	_____		

4. Identify sources and estimate % of support (materials, facilities, salaries) contributing to the development of the invention :

Government Funds (IRPA, grants and /or contract)	***100*** %
UTM-RMC Funds	*0* %
Other Institution (s) :	
Name : _____	%
Other source : _____	%

5. If developed with Government Funds :

   Has invention been reported to granting agency ?   Yes ☐   No ☑

   Agency Name : ***IRPA***   Report Date: _____

   Grant Number : ***74535***

   Has notification been made to the relevant Government Agency for retention of rights to invention ?
            Yes ☐   No ☑

   Please attach copies of any correspondence with any Government agency related to disclosure of invention or rights to invention.

6. If developed with other funds (industry sponsor, foundation grant, etc.) :

   Has the invention been reported to the sponsor?   Yes ☐   No ☐

   Source name : _____ Report Date : _____
   Please attach copies of relevant correspondence with the sponsor.

7. Record of Invention :

    7.1 Invention was first conceived on or about (Date) : **12/01/2004**

    7.2 An oral disclosure has been made :

        (Name) **Wahyu Mulyo Utomo** _____ on (Date) **01 / 11 / 2005**

        (Name) _____ on (Date) _ / __ / ____

    7.3 First sketch or drawing was made on (Date) : ____ / ____ / _____ disclosed to and understood by (Name) : **Wahyu Mulyo Utomo** _____ on (Date) : **12 / 01/ 2004**

        That document is now located at: **P07-112-01**_____

    7.4 First written description was completed on (Date) : ____ / ____ / ____ and that document is now located at : _____

    7.5 First reduction to practice was successfully tested on (Date) : ____ / ____ / ____ and the records of that test are now located at _____

    7.6 First publication disclosing the invention was dated (Date) : ____ / ____ / ____

8. List companies or individuals with whom you may have discussed this project and append copies, showing dates, of all correspondence relating to their interest.

    (Name) _____ (Correspondence Date) : ___ / ___/ ____

    (Name) _____ (Correspondence Date) : ___ / ___/ ____

    If you have communicated, via telephone, with any additional companies, please list the company names, giving dates, and append a brief summary of your conversations.

    (Name) _____ (Communication Date) : ___ / ___/ ___

    Summary of conversation: _____

    (Note : Valuable rights to inventions may be lost if disclosed to outside parties unless signed Confidentiality Agreement is obtained)

9. Has invention or components thereof been described in a draft of an article or lecture ? If so, please attach copies of drafts of abstracts, manuscripts, or reprints and give proposed presentation and/or publication dates.

    (Type & Title of Draft) : _____

    (Proposed Presentation Date) : ____ / ____ / ____
    (Note : Premature disclosure of invention in lectures, articles, etc. may result in loss of all right to obtain patent)

10. Briefly outline your views regarding potential commercial application of your invention :

    10.1 List potential licensees or manufacturers or companies active in this field.

        Name : **Focus Dynamic Technology Bhd.**

        Name : **Schneider Scott & English Electric Sdn Bhd.**

        Name : **Advance Control Engineering Sdn Bhd.**

10.2 What is potential market ?

Focus Dynamic Technology Bhd

_____

_____

_____

_____

10.3 Estimate commercial market in RM and USD :   RM **5,000**   USD _____

11. List independent referees with expertise in the area of the invention with whom we may communicate for additional information (with your approval) :

(Name, address, contact nos.) : **Sio Kee Hong, 03-78450896**

(Name, address, contact nos.) : **Nik Rumzi Nik Idris, 019-7205854**

12. Please append a full description of the invention which should include the following :

   12.1   Drawings, diagrams, figures, flowcharts, sketches etc. which illustrate the invention.
   12.2   Chemical structural form (if the invention is a new chemical compound).
   12.3   List of equivalents which can be substituted for the invention or for components of the invention.
   12.4   Reprints of articles or patents describing inventions, methods etc. similar to the one described in this disclosure.
   12.5   Describe why your product or process is sufficiently novel compared to those already available to warrant patentability.

Principal Inventor : _____   Dean/Director : _____
                    (Signature)   of Faculty/Centre/Institute   *(Signature)*

Name :   **Prof. Dr. Abdul Halim**   Name :
         Mohd Yatim

Address :   **ENCON, FKE, UTM**   Address :

Telephone / Fax : **5535860/5578150**   Telephone / Fax :

Date : **12 / 01 / 2006**   Date : ____ / ____ / ____